THE UNIVERSITY OF ALBERTA

RELEASE FORM

NAME OF AUTHOR W.A. Ruzycki

TITLE OF THESIS Fatigue Failure of Total Hip Prostheses

DEGREE FOR WHICH THESIS WAS PRESENTED MASTER OF SCIENCE

YEAR THIS DEGREE GRANTED Fall 1979

THE UNIVERSITY OF ALBERTA

Fatigue Failure of Total Hip Prostheses

by

W.A. Ruzycki

A THESIS

SUBMITTED TO THE FACULTY OF GRADUATE STUDIES AND RESEARCH
IN PARTIAL FULFILMENT OF THE REQUIREMENTS FOR THE DEGREE
OF MASTER OF SCIENCE
IN
Mechanical Engineering

EDMONTON, ALBERTA
Fall 1979

THE UNIVERSITY OF ALBERTA

FACULTY OF GRADUATE STUDIES AND RESEARCH

The undersigned certify that they have read, and recommend to the Faculty of Graduate Studies and Research, for acceptance, a thesis entitled Fatigue Failure of Total Hip Prostheses submitted by W.A. Ruzycki in partial fulfilment of the requirements for the degree of MASTER OF SCIENCE in Mechanical Engineering.

Abstract

The problem of fatigue failure of total hip prostheses implanted in the human body is investigated. An experimental model is developed to simulate in vivo loading and various femoral components of total hip prostheses are tested in order to determine their projected life.

In addition, certain important mechanical properties of the materials used in the component are established. The effects of improper positioning of the component is also investigated.

Acknowledgements

The author expresses his appreciation and thanks to

Dr.K.J. Russell for initiating this project and for providing a great deal of help and guidance throughout,

Dr.J.R. Colbourne for supervising this project and providing the academic guidance and help,

Tony Dyke, Brian Cielin, Tom Villett, Terry Nord, Dennis Jessey, and Bob Welker for their individual expertise in the technical design and construction phase of this work,

the University of Alberta Hospital Special Services and Research Committee for providing the majority of the funding for this project,

the DePuy Co., the Howmedica Co., the Zimmer Co., and the Richards Co. for donating their products and information.

Table of Contents

Chapter Page

List of Tables

List of Figures

List of Photographic Plates

List of Symbols

MPa - mega Pascals, Pascals * 10^6

GPa - giga Pascals, Pascals * 10^9

kN - kilo-Newtons

R - ratio as defined in the text

σ_y - yield stress

σ_e - endurance limit

σ_u - ultimate stress

K - stress intensity factor

K_c - critical stress intensity factor, fracture toughness

s - denotes small stem size

mm - millimeter

F_t - a force as defined in the text

F_a - a force as defined in the text

F_w - a force as defined in the text

W - body weight

N - Newtons

y - a distance as defined in the text

x - a distance as defined in the text

micro m/m - strain measurement, meter * 10^{-6} per meter

Nm - Newton meter

m - meter

R_y - a radius as defined in the text

E - Young's modulus, the modulus of elasticity

ν - Poisson's ratio

I. Introduction

The Problem

There are many painful or debilitating conditions that can occur in the hip joint. In certain circumstances, such as severe osteo-arthritis of the hip joint, replacement of the entire hip joint is considered by orthopaedic surgeons to be the best course of treatment. The operation entails the replacement of the upper end of the femur, the head and neck, with a metallic ball and stem. In addition, the pelvic side of the joint, the acetabulum, is replaced with a plastic socket.

A significant number of the total hip replacement stems have fractured after being in use several months or longer. Recently new metals have been developed for use in the stem. No study exists that adequately assesses the design and materials currently used in total hip replacements.

A. Literature Survey

Overall History of Total Hip Replacements

As detailed by Newman [1], total hip replacement has been practised for over 75 years. In 1891, Gluck implanted an ivory ball and socket hip joint, secured with screws. Wiles followed, in 1938, when he implanted six stainless steel hip joints. The early 1950's saw Charnley and McKee seperately begin developmental work on total hip replacement, on which many of today's principles are based. In 1960 Charnley advocated the use of methylmethacrylate for fixation of total hip replacement components.

Since 1960 the basic shape of the femoral component has not changed significantly. The modern prosthesis generally consists of a metal stem and ball, known as the femoral component or stem, and a plastic socket, which is called the acetabular component. A typical hip prosthesis is shown in Plate 1.

---

[1] Newman, P.H.; Development of Total Hip Replacement, Total Hip Replacement, Jayson, M., J.B.Lippincott Company Toronto,1971, pg. 13-25.

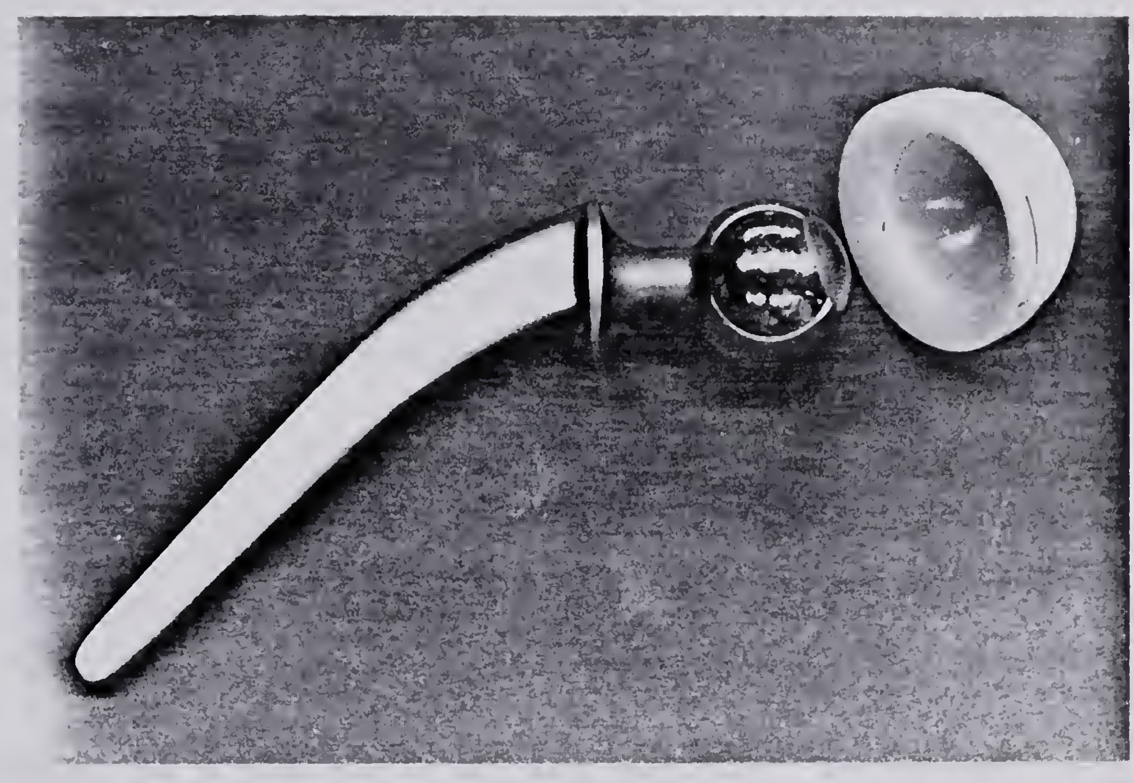

Total Hip Prosthesis (1/2X)

Plate 1

Definition of Terms

Frontal and Lateral Planes in the Human Body

Throughout this work reference is made to the frontal plane or the lateral plane. The frontal plane is the plane such that the normal to the plane points forwards. The lateral plane is the plane such that the normal to the plane points sideways. The frontal plane is seen from the front view, while the lateral plane is seen from the side view. These planes are depicted in Figure 1.

Basic Hip Anatomy

Figures 2 and 3 show the basic hip anatomy. For reasons of clarity only the anatomy referred to in this thesis is shown.

The 'lateral' and 'medial' directions are depicted in Figure 1. The lateral direction is away from the body centerline, while the medial direction is towards the body centerline. A total hip stem thus has a lateral side or face, a side furthest from the body centerline, and a medial side, a side nearest the body centerline.

Valgus and Varus Stem Position

The terms 'valgus' and 'varus' are used several

times in this work. Valgus means bent outward, denoting a deformity in which the angulation of the distal part is away from the midline of the body. Varus, on the other hand, means bent inward, denoting a deformity in which the angulation of the distal part is toward the midline of the body. The relation of these terms to the position of the femoral component is shown in Figure 4.

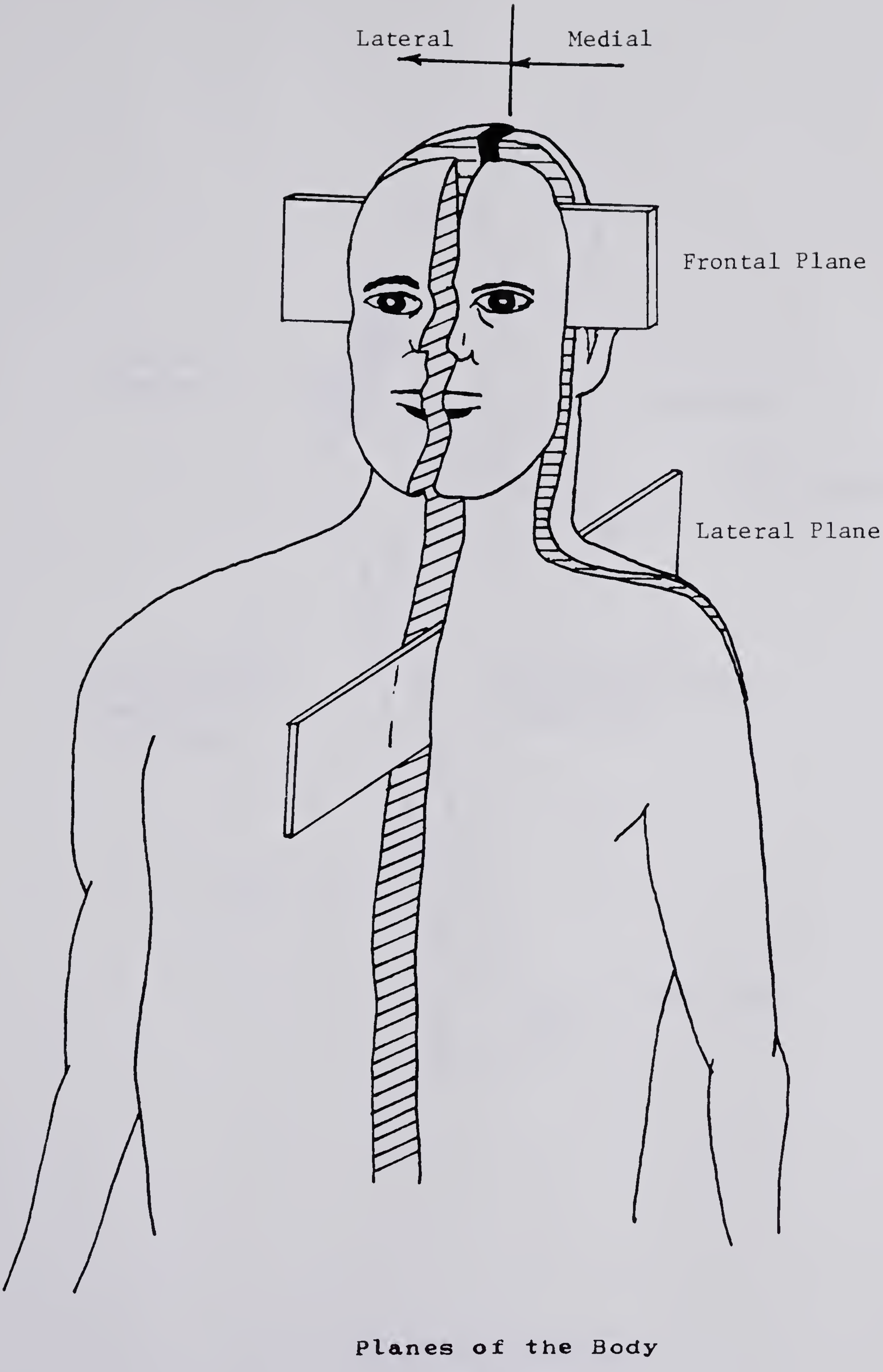

Planes of the Body

Figure 1

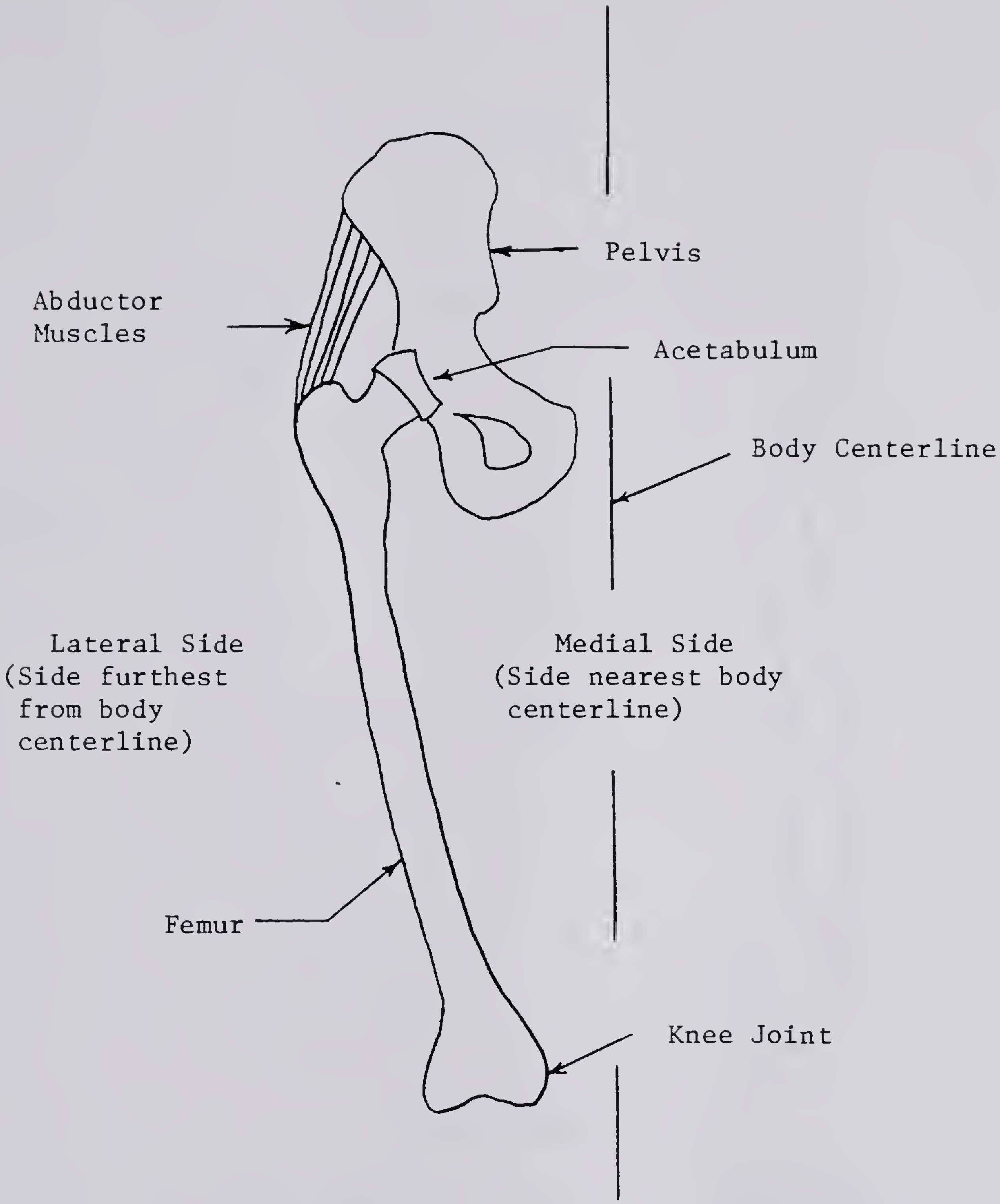

Basic Hip Anatomy

Figure 2

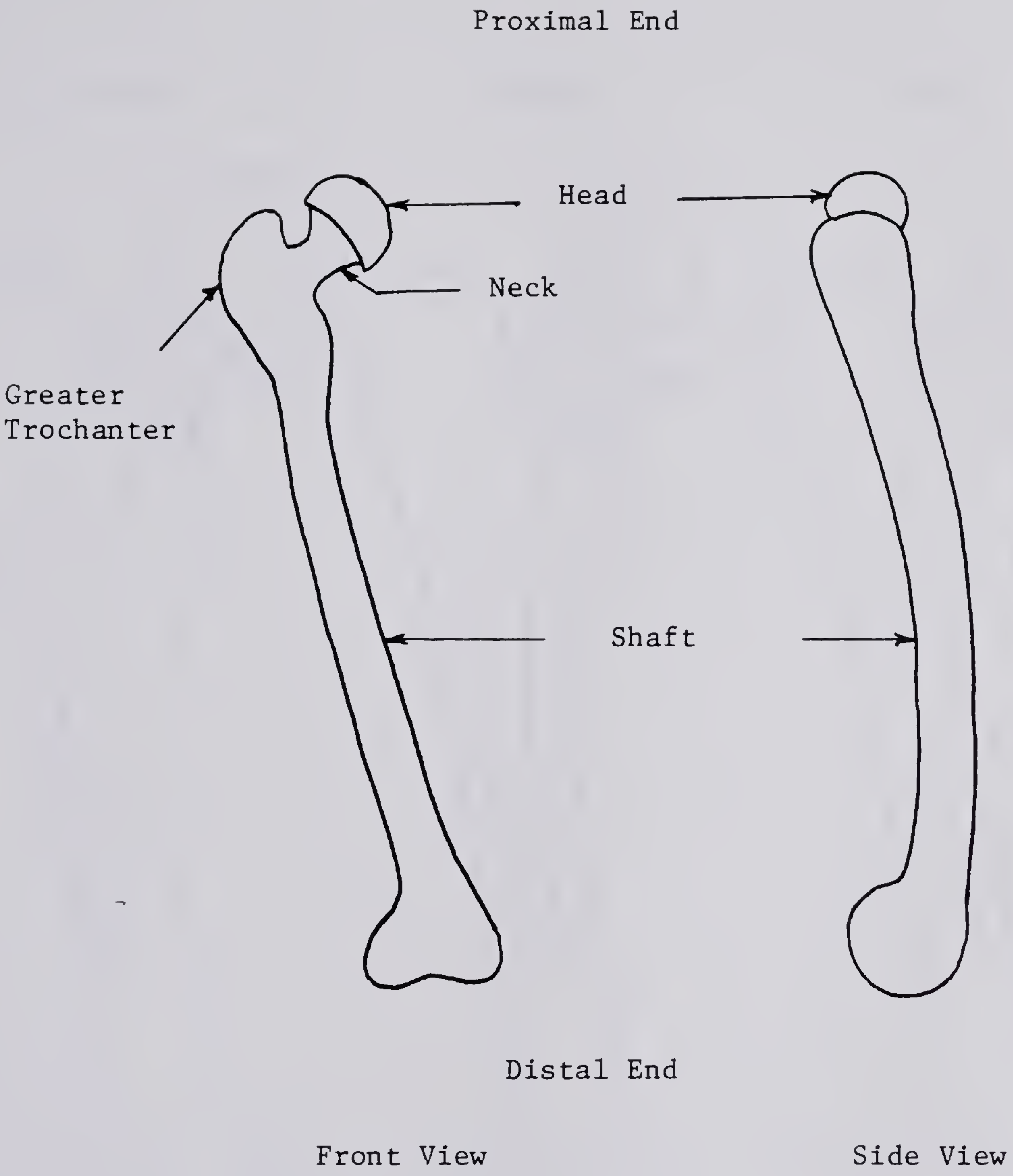

Basic Anatomy of the Femur

Figure 3

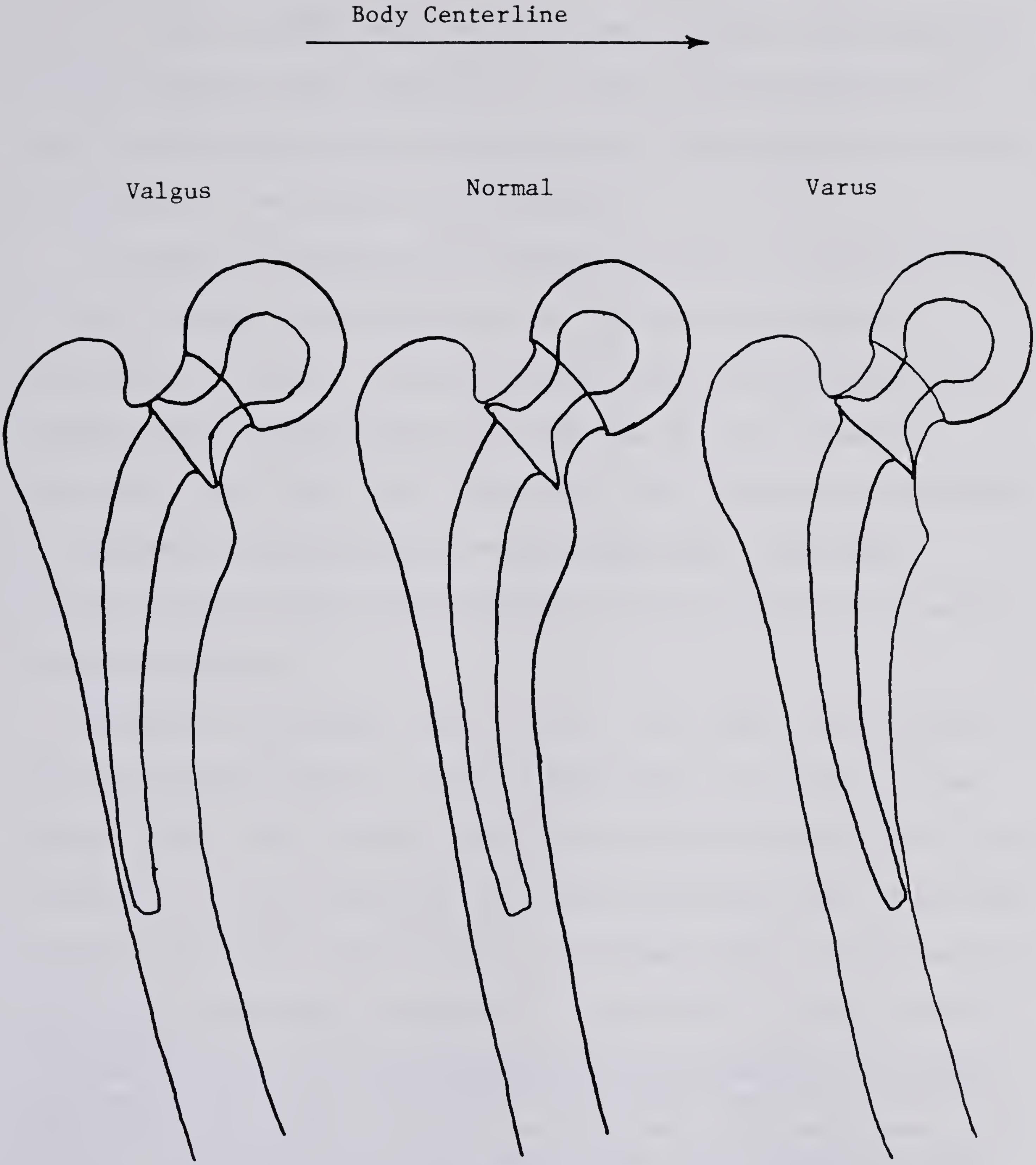

Valgus and Varus Stem Position

Figure 4

Previous Femoral Stem Studies

In 1973 Walker [2] calculated that a femoral stem stress of 20.7 MPa (30,000 psi.) could result from a load applied at the head of the prosthesis of only 2.22 kN (500 lb.) . He used a simplified set of assumptions, and simple beam theory to calculate the stress in the stem.

In 1974 Martens et al [3] described the in vivo failure of six femoral components. An accompanying study, to determine the cause, indicated the failures were due to improper stem positioning and the use of low strength materials. Although they identified the failures as fatigue, no fatigue strength values were presented. The study involved strain gage instrumented stems partially embedded in epoxy blocks.

Galante, Rostoker, and Doyle [4], in 1975, presented a two dimensional finite element analysis of stress in the femoral stem. They determined the important factors as being stem position and material fatigue strength. They also made the statement:"It was further indicated that current designs should be regarded as marginal in relation to long service

---

[2] Walker, Peter S.; The Optimun Use of Materials In Total Hip Design, The Hip 1973, The C.V. Mosby Company, pg.46-66.
[3] Martens, M.; Aernoudt, E.; de Meester, P.; Ducheyne, P,; Mulier, J.C.; de Langh, R.; Kestelyn, P.,; Factors in the Mechanical Failure of the Femoral Component in Total Hip Prosthesis, Acta Orthop. Scand. 45, 693-710, 1974, Munksgaard International Booksellers and Publishers Ltd., Copenhagen K, Denmark.
[4] Galante, J.O.; Rostoker, W.; Doyle, J.M.; Failed Femoral Stems in Total Hip Prostheses, The Journal of Bone and Joint Surgery March 1975, pg. 230-236, The Journal of Bone and Joint Surgery Inc., Boston, Massachusettes.

life until more fatigue information is available on the metallic materials currently in use."

B. Weightman [5] extended the earlier work of Martens. In 1976, he presented data concerning six instrumented stems implanted into cadaver femurs, and compared his data to results obtained using Martens' fixation method. The agreement between the two methods was not very close.

Zwicker and Schmid [6] presented a study in 1976 on fatigue testing of certain prosthetic stems. However, it showed a broad scattering of results for similar prostheses and support conditions.

Andriacchi et al [7], in 1976, combined fatigue strength values and Galante's stem stress analysis to estimate stem fatigue life. They considered only one type of prosthesis and material.

---

[5] Weightman, B.; The Stress In Total Hip Prosthesis Femoral Stems: A Comparative Experimental Study, Advances in Artificial Hip and Knee Joint Technology, Ed. M. Schaldach and D. Holmann, Spinger-Verlag, 1976, pg.138-147.

[6] Zwicker, H.U. and Schmid, H.J.; Mechanical Properties of Metallic Materials for Longterm Use in Highly Stressed Locomotor Systems, Engineering in Medicine Vol.2, pg.347-361, Institution of Mechanical Engineers.

[7] Andriacchi, T.P.; Galante, J.O.; Belytschko, T.B.; Hampton, S.; A Stress Analysis of the Femoral Stem in Total Hip Prostheses, The Journal of Bone and Joint Surgery, Vol.58-A, July 1976, pg.618-624, The Journal of Bone and Joint Surgery Inc., Boston, Massachusettes.

Material Properties

Endurance Limit

The endurance limit is an important fatigue parameter. It is the maximum cyclic stress a material can be subjected to, without failure, for an infinite number of cycles. In engineering practice, material behavior at 10 million cycles is taken as being representative of material behavior at an infinite number of cycles.

The endurance limit exhibited by the material is affected by the maximum and minimum values of the cyclic stress. The ratio of the minimum stress to the maximum stress in a load cycle is called the R ratio. A load cycle which produces a maximum tensile stress and a compressive stress of zero has an R ratio of zero. This type of stress cycle is representative of that produced on the lateral face of a femoral hip component in vivo, namely the side furthest from the body centerline, as shown in Figure 2.

There are no published endurance limits for an R ratio of zero ($R = 0$) for the materials now used in total hip replacements. However, the Goodman diagram, as

shown by Shigley [8], can be used to estimate the endurance limit at R = 0 if certain other mechanical properties of the material are known. These include the endurance limit at R = -1, the yield stress, and the ultimate stress. The Goodman diagram for forged cobelt-chrome is shown in Figure 5.

To obtain the endurance limit at R = 0 a line representing alternating stress equal to mean stress is drawn from the origin to the modified Goodman line. The coordinates of the intersection of these lines give the values of the alternating and mean stresses for the endurance limit at R = 0. The endurance limit is the sum of the two stresses.

A non-graphical method of obtaining the endurance limit at R = 0 is easily obtainable. It can be stated as:

> The endurance limit at R = 0 is the lesser of the yield stress, σ_y , and $2\sigma_e/(1 + \sigma_e / \sigma_u)$, where σ_e is the endurance limit at R = -1 and σ_u is the ultimate tensile stress.

When it was possible to obtain sufficient material for specimens, the endurance limit at R = 0 was measured directly. This was done by cyclic loading of the specimens as will be detailed later.

---

[8] Shigley, J.E.; Mechanical Engineering Design, McGraw- Hill Book Company, Toronto, 1963, pg. 177-183.

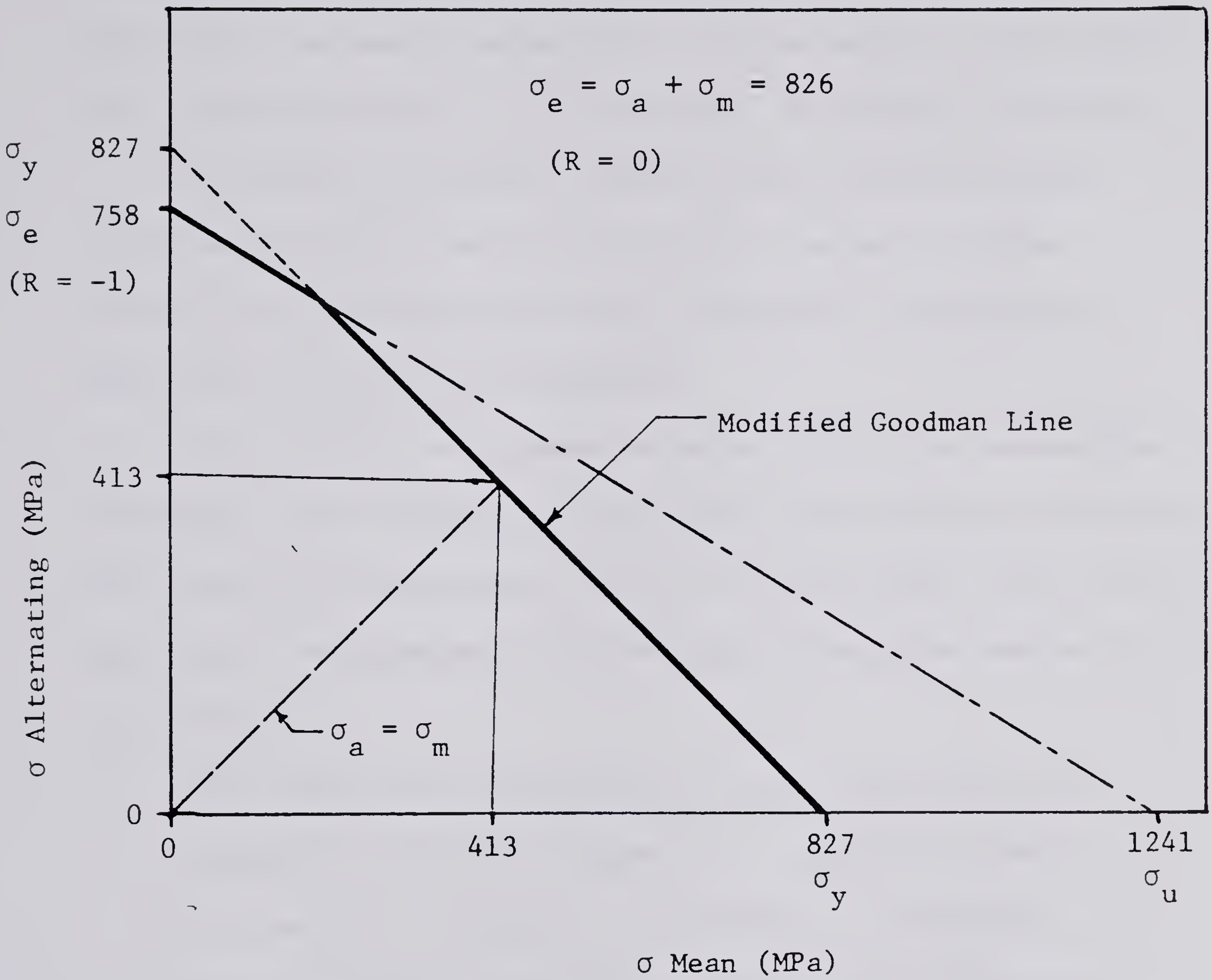

Goodman Diagram for Forged Cobalt-Chrome

Figure 5

Fracture Toughness

Fracture toughness is defined as the ability of a material to absorb energy and resist crack propagation. If the crack size and the stress level are known, fracture toughness principles can be used to determine the susceptibility of a structure to brittle failure.

A brittle fracture occurs with little plastic deformation and usually is aligned normal to the direction of principal stress. Tensile stresses are required for brittle fracture.

The science of linear-elastic fracture mechanics contains the methodology by which the relations between the material toughness, flaw or crack size, and stress level may be studied. The basis of fracture mechanics is as follows:

> When the stress intensity at the crack tip, K, reaches a critical value, K_c, unstable crack propagation occurs. K is related to both the nominal stress level and the size of the crack present. The nominal stress level is the stress that would exist if no crack were present. K_c represents the fracture toughness of the material. If the material toughness is known then the critical crack length for a given stress field can be calculated.

In this study material toughness values were determined by testing Charpy V notch specimens and theoretically correlating the results to toughness values. When sufficient material was available the Charpy specimens were precracked by fatigue loading them. This was done in an attempt to attain the sharpest possible notch which is necessary, according to Brown and Srawley [9], to obtain the lowest possible K_c. This is described in detail in the appendix.

B. Objectives

In 1977, Dr. K.J. Russell asked for assistance from the Mechanical Engineering Department at the University of Alberta. He had become concerned with the rising number of fracture failures of total hip prostheses both at the University Hospital and as reported by Collins [10] and others. He requested that a thorough engineering study be undertaken to review the design of total hip replacements and that a recommendation be made for the best prosthesis, from the point of view of resistance to failure.

The objective of this research is to compare the resistance to fracture of existing commercially available

---

[9] Brown Jr., W.F.; Srawley J.E.; Commentary on Present Practice, Review of Developments in Plane Strain Fracture Toughness Testing, ASTM STP 403, American Sociey for Testing and Materials, Philadelphia Pa. 19103, Pg 229.

[10] Collins, D.K.; Femoral Stem Failures in Total Hip Replacement, The Journal of Bone and Joint Surgery Vol.59-A, Dec. 1977, pg.1033-1041.

prostheses, in order to assist the orthopaedic surgeons at the University of Alberta Hospital in their selection of a particular brand of prosthesis. The most important parameters required for the evaluation of each type of stem are the maximum expected stress, the material endurance limit, and the material fracture toughness. A knowledge of these properties will aid in the selection of a prosthesis type with the objective of reducing the probability of stem failures such as those shown in Plates 2-5.

Broken Stems

Plate 2

View of One Cracked Stem (2X)

Plate 3

End-on View of Fracture Surface (25X)

Crack Began in Upper Right Corner

Plate 4

Fatigue Striations (5000X)

Plate 5

C. Analysis of the Problem and the Issues to be Resolved

There are many different shapes and materials presently being used in total hip prostheses. The important parameters, for evaluation of each prosthesis, are those related to the fracture characteristics of each type, with emphasis on the fatigue failure aspect. A realistic, precise method of testing each stem design is required. It is necessary to determine which properties of the materials are important, then to determine their values. The stem evaluations can then be made considering both the shape of the stem and the material involved, on a comparative basis.

Of secondary importance is the determination of the effect of improper stem positioning. Malpositioning includes the medial or lateral implantation of the distal end of the stem in the shaft of the femur, as seen in Figure 4. It also includes the medial or lateral shift of the position of the knee, in the case of a knock-kneed or a bowlegged patient.

Description of the Stems

Of the 25 femoral components tested there were only six basic stem cross-sections. The cross-sectional areas and lengths of the stems varied somewhat and necessitated grouping the components into two categories for comparison purposes. The small size category contained four stems and the large size category contained 21 stems. A selection of

various stems is shown in Plate 6.

Total Hip Stems

Plate 6

Testing Procedures

In order to compare prosthesis stems on a fatigue basis, two approaches were considered. One approach would be to subject many components to appropriate cyclic loads and estimate the maximum load possible for no failure at 10 million cycles. This would require a very durable mounting method and a considerable number of samples to achieve reliable results.

The second approach would be to estimate the maximum stress produced in each prosthesis, and then to compare this with the endurance limit for the particular material. This would give an indication of the load level that the stem could withstand without failure. The stresses could be calculated by measuring the strains in the component in a static test.

The second approach was the one chosen. The problem then became one of developing a suitable method for loading the component.

Two possible procedures were again considered. In the first, the stems would be mounted in cadaver femurs and loaded appropriately. This would require at least as many femurs as stems and has the additional drawback that the femurs would not be uniform in either size or mechanical properties.

The second possibility, and the one chosen here, required the development of a suitable mounting and loading

method. It was necessary that the stems be mounted and loaded in a manner that would give stresses similar to those found in vivo, and that these stresses should be repeatable. To ensure that this occured, the stems were fixed in aluminum tubes, with carefully specified dimensions, loaded, and the stresses then compared with the stresses produced in stems mounted and loaded in cadaver femurs.

Forces Acting on the Stem

The force applied to the head of the stem is depicted in Figure 6. Equilibrium of the stem is ensured by the reaction forces exerted by the femur on the stem. Since the distribution of these forces is unknown, it was necessary to measure the stem strains experimentally, and to use the measured strains to calculate the stresses.

When the femur and the stem are considered as a free body, as shown in Figure 7, the only significant forces acting are the abductor muscle pull, the knee force, and the stem head force.

In measuring the strains it was assumed that the system was linear, so that the principle of superposition applies, and the strains due to the abductor muscle force and those due to the knee joint force could be measured separately. The method by which this was done, and the manner in which the total strains were determined, will be described later.

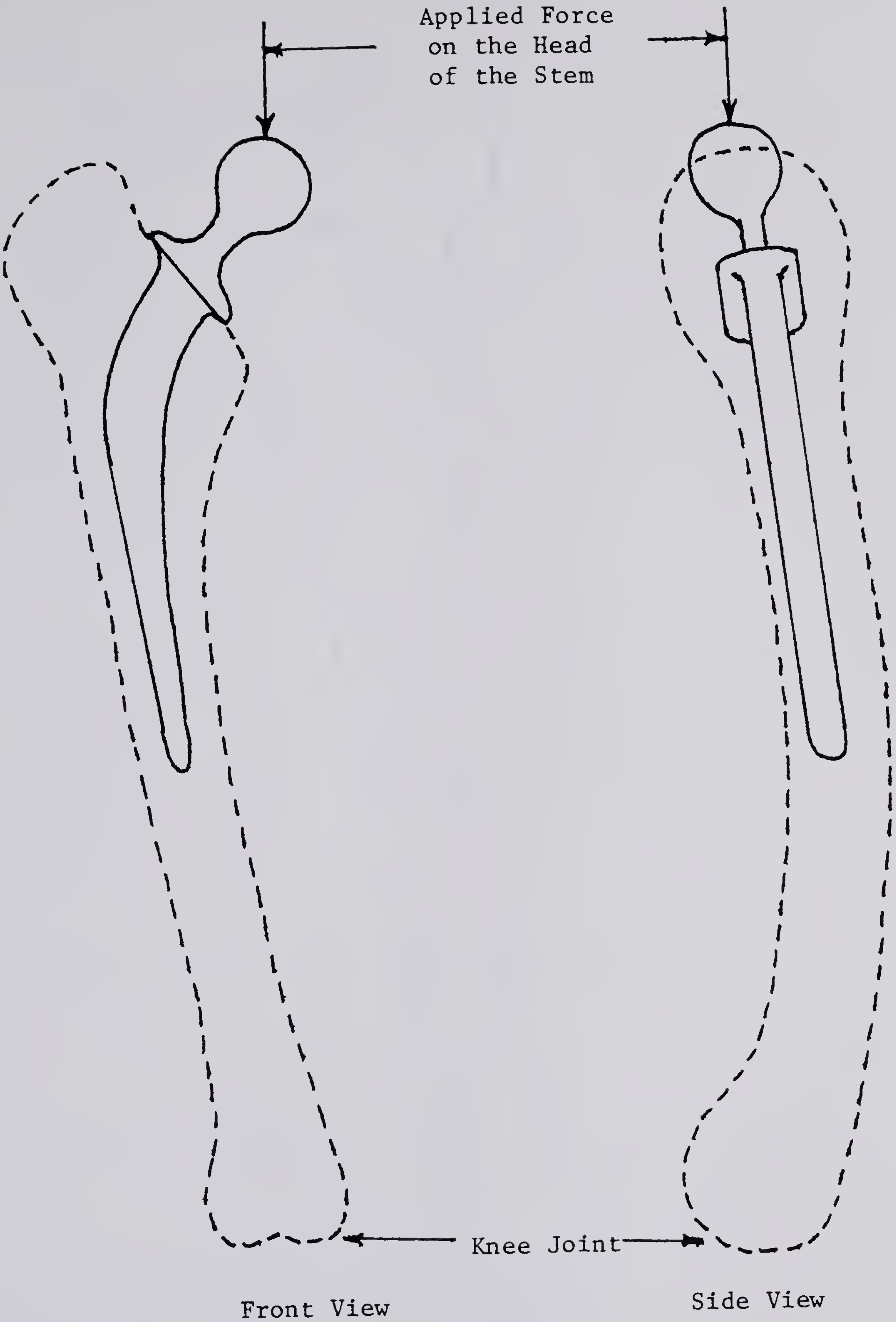

Applied Force Acting on the Stem

Figure 6

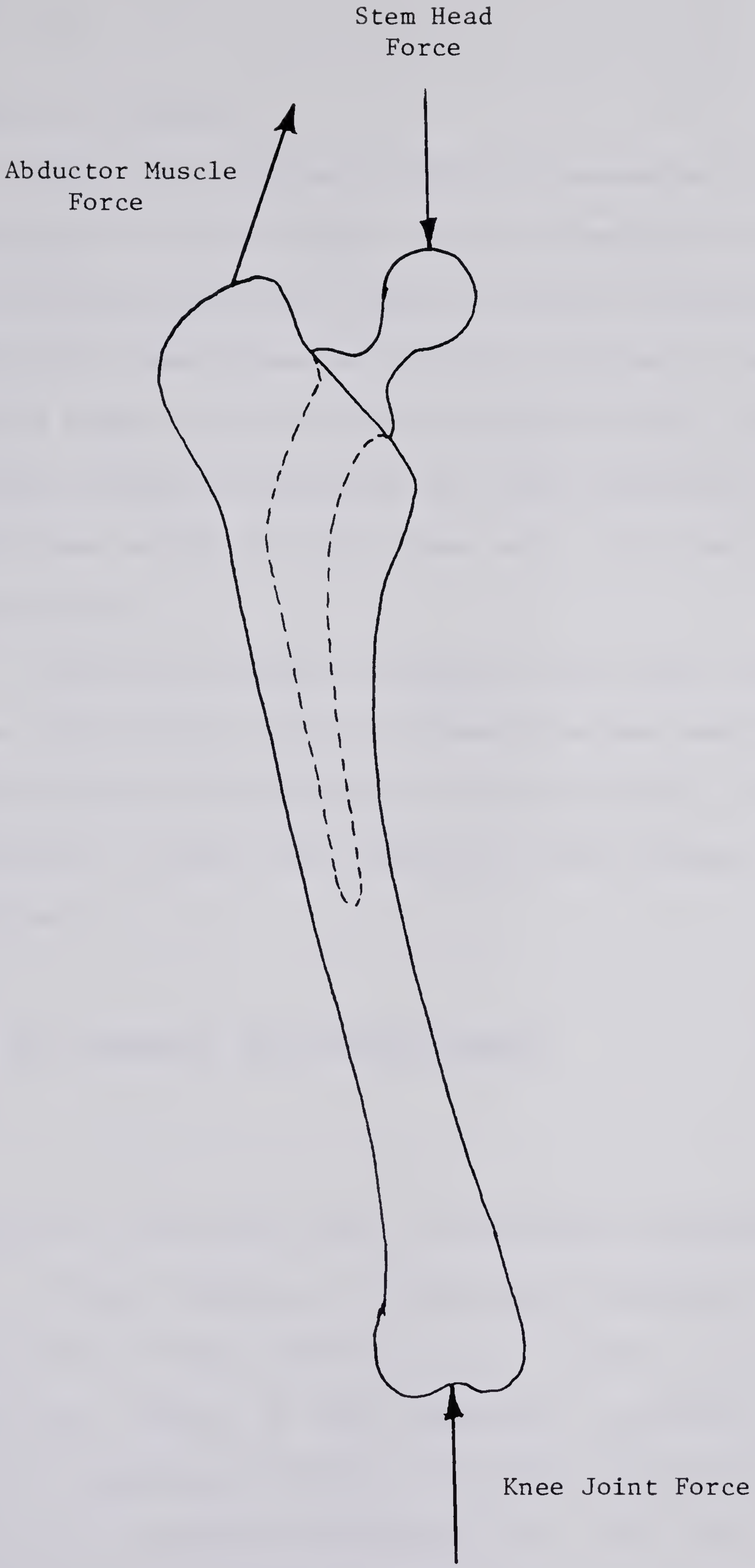

Free Body Diagram of the Stem and Femur

Figure 7

Material Testing

The most important material parameter, from the viewpoint of this study, was the endurance limit, since, as mentioned earlier, previous stem fractures have been generally identified as fatigue failures. The endurance limits were arrived at both theoretically, using the Goodman diagram approach, and experimentally, using specimens which in most cases were cut from femoral components.

Material fracture toughness was also considered in this study since little information was available concerning this property of the materials. Fracture toughness values were calculated from Charpy V notch specimens.

Effects of Improper Stem Positioning

Improper Positioning Due to Insertion Technique

Certain authors, as mentioned earlier, have identified stem position, in the femur, as being an important factor in stem fracture. To study the effects of the mounting position, stem #23 was mounted several times in different aluminum tubes. That is, once in extreme valgus, once in extreme varus, and twice on the centerline of the tube. The term 'extreme' is used since

the large inner diameter of the tube allowed more of a valgus or varus placement of the stem than would be possible if the stem was inserted into the relatively smaller medullary canal of a femur. The medullary canal is the marrow filled cavity in the center of the femur. Stem #23 was chosen because it was one of the smallest of the medium category stems. This, again, allowed a greater range of positions for the distal end of the stem.

Improper Position Due to Deformities

The effects on stem stress of improper positioning, due to deformities such as knock-knees and bowlegs, was investigated by loading the aluminum tubes appropriately. The loading method is explained in the section desribing the apparatus and testing methods.

II. Subjects, Apparatus, and Testing Methods

A. Subjects

Stems

Twenty-five total hip stems were evaluated in this work. There were eight different materials used in the stems. The materials are listed in Table 1, along with the distributor of the stem and the trade name, if any, of the material. The chemical composition of these materials is listed in the Appendix.

There were, as mentioned previously, six basic cross-sections among the twenty five stems. These are shown in Figure 8.

Table 2 correlates the stem number with the cross-sectional shape, the length of the stem, and the stem material. Table 2 also contains the distributor's description of the stem and identifies the distributor, by an initial preceding the material code. That is, Howmedica is represented by an 'H', Zimmer by a 'Z', DePuy by a 'D', and Richards by an 'R'. The first four stems listed were relatively smaller than the rest and are denoted by an 's' following the stem number. The remainder of the stems would normally be classed as medium or large size stems.

Table 1

Materials and Distributors

Material	Material Code	Distributors	Trade Name
Cast Cobalt-Chrome	CCC	Howmedica	Vitallium
Cast Stainless Steel	CSS	Richards	-
MP-35N	MPN	DePuy	Protasul-10
Forged Stainless Steel	FSS	Richards, Zimmer	-
Hot Isostatically Pressed Cobalt-Chrome	HCC	Zimmer	Zimalloy
Forged Cobalt-Chrome	FCC	Howmedica	FHS Vitallium
Ti-6Al-4V	TAV	Zimmer	Tivanium

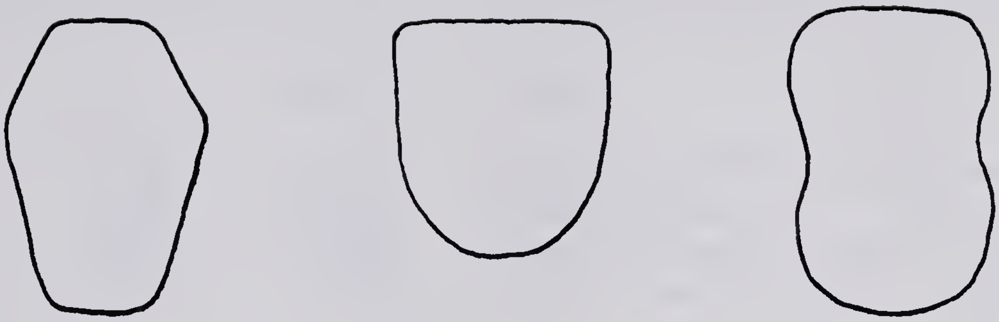

Hexagonal (HEX)

Semi-Round (SR)

'I-Beam' (IB)

Trapezoidal (TZ)

Oval (OV)

Rectangular (RE)

Stem Cross Sections

Figure 8

Table 2

Stem Descriptions

Stem No.	Section Shape	Length (mm)	Material	Distributor's Description
			Small	Stems
5-s	RE	123	Z-HCC	Straight Stem, Medium Neck
6-s	IB	127	H-FCC	Small Stem
7-s	TZ	128	Z-FSS	Medium Neck, Small Stem
19-s	HEX	114	D-MPN	Short Neck, Short Stem
		Medium	and	Large Stems
1	TZ	142	Z-CCC	Medium Neck, Long Stem
2	SR	140	R-CSS	3/8" Reg. Stem, 2 1/4" Neck
4	SR	137	Z-TAV	T-28 Tivanium
8	SR	137	R-CSS	3/8" Str. Stem, 1 3/4" Neck
9	SR	139	R-CSS	3/8" Reg. Stem, 1 3/4" Neck
10	SR	138	R-CSS	5/16" Reg. Stem, 1 3/4" Neck
11	SR	137	R-CSS	5/16" Str. Stem, 1 3/4" Neck
12	TZ	142	Z-HCC	Long Neck, Large Stem
13	IB	125	H-CCC	6993-1, Medium Stem
14	IB	112	H-CCC	6988-2, Large Stem
15	IB	126	H-FCC	Med. Neck, Large Stem
16	IB	128	H-FCC	Med. Neck, Medium Stem
17	HEX	133	D-MPN	Std. Neck, Std. Stem
18	HEX	133	D-MPN	Long Neck, Std. Stem
20	RE	140	Z-HCC	Medium Neck, Large Stem
21	OV	136	R-FSS	Medium Stem, 1 3/4"Neck
22	OV	135	R-FSS	Medium Stem, 2 1/4" Neck
23	OV	133	R-FSS	Small Str., 2 1/4" Neck
24	OV	136	R-FSS	Small Str., 1 3/4" Neck
25	TZ	134	D-MPN	Large Stem

Specimens

The specimens used for determining the material properties were generally machined from stems. The MP-35N, however, was supplied by the distributor in bar stock form and some of the forged cobalt-chrome material was supplied before it had been machined.

Endurance Limit Specimens

These specimens were dog bone type threaded specimens as shown in Figure 9. Dimensions for the specimens are shown in the figure.

Charpy Specimens

The Charpy specimens used were machined as close to standard dimensions as possible. In some instances, in particular when specimens were machined from stems, the specimens were slightly undersize. The standard Charpy dimensions are shown in Figure 10.

There was enough of the HCC material available to allow for the fatigue cracking of two of the specimens. This was not practical for the other materials as the fatigue cracking procedure provided usable specimens only 50% of the time, and material was scarce. The difficulty in the fatigue cracking procedure was determining the correct load to use to cause a fatigue crack of the necessary length.

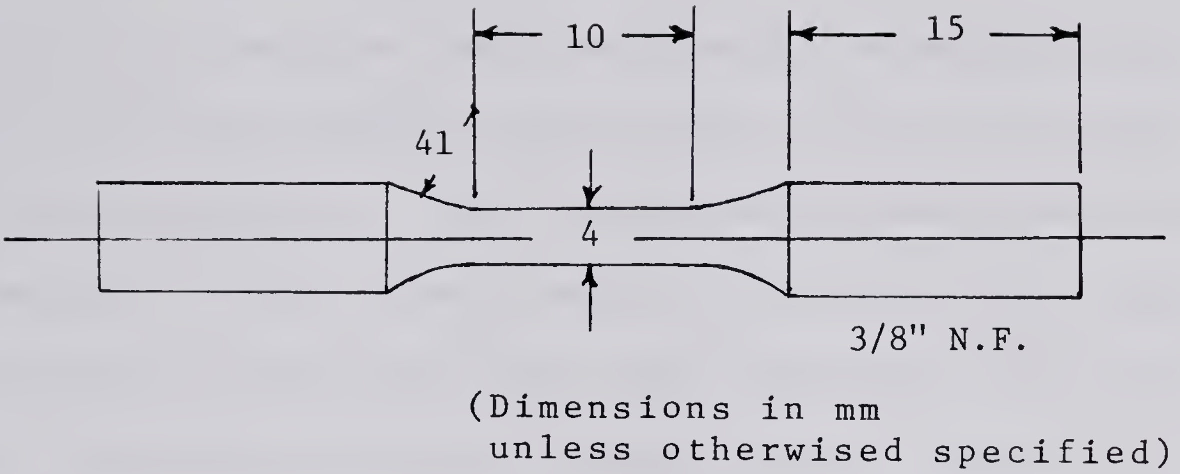

Fatigue Specimens

Figure 9

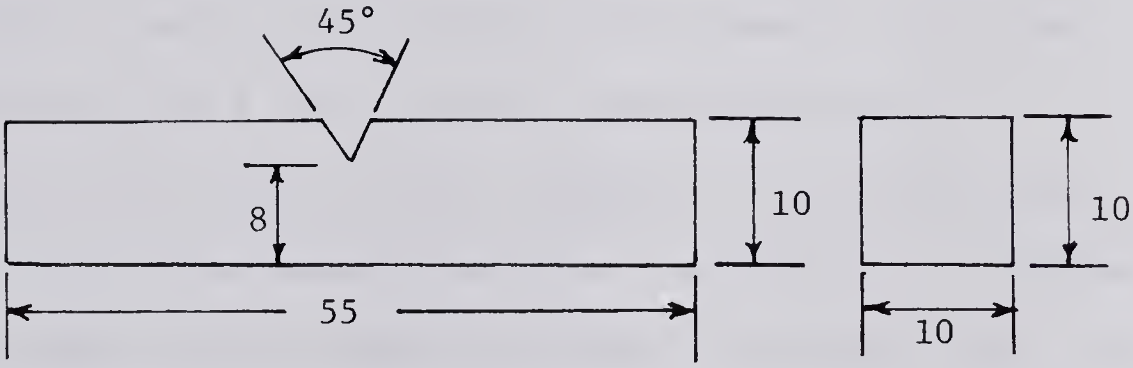

Charpy Specimens

Figure 10

B. Apparatus

Strain Measurement Apparatus

In order to measure the stem strains corresponding to the principal stem bending moment caused by the applied force shown in Figure 6, five strain gages were mounted on the centerline of the lateral face of the stem. The gages were positioned beginning 20 mm from the distal end and were spaced at intervals of 20 mm. On four stems, gages were mounted on the centerline of the front face of the stem as well as on the lateral face. A typical instrumented stem is shown in Figure 11 and Plate 7.

The front face gages measured the strains caused by out-of-plane bending. This occurs because the applied force on the head of the stem is not exactly in the plane of the stem, as shown in the side view of Figure 6.

The strain gages were metallic foil gages with gage factors ranging from 1.99 to 2.10. Additional gage specifications are found in the Appendix. The gages were wired using the recommended procedure and then were coated with a thin layer of silicone caulking. The stem, from the neck down, was then wrapped with plastic tape. The application of caulking was found necessary to protect the gages from the methylmethacrylate. If it was not applied, the methylmethacrylate reacted with the glue bonding the gages to the stem, and allowed the gages to lift. The

strains were recorded on a Vishay Digital Strain Indicator, model VE-20.

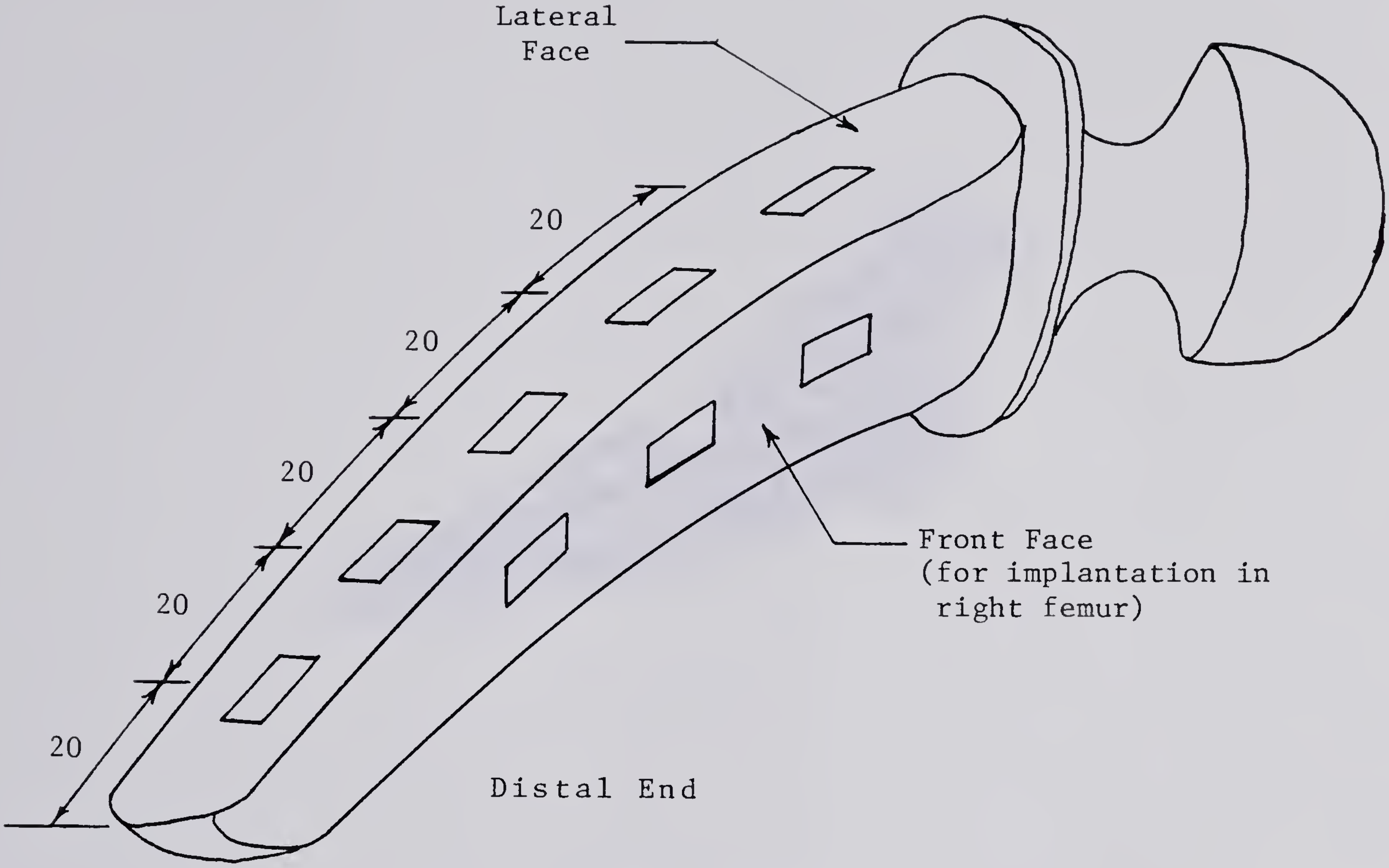

Diagram of Strain Gages

Figure 11

Strain Gages

Plate 7

Mounting and Loading Apparatus

It was necessary to develop a loading device for the stems that would produce strains, hence stresses, in the stem similar to those found in vivo.

The stem support characteristics provided by the femur were duplicated by reproducing, with the apparatus, the flexural support characteristics of the upper end of the femur and the following femoral dimensions, measured from an x-ray of an average size male femur.

1. The length of the femur from the bottom of the neck to the knee joint was 390 mm.
2. The femur as seen from the front view was straight.
3. The femur as seen from the side view had a slight forward bow. The offset at its midpoint was about 10 mm.

The force acting on the head of the stem, in vivo, can be estimated if it is assumed that critical loading of the stem occurs when a person is walking down a flight of stairs. Zwicker[11] has shown that the force acting on the foot can be as high as 3.5 times the body weight, when walking down 210 mm high stairs. The following simplifyng assumptions are also necessary:

1. The abductor muscles (gluteus medius and minimus) are the main muscle group acting on the femur.
2. No lateral shift of the pelvis or shoulders occurs.

---

[11] H.U. Zwicker and H.J. Schmid; Mechanical Properties of Metallic Materials for Longterm Use in Highly Stressed Locomotor Systems, Engineering in Medicine Vol.2, pg.347-361.

3. The angular momentum of the body about an axis through its mass center in the forward direction can be neglected.
4. The distance from the center of the head of the stem to the centerline of the body mass is normally twice the distance from the center of the head of the femur to the line of action of the abductor muscles[12], or about twice 63.5 mm (measured on femurs #5 and #6).
5. The center of mass of the body lies in a frontal plane that contains the centers of the head of the stem and the head of the opposite femur.
6. The maximum stress occurs in the stem when the knee joint is located on the vertical line connecting the center of the head of the stem and the foot.
7. The mass of one leg from the hip joint down is approximately 14% of the body mass, and from the knee down approximately 6% of the body mass.

---

[12] M.E.Muller; Osteotomy of the Greater Trochanter, The Hip 1974, The C.V. Mosby Company, pg.231-251.

Consider the free body diagram shown in Figure 12. It depicts the forces acting on the body above one hip joint when only one foot is in contact with the ground, in this case when walking down stairs.

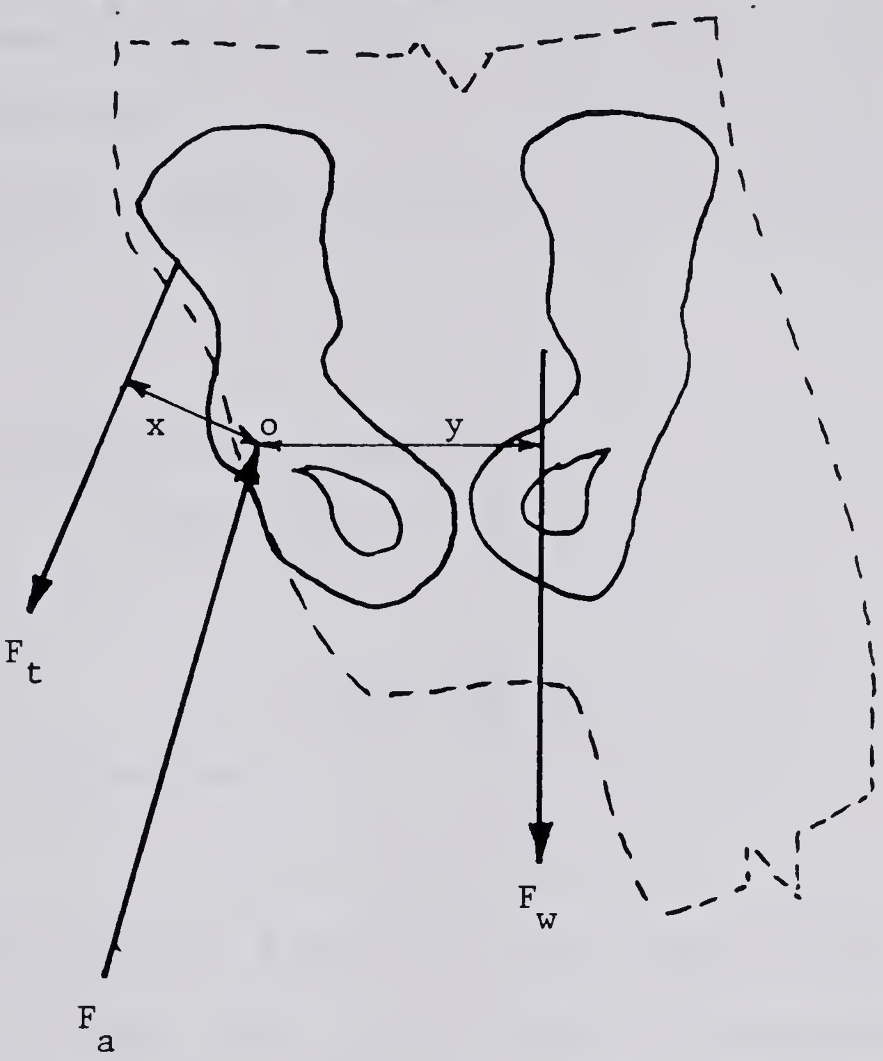

Free Body Diagram of the Body Above One Hip Joint

Figure 12

F_t = the force of the abductor muscles on the pelvis.

F_a = the force of the head of stem on the acetabulum.

F_w = the force due to the body weight, excluding one leg.

F_w was taken as 3.5(0.86W). The body weight used for medium and large stems was taken as 784 N, and for small stems 468 N, corresponding to body masses of 80 kg and 47.8 kg respectively.

x = the distance from the center of the head of the stem to

the line of action of the abductor muscle force. This distance, measured in millimeters, varies with each stem and was measured using a template of one of the femurs. This is described in detail in the Appendix.

y = the distance from the head of the stem to the line of action of the weight (F_W). The value of 'y' used in this study was 148 mm, calculated using a 'y' of 127 mm for two legged stance.

Summing the moments about point O:

$$3.5(0.86W)y - F_t * x = 0$$

Hence:

$$F_t = 3.5(0.86W)y / x \qquad (1)$$

Substituting the value of 'y' into (1):

$$F_t = 446 * W / x \qquad (2)$$

Referring back to Figure 7, the forces acting on the femur are now known. That is, the pull of the abductor muscles is F_t and varies with each stem, while the knee force is approximately 3.5 times the weight of the body not including the leg below the knee, or about 3.3 W. The total stresses in the stem will be those caused by the knee force plus those caused by the abductor muscle force.

The knee force was duplicated in the loading of each stem, as will be described later. The method by which the effect of trochanter loading on stem strain was measured is detailed in the section entitled 'Loading the Greater Trochanter'. An 'effective knee joint force' was arrived at

by adding the effect of the trochanter load on the stem stress to the knee force. This allowed measurement of the maximum strains that could occur in the stem to be made by loading only the knee joint and the head of the stem. This is detailed in the section entitled 'Effective Knee Joint Force'.

Stem-Aluminum Tube Apparatus

To duplicate the stem support conditions provided by the upper half of the femur, the stems were cemented into aluminum tubes. Each tube was 25.4 mm in diameter, 205 mm long, and had a 1.47 mm (0.058 inch) wall thickness (as manufactured). The lower 140 mm of the tube was straight, with the upper 65 mm bent uniformly to a 'stem neck' angle of approximately 126 degrees. The cement used was surgical methylmethacrylate, 'Simplex-P'. This stem-tube combination can be seen in Figure 13. The lower end of the stem was centered using a methylmethacrylate plug, with a cone machined into one end of it, as a guide.

The necessary dimensional characteristics of the lower part of the femur were obtained by securing the lower end of the aluminum tube in a holder, as seen in Figure 14. The knee joint was approximated by a ball joint, at the bottom of the device. The 10 mm offset at the midpoint of the femur was duplicated by offsetting the ball joint, towards the rear a distance of 20 mm. The total length of the apparatus was 390 mm, measured from the ball joint on the bottom to the point 'A', as seen in Figure 14. The point 'A' is comparable to the bottom of the neck of the femur. The complete apparatus is shown in Plate 8.

The bar on the lower half of the apparatus allowed

the ball joint to be moved, relative to the lower end of the holder. This allowed duplication of the support conditions that would occur when a stem is used in a patient who is either knock-kneed or bow-legged. These configurations are shown in Plates 9 and 10.

The ball at the bottom end of the apparatus was held in position, directly under the stem head, with a socket that had been machined into a steel plate. The steel plate was secured to the bottom of the testing machine.

Force was applied to the head of the prosthesis through an acetabular cup cemented into a steel fixture. The cup was mounted at a 45 degree angle to the vertical. This is the normal angle of installation of this component at the University Hospital, and falls within the normal physiological range of 24 to 48 degrees [13]. The steel fixture was bolted to the upper head of the testing machine.

The testing machine used for all static loading was the Instron TT-K Universal Testing Machine. This is a hydraulicably powered machine with a bearing screw crosshead drive.

---

[13] Stulberg, David and Harris, William H.; Acetabular Dysplasia and Developement of Osteoarthritis of the Hip, The Hip, The C.V. Mosby Company, 1974, pg.82-91.

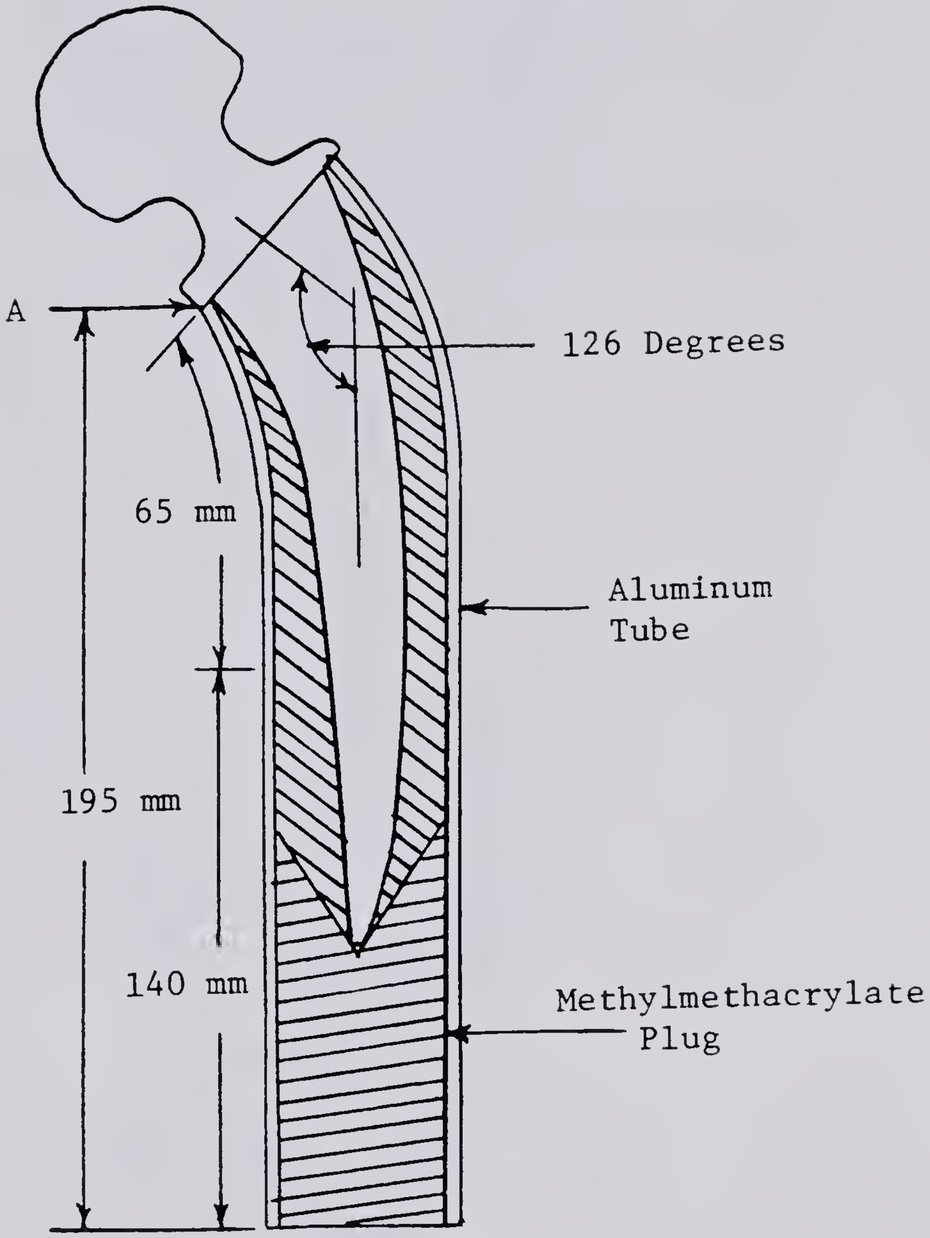

Tube-Mounted Stem

Figure 13

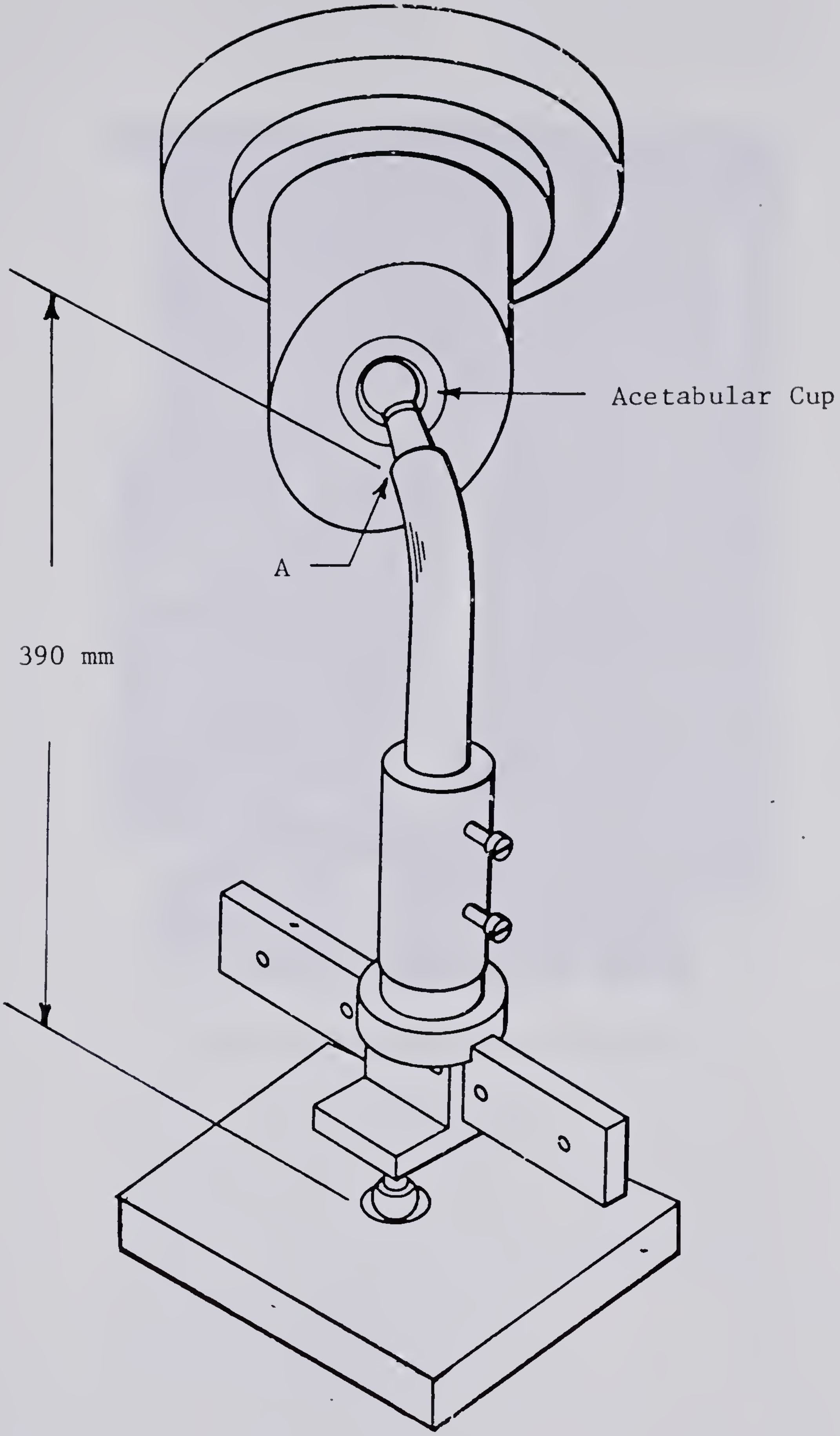

Complete Stem-Tube Apparatus

Figure 14

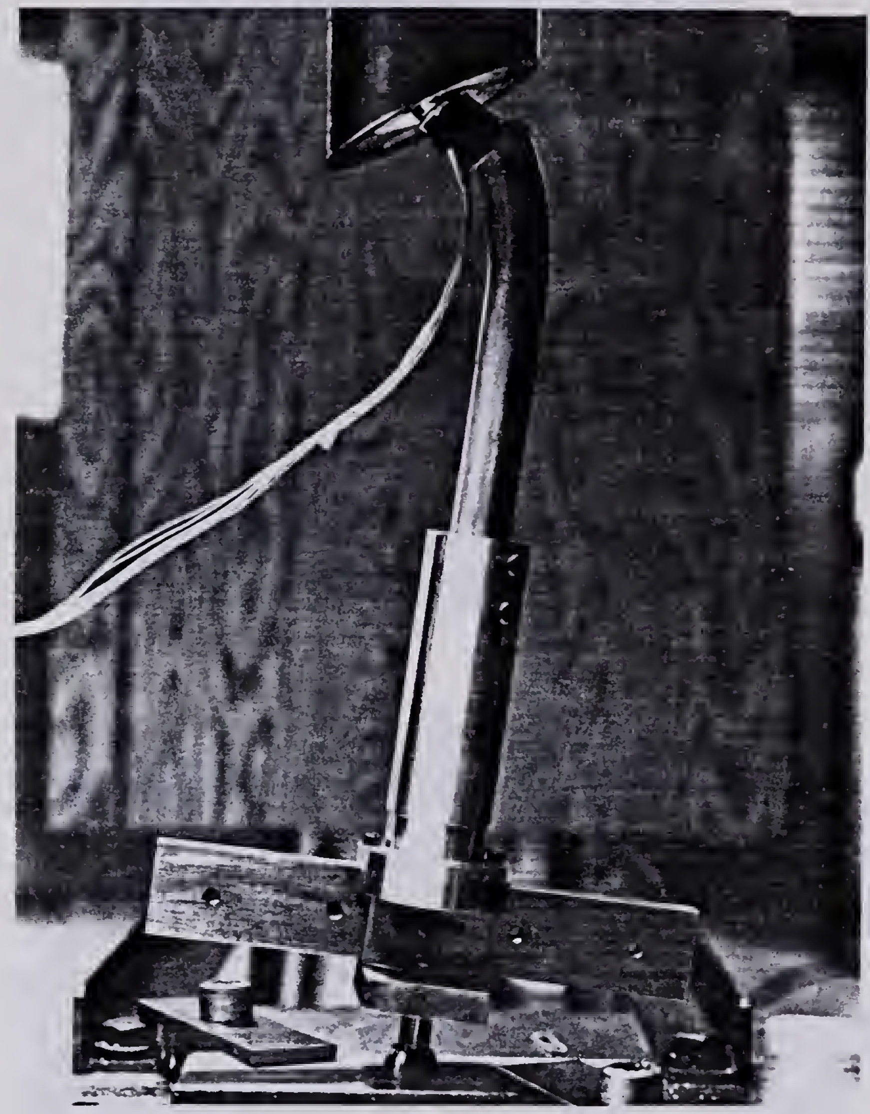

Stem-Tube-Instron Apparatus

Plate 8

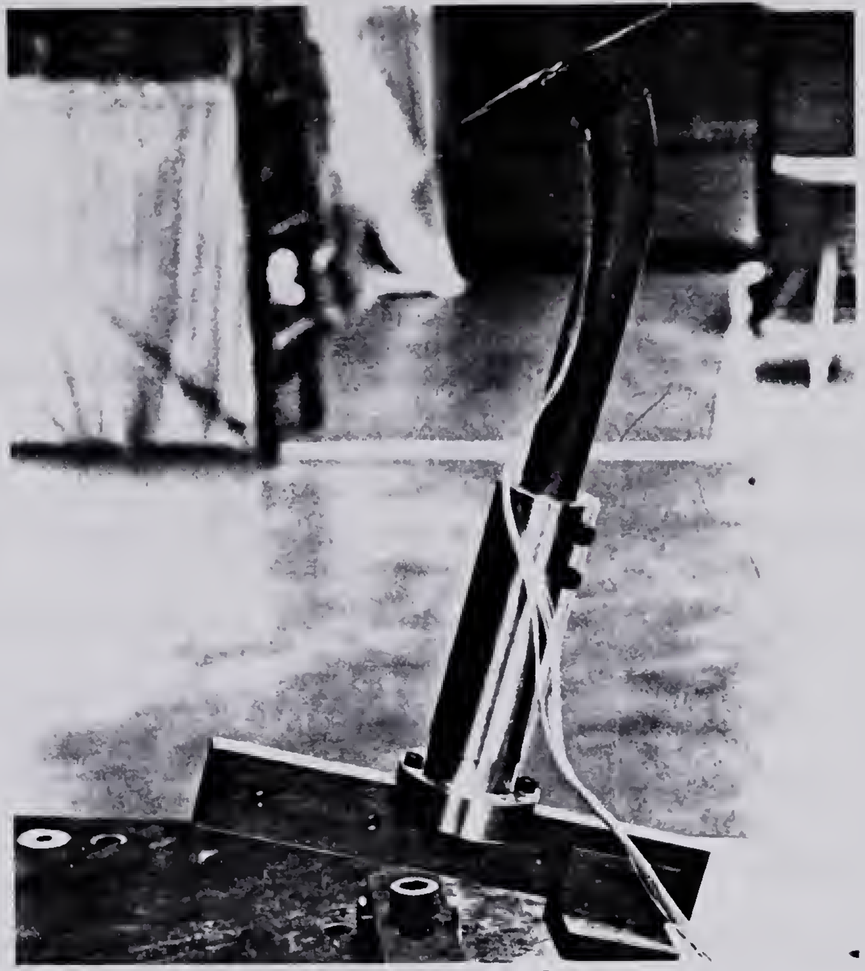

Knock-Knee Simulation

Plate 9

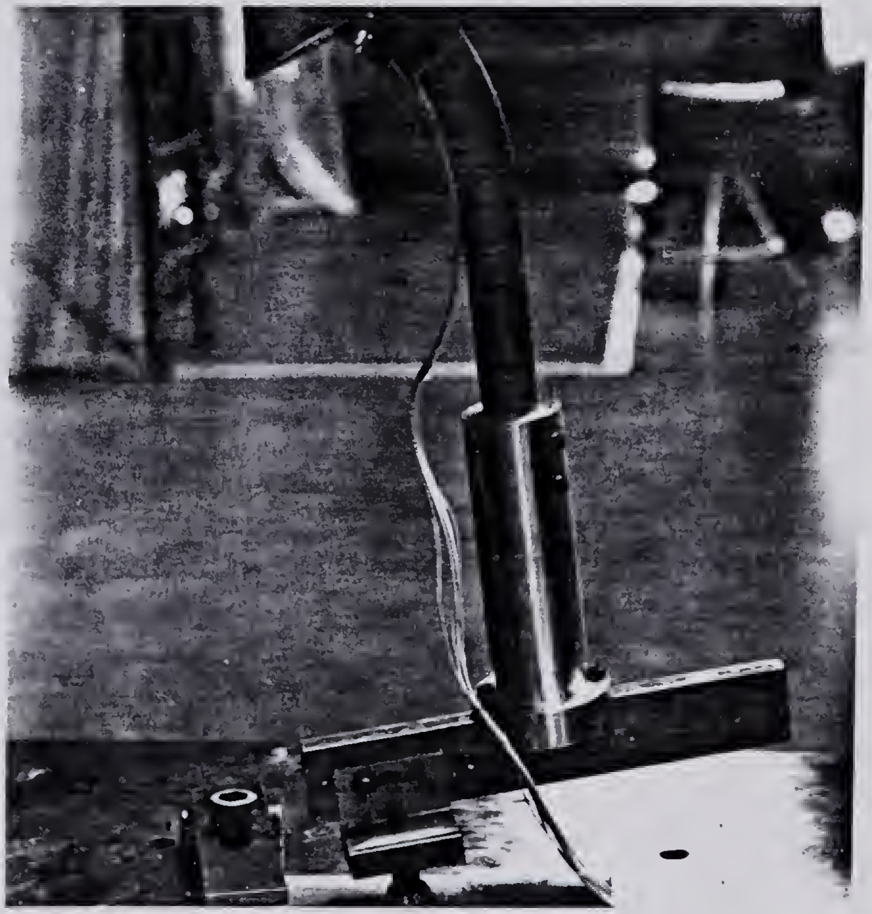

Bowlegged Simulation

Plate 10

Stem-Femur Loading Apparatus

To determine whether the flexural support conditions provided by the aluminum tube duplicated those of the femur, it was deemed necessary to mount and test several stems in femurs. It was also considered necessary to determine the stem stress caused by the abductor muscle force exerted on the greater trochanter, as shown in Figure 7. This was accomplished by testing the stems fixed in the upper end of human femurs, in place of the tube in the mounting and loading apparatus.

To determine the effect of the abductor muscle force, the cable loading device shown in Figure 15 was used. As can be seen, the same holder which was used with the aluminum tube was also used to hold the femur. The abductor muscle pull was simulated by applying a force, by means of a cable, to a trunnion fixed to the greater trochanter. The strain gage wires and terminal box are also shown in this figure. A femur mounted stem is shown in Plate 11.

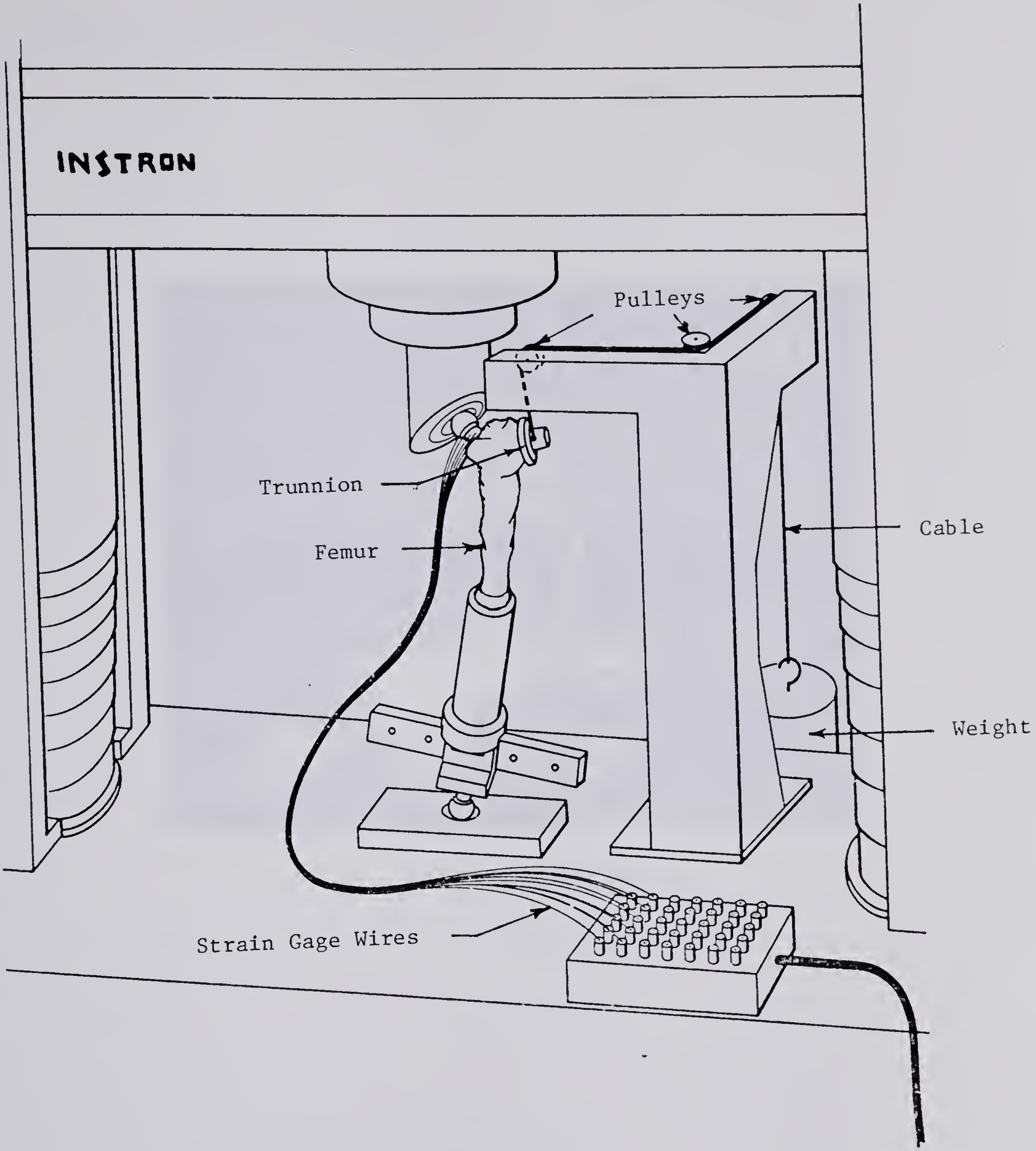

Femur Loading Apparatus

Figure 15

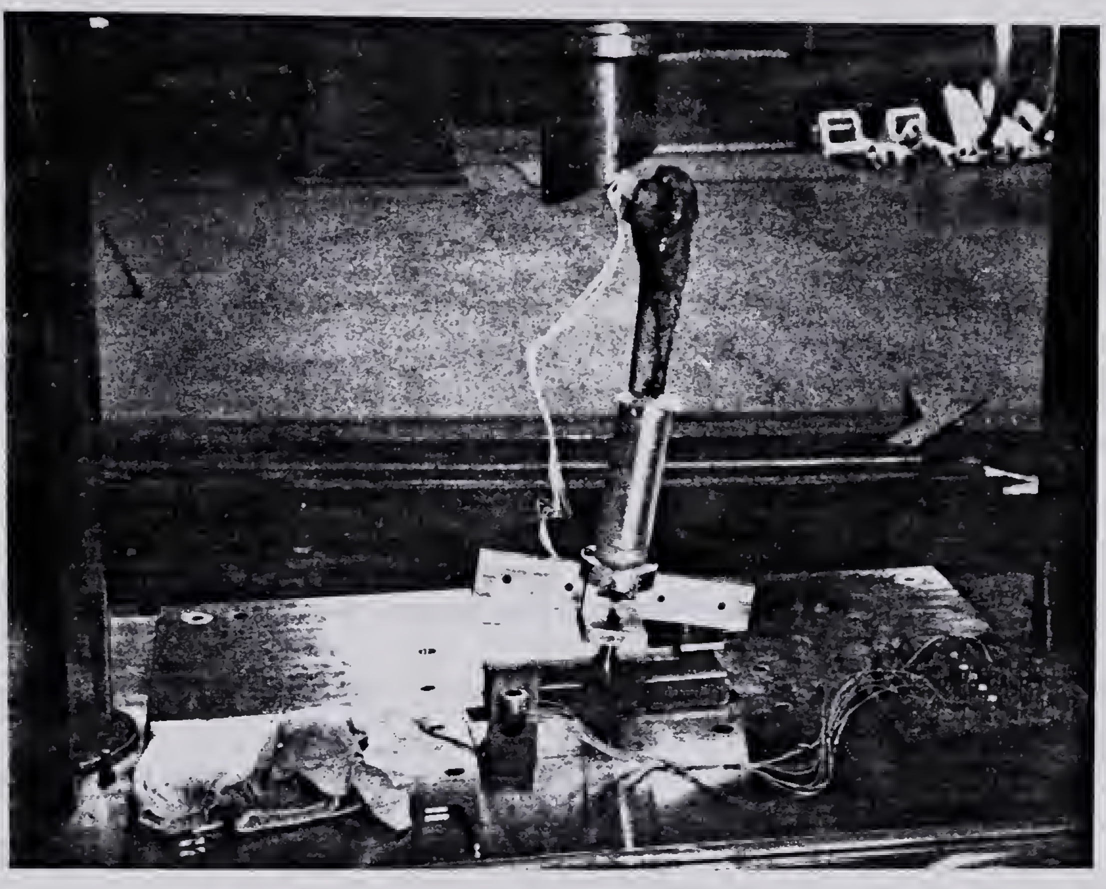

Femur Mounted Stem

Plate 11

[illegible]

Fatigue Loading Apparatus

Specimens

The fatigue testing of specimens was carried out on a Vibrophore high frequency testing machine. This is shown in Plate 12. Up to 166 load cycles per second were attainable using this machine.

Stems

In addition to testing the properties of the materials themselves, a number of fatigue tests were carried out on the complete tube-mounted stems. No attempt was made to fatigue test the stems mounted in femurs, since it was assumed that the endurance limit of a cadaver femur would be very low.

The testing was done using the apparatus shown in Figure 16. The stems were cemented into tubes that were identical to those used for the static tests. The bottom half of the apparatus was simpler, in that the bar, for knee position variation, was not included. The overall dimensions were the same as those used earlier. That is, the length from point 'A' to the bottom of the device was 390 mm, and the offset at the middle of the device was 10 mm.

The acetabular cup fixture was bolted to the upper

head of an MTS Load Frame. The ball at the bottom end sat in a socket machined into a plate. The plate was attached to the MTS Load Frame piston. The MTS testing machine was run in conjunction with a Univeral Testing Systems Controller and the loading rate was 24 cycles per second. The complete unit is shown in Plate 13.

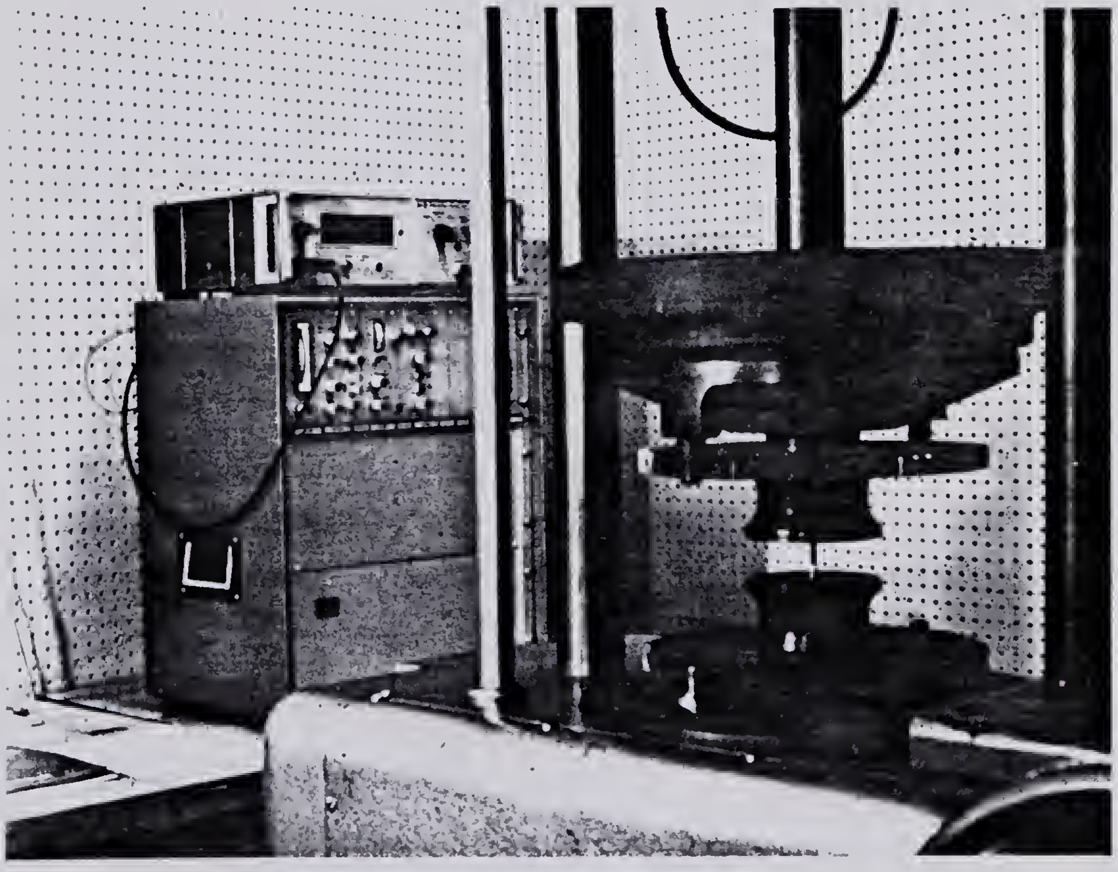

Vibrophore Testing Machine

Plate 12

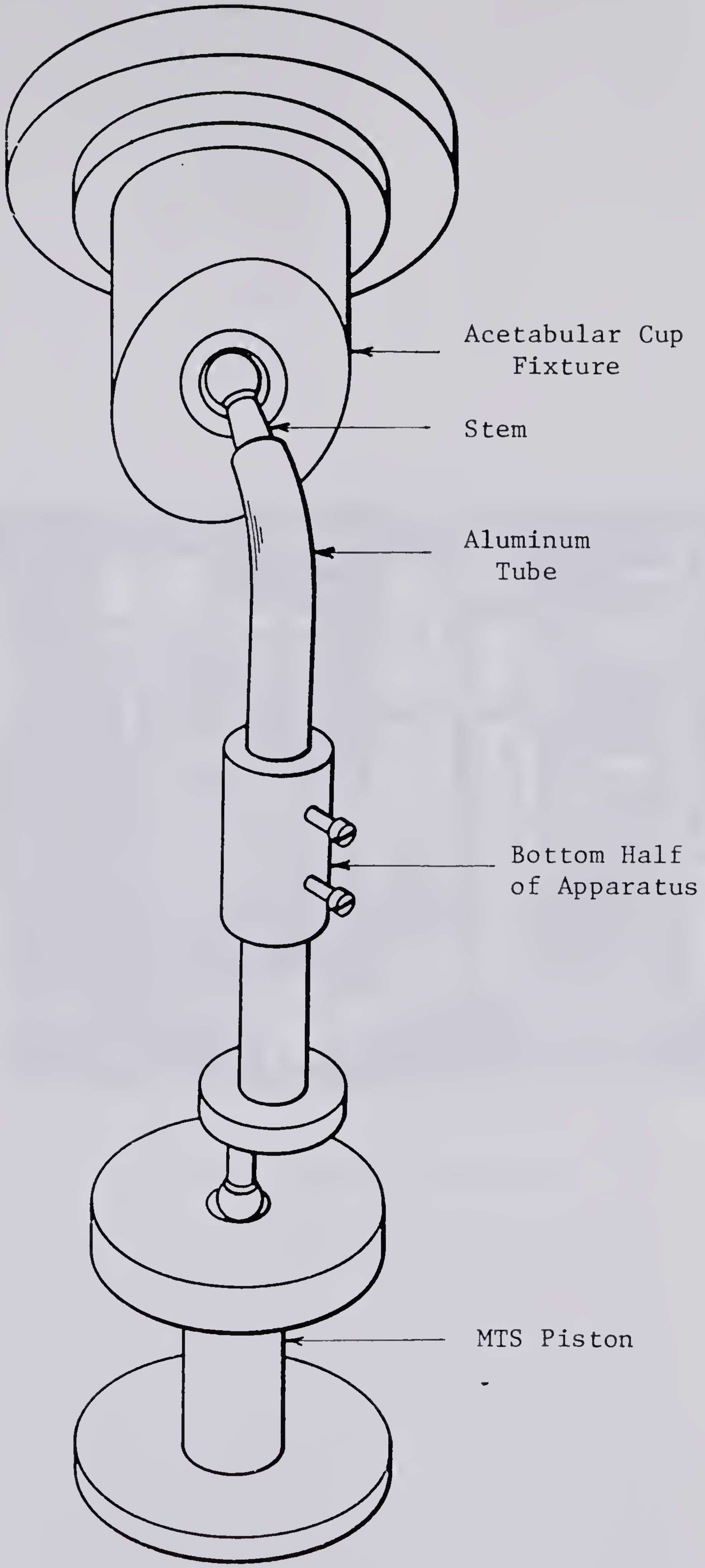

Stem-Tube Fatigue Apparatus

Figure 16

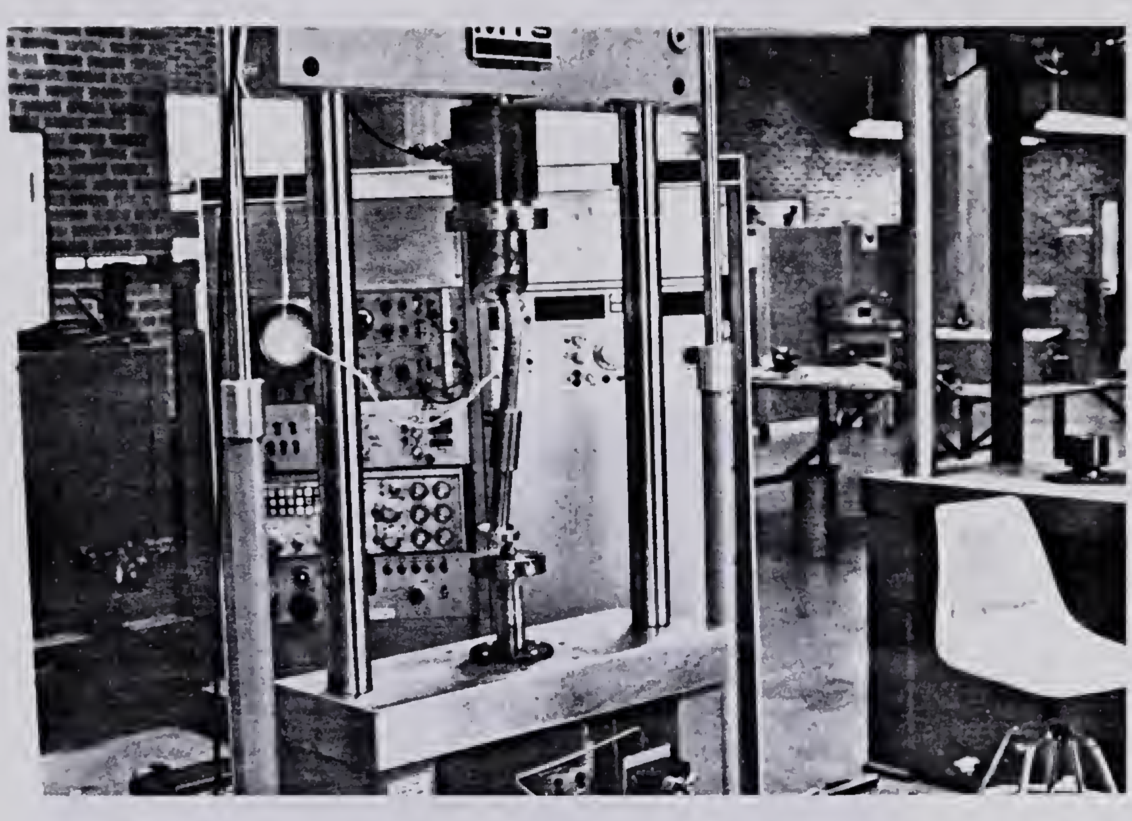

MTS Testing Machine

Plate 13

[illegible]

[illegible]

Charpy V Notch Testing Apparatus

Charpy V notch specimens were tested in the Tinius Olsen machine shown in Plate 14. Fatigue cracking of the hot isostatically pressed cobalt-chrome Charpy specimens was carried out on the apparatus shown in Plate 15. This apparatus was mounted in the MTS fatigue machine mentioned previously.

Tinius Olsen Impact Machine

Plate 14

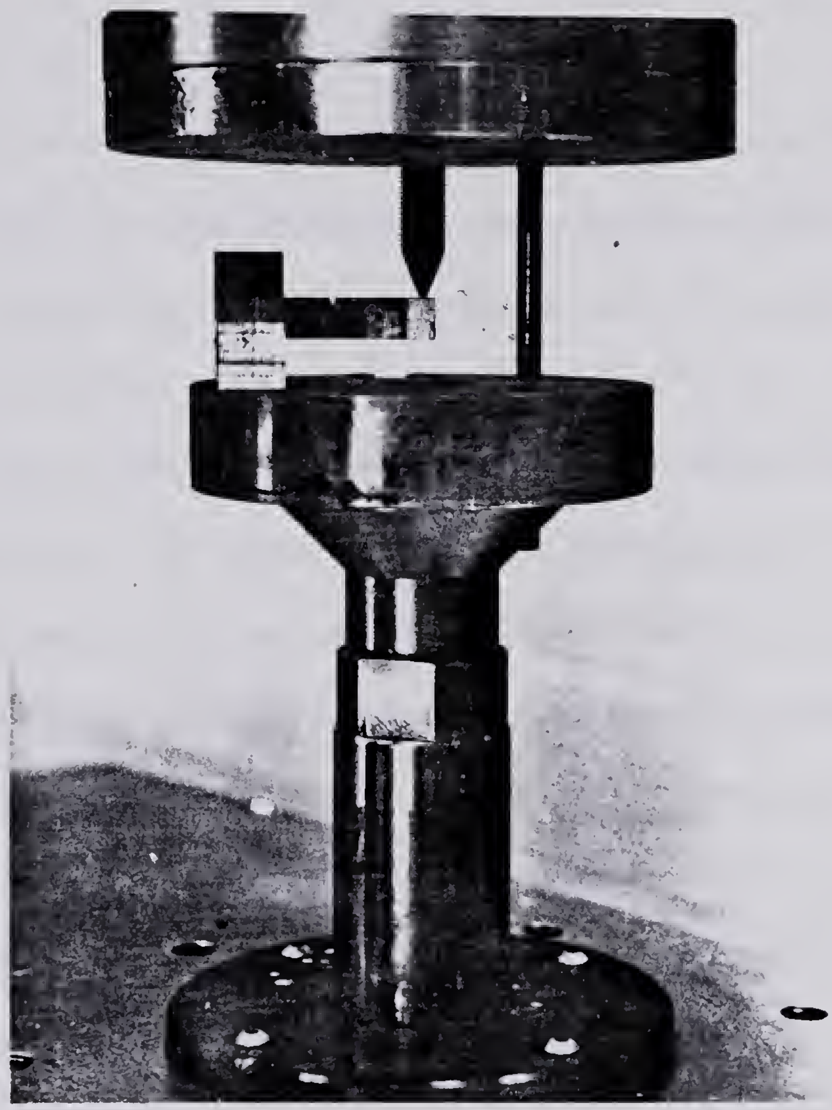

Charpy Specimen Fatigue Apparatus

Plate 15

C. Testing Method

Strain Measurement in Tube Mounted Stems

Mounting the Stems in Tubes

Most of the stems were positioned, in the aluminum tubes, using a jig designed for that purpose. Using this method, however, the positioning of the stems could not be checked until they were cut out of the tube and cement, and some of them were incorrectly mounted. A better method for centering the distal end of the stem, using the machined plug shown in Figure 13, was developed near the end of the testing program.

Cementing of the stems in the tubes, using the machined plug, was relatively simple. The machined plug was first inserted into the bottom end of the tube. Methylmethacrylate was mixed, in the bag, kneaded until it had reached the proper consistency, then inserted into the upper end of the tube. The stem was pushed into the upper end of the tube, displacing excess cement. Excessive heating of the tube, due to the exothermic cement polimerization reaction, was prevented by wrapping it with a water soaked rag. The cement was allowed to set for at least 24 hours prior to loading.

Loading the Tube-Mounted Stem

Before loading the stem-tube combination, the Instron testing machine was calibrated with a proving ring (400 lb. Moorehouse #4005). The acetabular cup was then aligned with the socket in the bottom plate of the loading device. The stem to be tested was mounted in the apparatus, as shown earlier in Figure 14, and placed between the Instron crossheads. This was done with the ball joint at the bottom in the 'normal knee' position. A tube mounted stem was shown in Plate 8.

The stem was repeatedly loaded up to 1 kN then unloaded, a total of 20 times, to eliminate any initial wear-in effects. After the wear-in loading runs, the gages were balanced on the digital strain indicator and the appropriate gage factor dialed in. One kN was applied to the ball of the stem and the resulting strains were recorded. The load was removed and the gages rebalanced. This was repeated twice.

After the three 'normal knee' position runs were completed the loading device was removed from the Instron and the ball position was changed to simulate knock-knee type loading. The previous procedure was repeated and the strains recorded. This loading setup was shown in Plate 10.

The experiment was repeated a third time with the ball in the position simulating the bow-legged support condition. This was shown in Plate 11.

Precision of Results

To ensure that the aluminum tube mounting method produced repeatable results, five stems were each mounted and loaded in several tubes. It was assumed that if a stem mounted and tested in one tube produced similar results to the same stem mounted and tested in a different tube, then the results could be repeated by others, provided similar methods and apparatus are used. As will be shown later, this testing method proved to be quite repeatable.

Strain Measurement in Femur-Mounted Stems

Mounting the Stems in Femurs

To prevent degradation, the femurs were kept cool and moist at all times with a solution of mercuric cyanide, and were used as soon as possible. The stems were inserted into the femurs in the manner described below, following the surgical procedure used in operating rooms as closely as possible. First, the head and neck of the femur were removed at the appropriate angle using a band saw. The femur was then shortened to the same length as the aluminum tubes, 195 mm, by removing some of the distal end. The medullary canal was rasped out using a standard surgical rasp, then cleaned of any debris. After the proper fit had been verified by a trial insertion of the instrumented stem the cement

was prepared. Packing of the cement into the medullary canal was followed by insertion of the stem. Proper positioning was verified by x-raying the femur.

Loading the Femur-Mounted Stems

The femur-mounted stems were loaded in exactly the same manner as the tube-mounted stems. It should be noted, however, that while the tubes could be secured in the bottom half of the apparatus with screws, it was necessary to cement the femurs in.

Loading the Greater Trochanter

In order to simulate the pull of the abductor muscles on the greater trochanter a trunnion was attached to it. This was done by hollowing out the weak spongy bone in the greater trochanter region and replacing it with methylmethacrylate. The methylmethacrylate acted as an anchor, which could be drilled and tapped. The trunnion was then screwed to this anchor.

With the stem-femur-holder positioned between the Instron crossheads, as shown in Plate 16, the greater trochanter load was applied. For this test, the Instron testing machine was used simply to support the stem-femur-holder, and no additional load was applied.

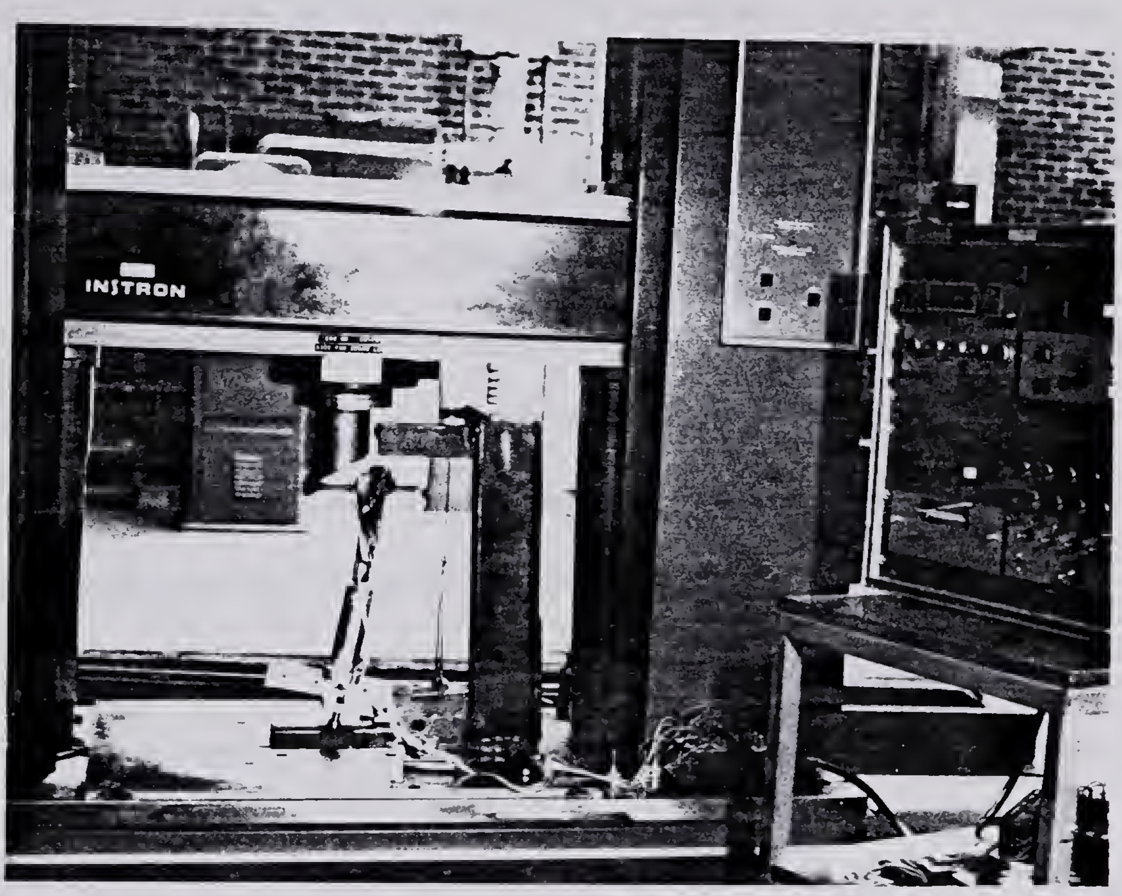

Greater Trochanter Loading

Plate 16

Specimen Fatigue Testing Method

An estimate of the endurance limit of the material being tested was first arrived at using the Goodman Diagram approach mentioned earlier. To do this, in some cases it was necessary to establish the yield strength of the material experimentally; the standard 0.2% offset yield stress was used. This was measured by instrumenting a specimen with two strain gages mounted on opposite sides of the specimen. Two gages were necessary to balance out possible bending stresses. The specimen was then axially loaded in tension and strain readings were taken at appropriate load intervals. The specimen was loaded to failure and the necessary properties calculated.

With the endurance limit estimate, the specimens could be tested. The specimens were mounted in the high frequency testing machine and the machine was adjusted to apply a mean load necessary to produce a stress of one half the estimated endurance limit. The variable load was adjusted to the same value, for an R = 0 ratio.

If the specimen failed before 10 million load cycles had been applied the stress level was decreased and the procedure repeated. This was continued until 10 million load cycles were reached. If the specimen, on the other hand, did not fail, a new specimen was used, the load level increased, and the procedure repeated. This was repeated until a failure occurred. When sufficient specimens were available

they were tested at the newly established endurance limit.

Stem Fatigue Testing Method

Fatigue testing of the stems was done at a load that the stem could be subjected to in vivo. The cyclic loads applied to the stems were usually 3.43 kN for the small stems and 5.49 kN for the remainder of the stems.

The stem-tube configurations cycled at the higher load only lasted for relatively few cycles before failure occurred in the aluminum tube. The failure, in general, was characterized by a split in the aluminum tube just under the neck of the stem, point 'A' as shown in Figure 13.

The configurations cycled at lower loads lasted considerably longer, about three million cycles. To reach the 10 million cycle limit the stems, subjected to the lower loads, were reimplanted into tubes several times. This procedure was not practical for the large stems, as it would have required replacing the aluminum tubes many times.

Fracture Toughness Testing Method

As described in the introduction, fracture toughness values were not measured directly, but were estimated from the results of Charpy tests carried out on a Tinius Olsen impact machine. ASTM specification E23-72 for this procedure was followed. The specimens were immersed in water at 37 degrees Centigrade for approximately 10 minutes prior to testing. They were removed from the water, positioned in the

Tinius Olsen, and tested within 5 seconds.

Two of the hot isostatically pressed cobalt-chrome Charpy specimens, as mentioned previously, were pre-cracked before testing. This was carried cut in the apparatus shown earlier in Plate 15. A cyclic load, sufficient to produce a nominal tensile stress of 50% of the yield stress at the notch tip was applied to the specimen. Approximately 21,000 load cycles were necessary to generate a fatigue crack for each of the two specimens.

Improper Stem Positioning

Stem Positioning in the Tube

Stem #23, as mentioned in the Introduction, was mounted in four different tubes, in three different positions. The malpositioned stems were loaded in the same manner as the other stems and the strains were recorded.

Knee Position

The effects of knee position on stem stress was investigated by varying the position of the ball joint at the bottom of the apparatus as described earlier. For this measurement, the ball joint position was moved 100 mm either medially or laterally.

III. Results

The strain gage data presented are the average of measurements taken while the stems were loaded at 1 kN three separate times. The variance in the strains was in the order of a few micro m/m and is not presented separately.

Strain Gage Data for Tube-Mounted Stems

Table 3 presents the five strain measurements from the lateral face of the stem for five selected stems. In the case of stems #4, #9, and #16 the measurements are the average of those taken from four, two, and two separate implantations respectively.

Table 3

Lateral Face Strains Measured on Tube Mounted Stems at 1 kN Load

Stem	Gage Position (mm), Strain (micro m/m)				
No.	20	40	60	80	100
4	253	497	585	669	326
9	179	340	445	476	-
12	243	320	338	329	319
16	118	271	338	315	149
18	395	589	615	530	417

Table 4 lists the average maximum strains measured on each tube-mounted stem. The entire set of strain measurements is listed in the Appendix. The position of the stem, if not on the centerline, is noted in the table. The term 'valgus', when applied to the positioning of the stem, was defined in the Introduction, and is shown in Figure 4.

Table 4

<u>Lateral Face Maximum</u>

<u>Strain Measurements at 1kN Load</u>

Stem No.	Max. Strain (micro m/m)	Gage Position (mm)	Stem Position
5-s	538	60	
6-s	557	80	
7-s	953	80	
19-s	598	69	slight valgus
1	496	80	
2	417	80	
4	669	80	
8	446	80	
9	476	80	
10	656	80	
11	560	80	valgus
12	338	60	
13	342	60	
14	248	60	valgus
15	276	60	valgus
16	338	60	
17	606	60	
18	615	60	
20	383	80	
21	343	60	valgus
22	328	60	valgus
23	539	60	
24	506	60	
25	274	60	

Table 5 presents the data obtained from the strain gages mounted on the front face of the stems. As noted earlier, the strain was caused partly by the axial force in the stem, and partly by the bending moment due to the fact that the applied force had a component out of the plane of the stem. In the case of stem #1, the compressive axial stress was greater than the tensile bending stress, hence a compressive strain was measured.

Table 5

Side Strains Measured on Four Stems at 1 kN Load

Stem	Gage Position (mm), Strain (micro m/m)		
No.	60	80	100
1	-75	-94	
4	55	76	
9	47	32	
11	47	54	40

Precision

Five stems were repeatedly mounted and loaded in different aluminum tubes to verify the precision of the testing method. The lateral face strains from stems #4, #16, and #23 are shown in Figures 17-19. Results from the remaining stems tested for repeatability have not been shown, since in each case two of the strain gages ceased to operate for part of the test. Similar precision, however, was observed in these two stems, with maximum strains, measured in stem #1 of 488 and 505 micro m/m, and in stem #9 of 493 and 459 micro m/m.

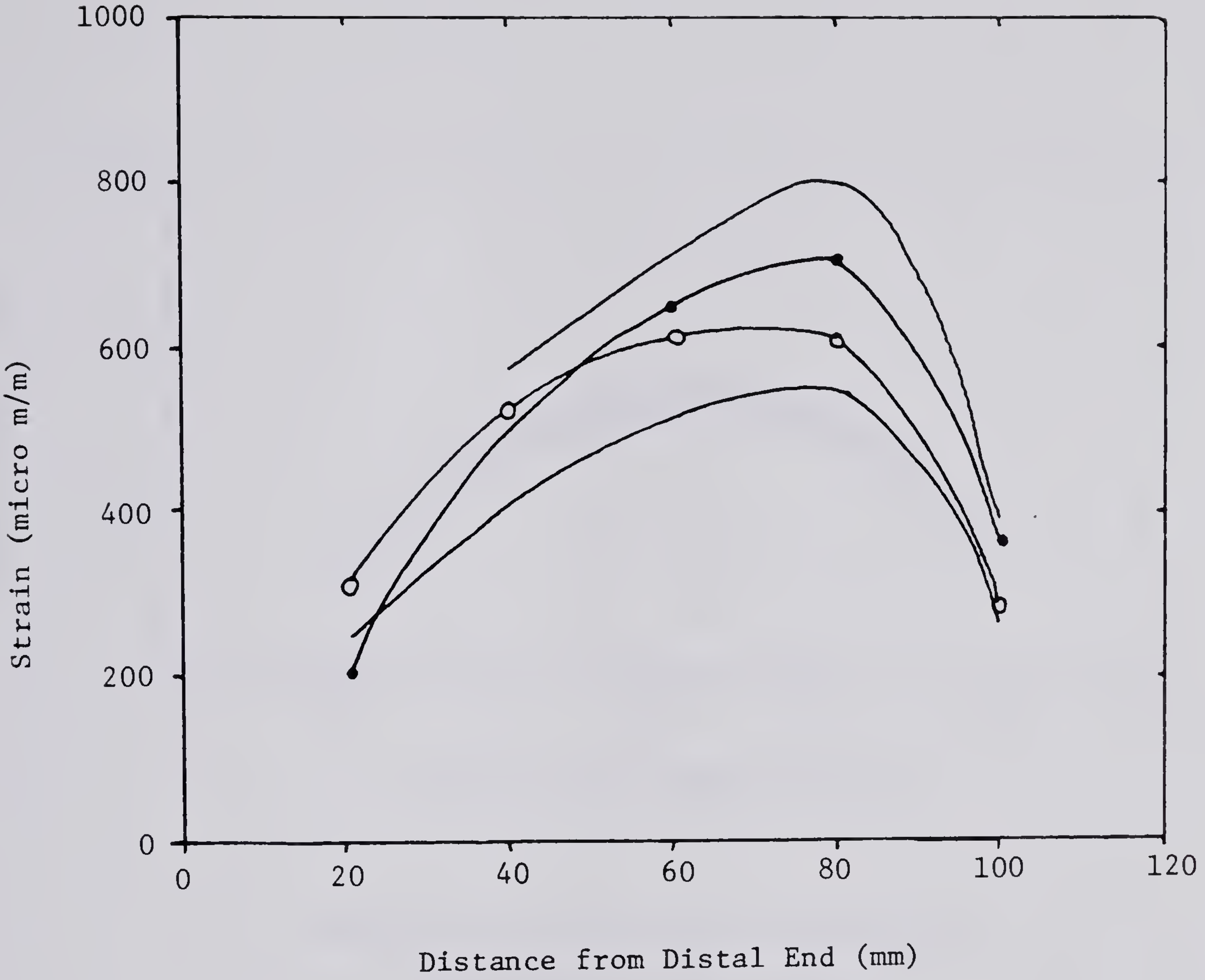

Lateral Face Strains Measured on Stem #4 in Four Tubes

Figure 17

[illegible]

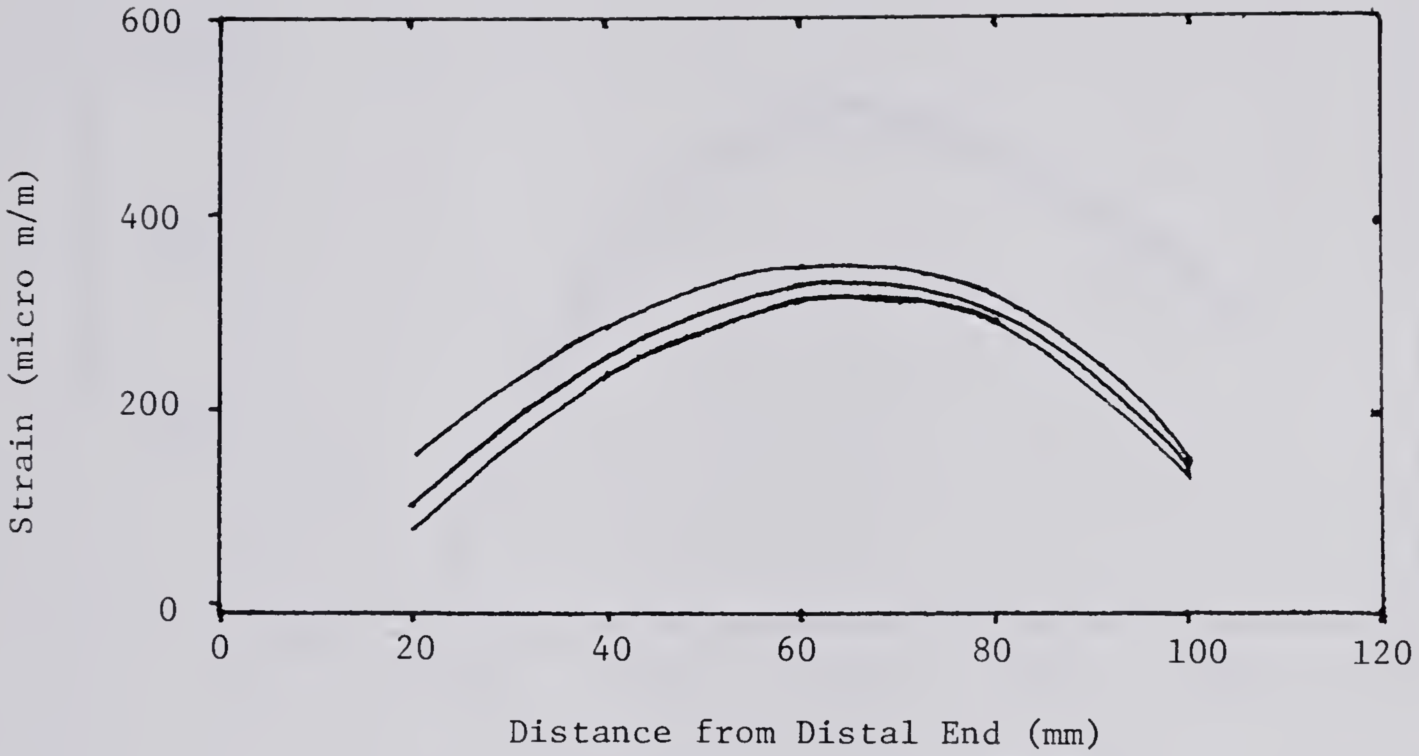

Lateral Face Strains Measured on

Stem #16 in Three Tubes

Figure 18

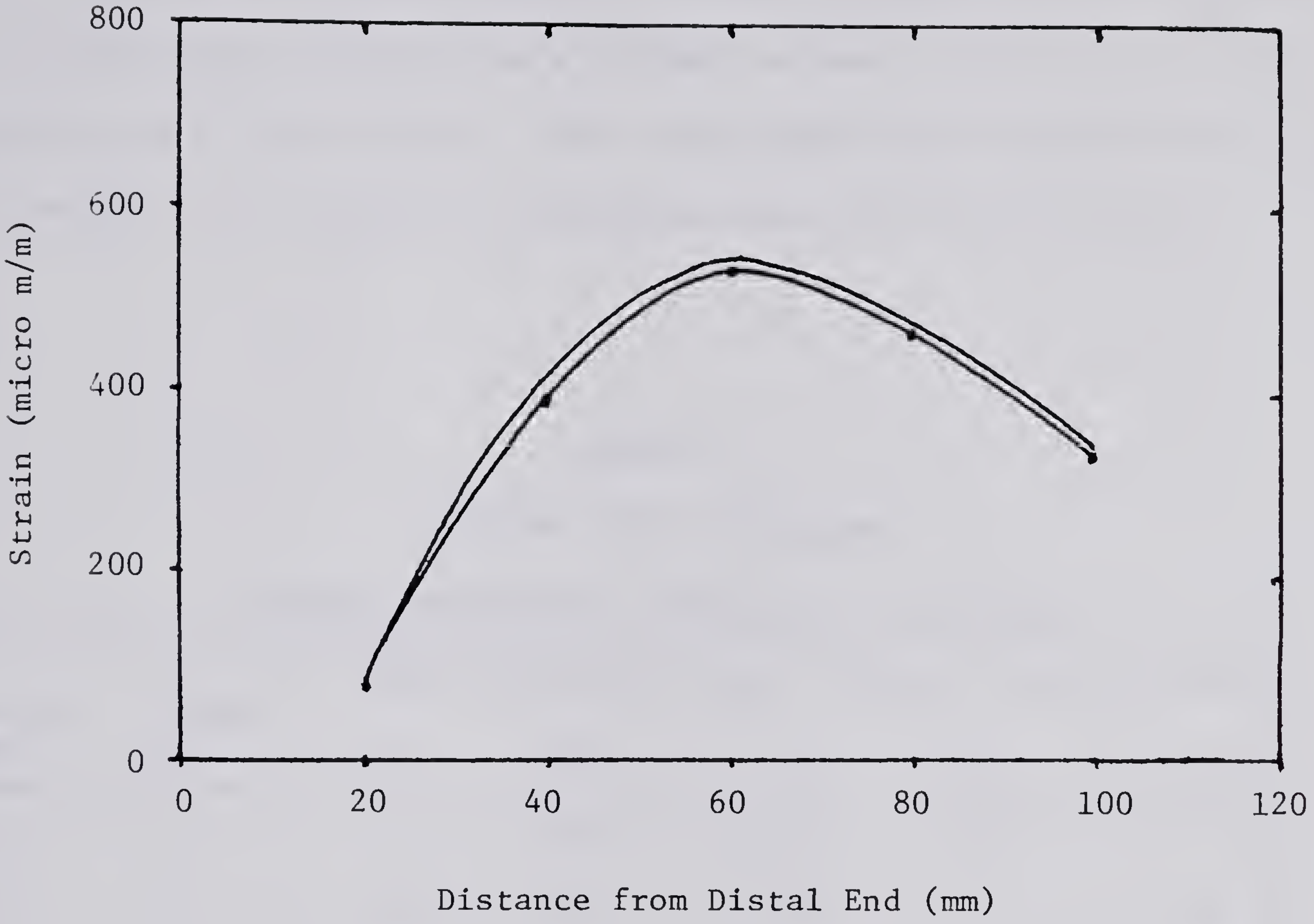

Lateral Face Strains Measured on

Stem #23 in Two Tubes

Figure 19

Strain Gage Data for Femur-Mounted Stems

Table 6 presents the data obtained from four stems mounted in five different femurs. No data was obtained from the first femur used because of strain gage failure. All of the stems were mounted in a slight valgus position. As the results will show later, this condition was expected to have the effect of slightly increasing the measured strain.

Table 6

Lateral Face Strains

on Femur-Mounted Stems at 1 kN Load

Stem No.	Femur No.	Gage Position (mm), Strain (micro m/m) 20	40	60	80	100
12	2	67	206	321	355	349
12	3	137	276	339	-	338
9	4	176	287	389	463	343
20	5	182	319	362	358	323
23	6	118	276	410	401	315

Comparison of Tube and Femur Results

In order to compare the strain measurements made on tube-mounted stems and femur-mounted stems, Figures 20-23 were prepared. They show the strains measured on the stem as a function of gage position. When more than one stem or femur was used for each stem the average strain readings were used.

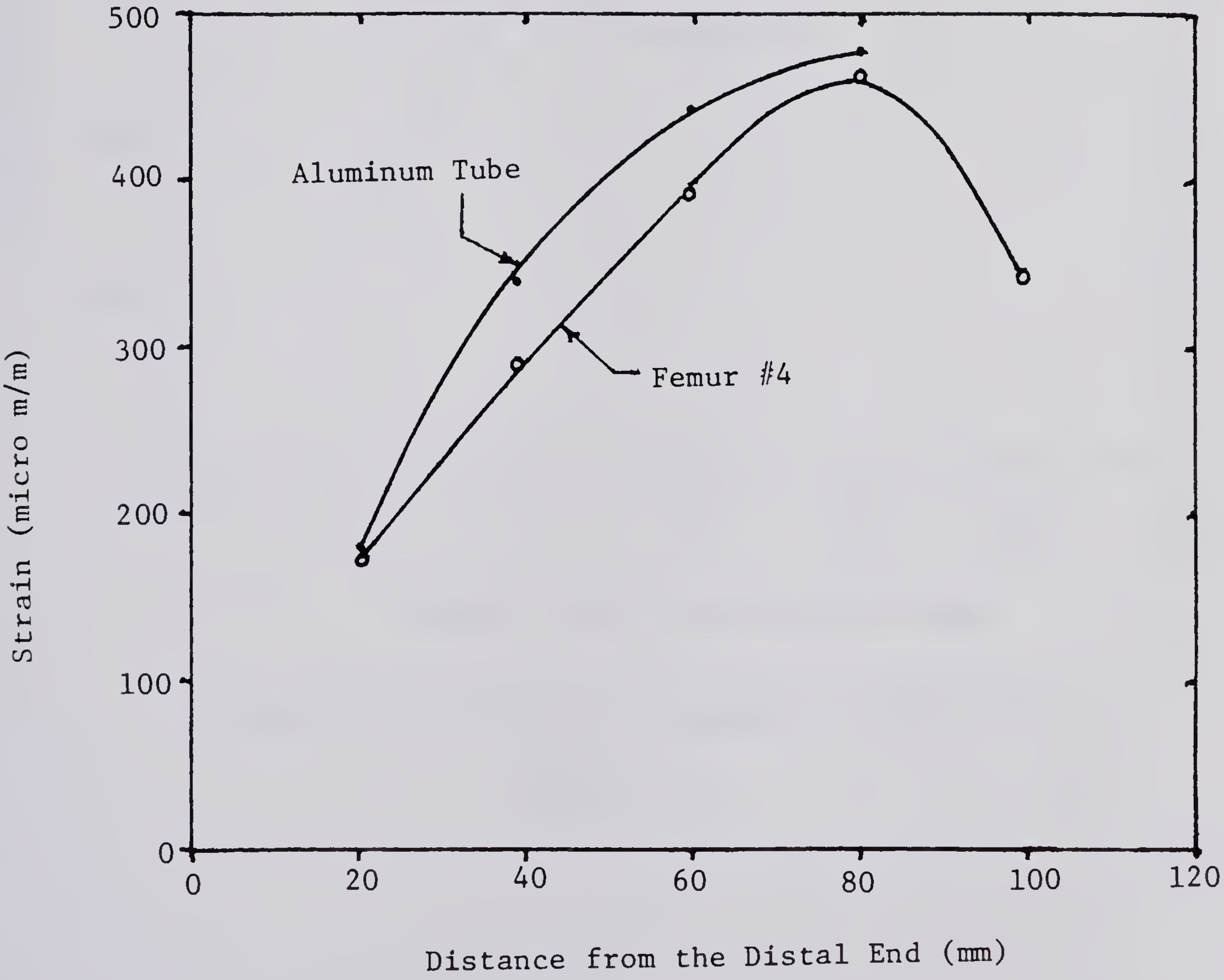

Lateral Face Strains Measured on Stem #9

Figure 20

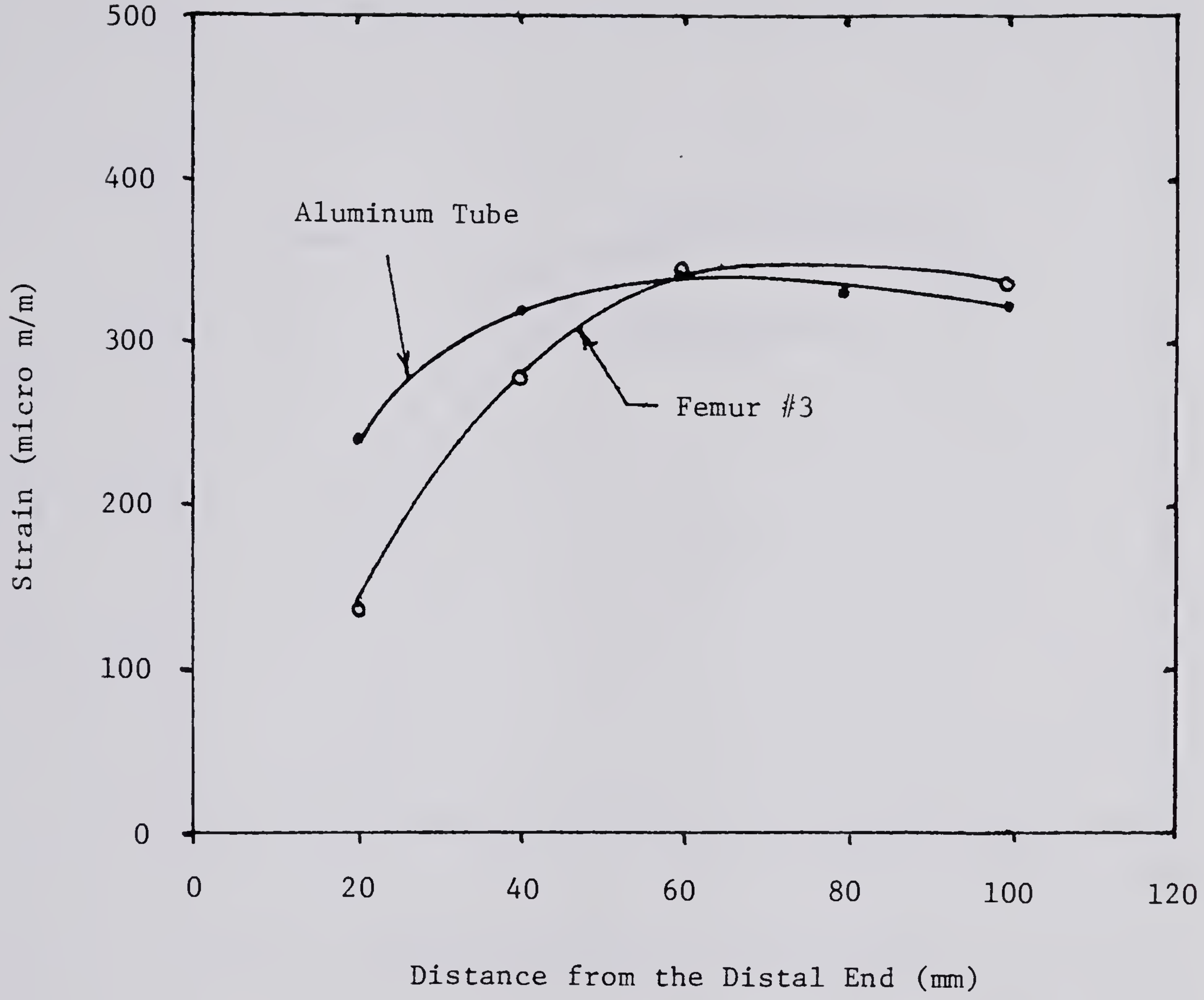

Lateral Face Strains Measured on Stem #12

Figure 21

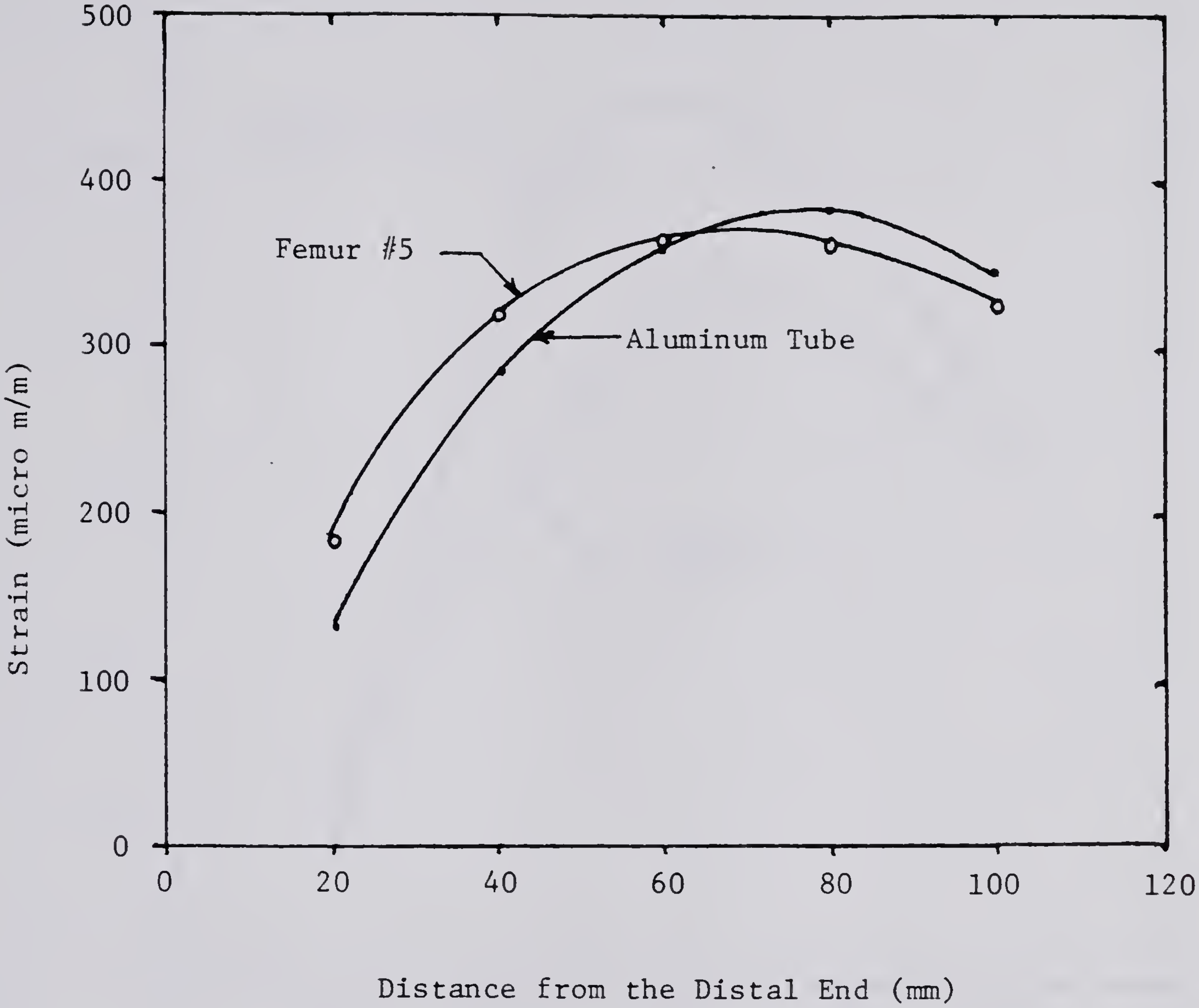

Lateral Face Strains Measured on Stem #20

Figure 22

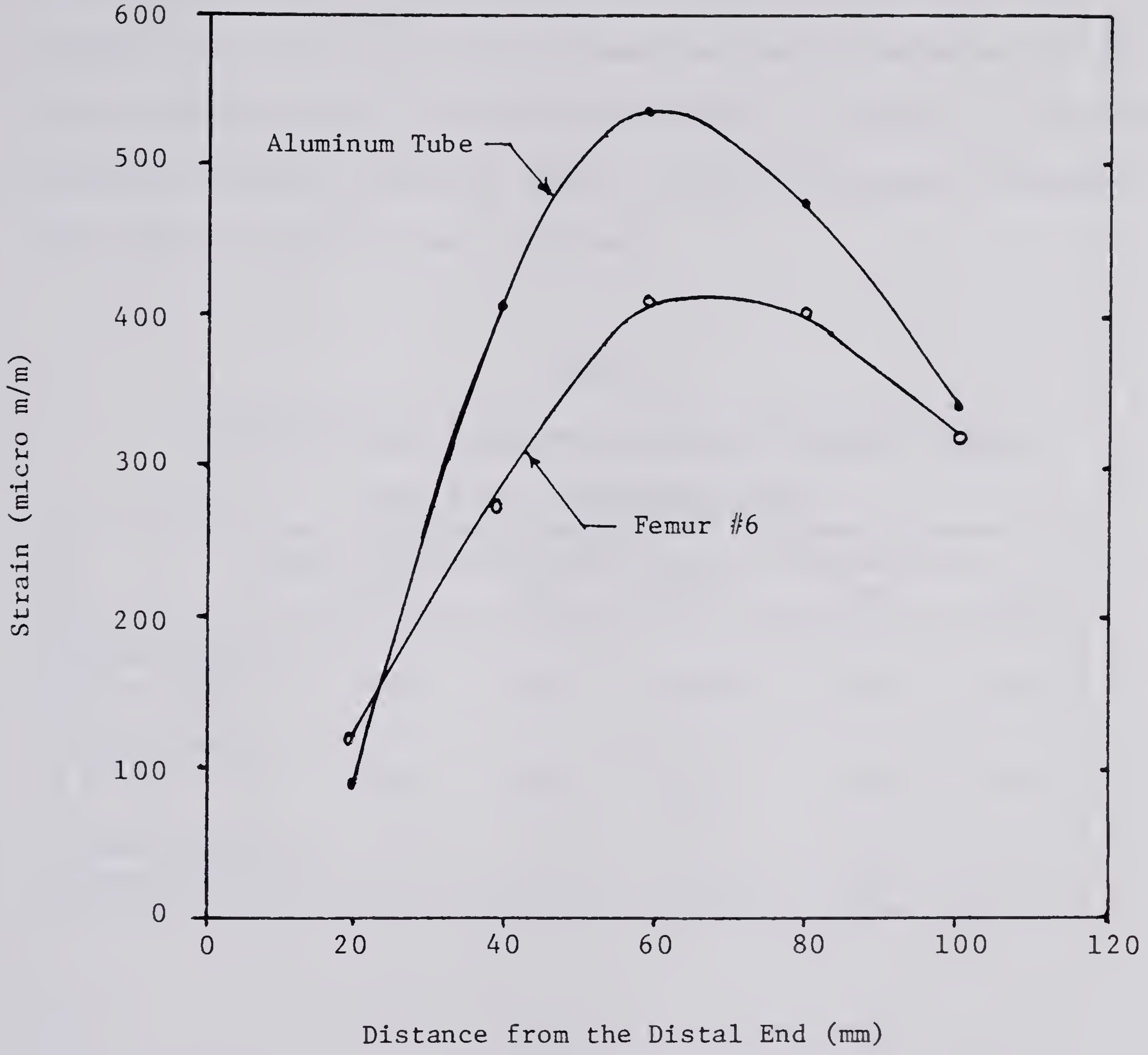

Lateral Face Strains Measured on Stem #23

Figure 23

Strains in Trochanter-Loaded Stems

Table 7 contains the strain measurements resulting from loading of the greater trochanter. All of the strains have been normalized to give the values that would have been measured at a load of 1 kN, assuming linear behavior. This was necessary since it was not possible to apply a 1 kN load using the method shown in Figure 15. The maximum trochanter load applied was in fact 0.69 kN.

Table 7

Lateral Face Strains on Femur Mounted Stems

at 1 kN Trochanter Load

	Gage Position (mm), Strain (micro m/m)				
	20	40	60	80	100
Stem #12 in Femur #3	124	191	180	180	152
Stem #9 in Femur #4	217	234	213	174	94
Stem #23 in Femur #6	79	171	182	132	71

Specimen Fatigue Data

The results of the fatigue tests for each of the metals tested are displayed in Figures 24-29. It should be noted that a dot on the diagram indicates the number of cycles at which a specimen failed at the indicated stress, while an dot with an arrow through it indicates that the specimen had not failed at the number of cycles shown.

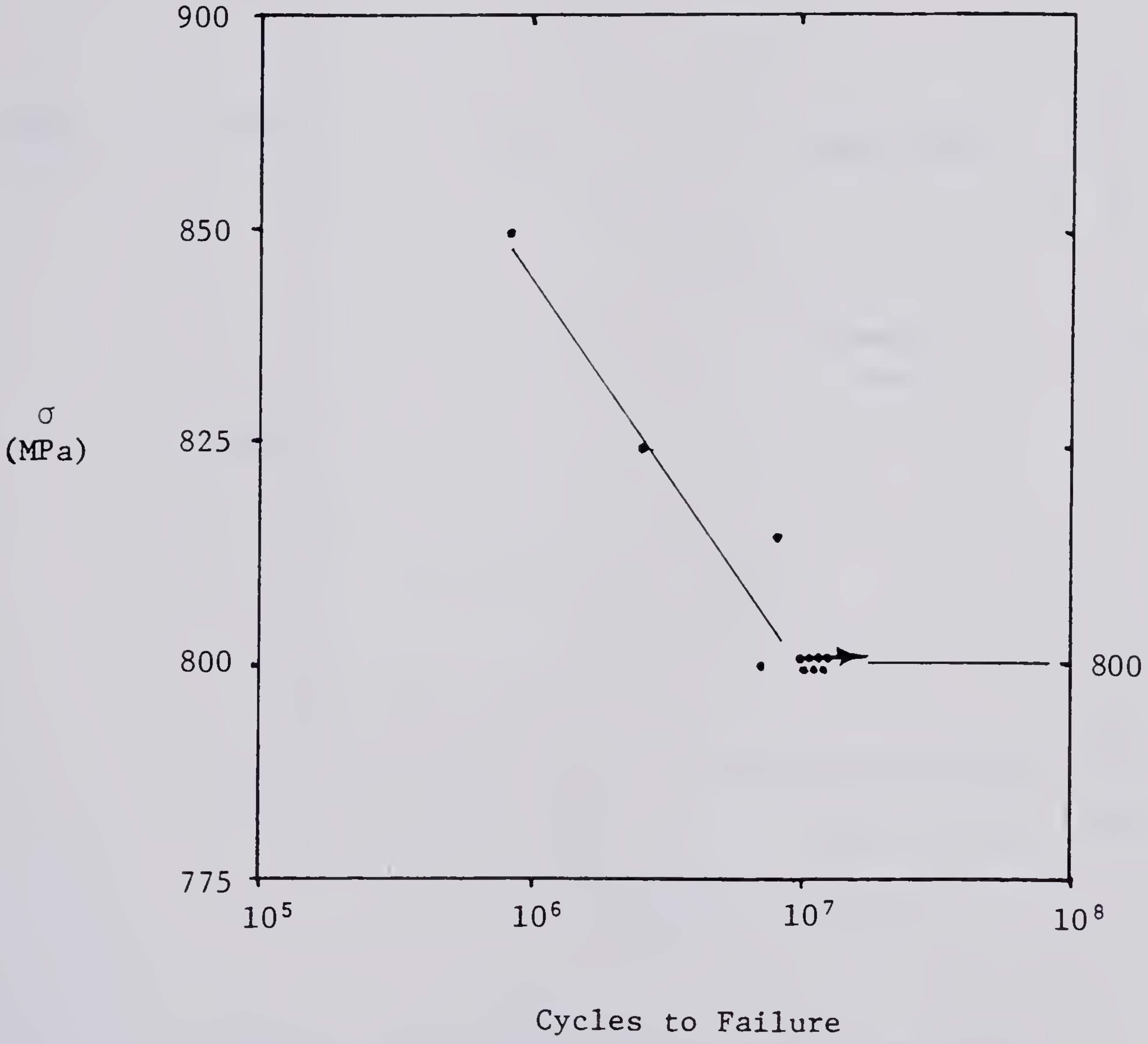

Fatigue Data for Hot Isostatically

Pressed Cobalt-Chrome

Figure 24

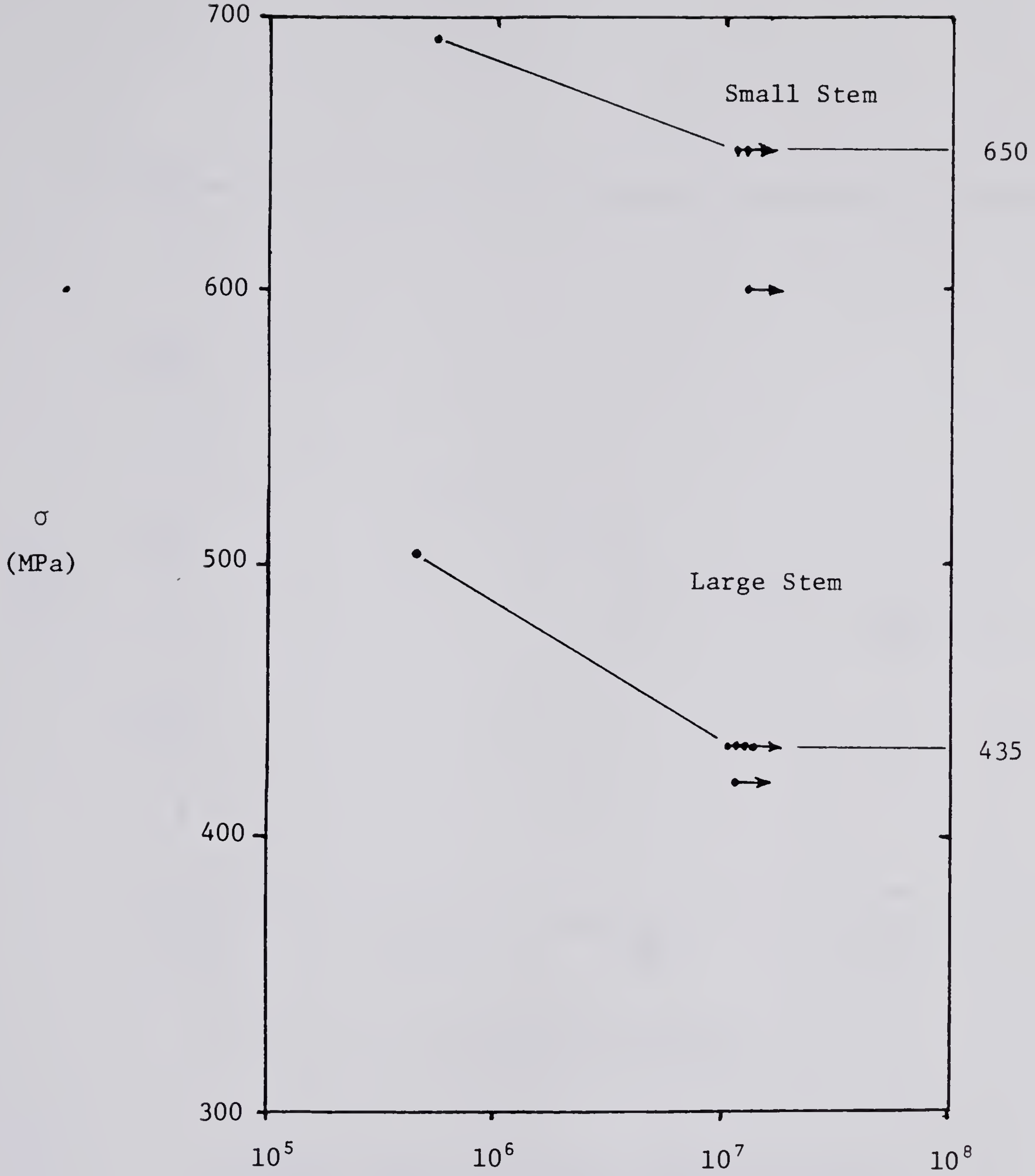

Fatigue Data for Forged Stainless Steel

Figure 25

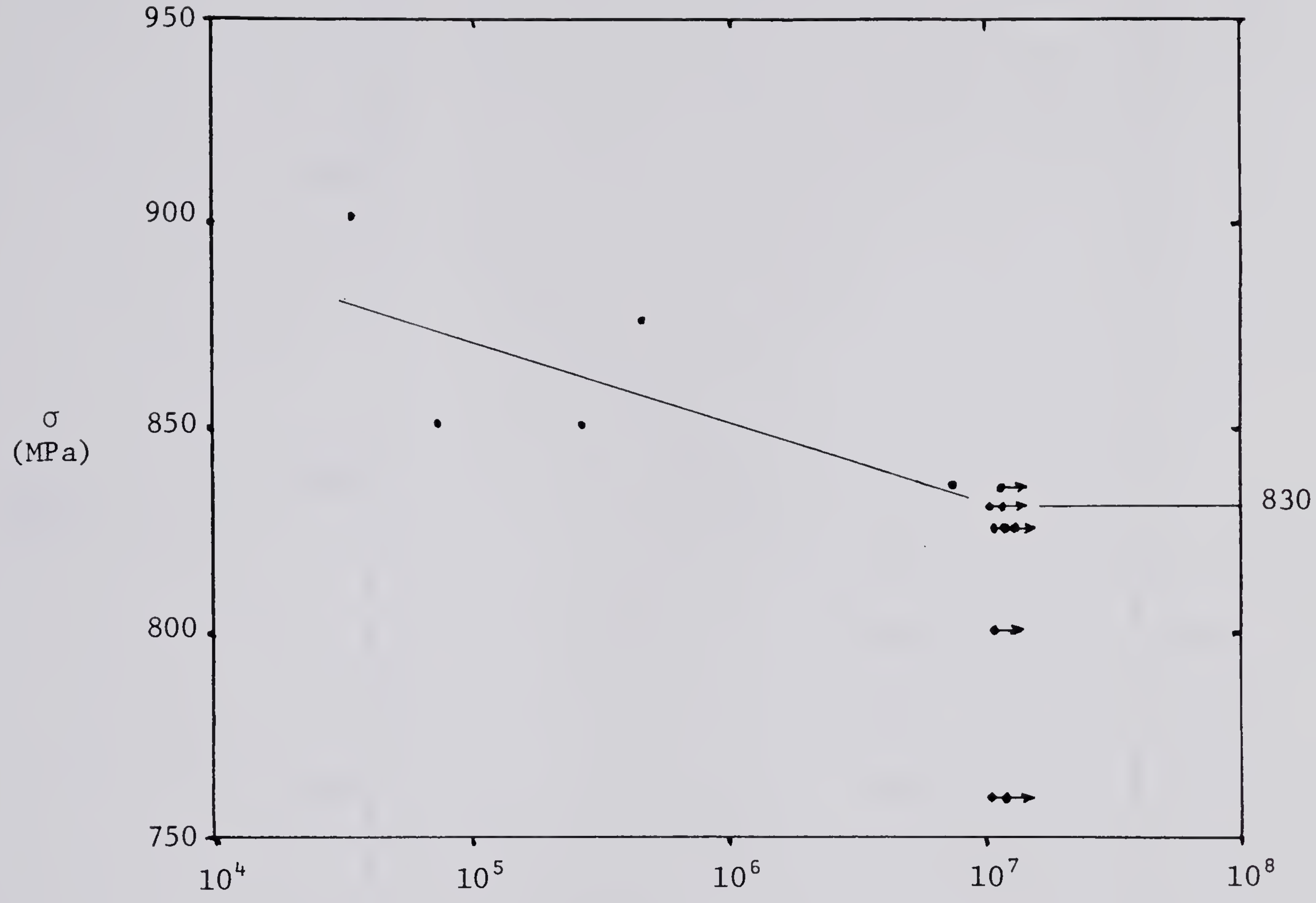

Cycles to Failure

Fatigue Data for Forged Cobalt-Chrome

Figure 26

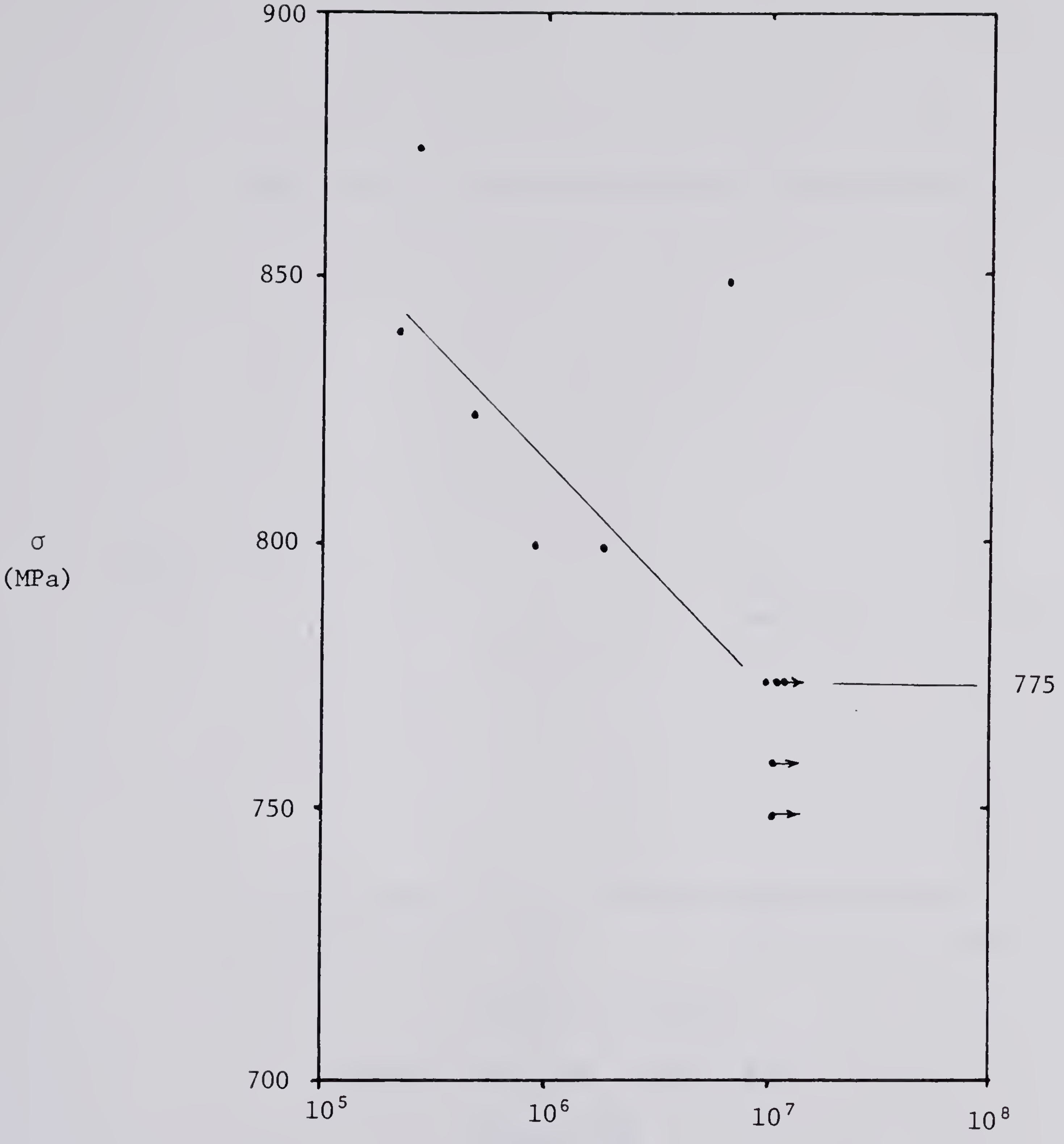

Fatigue Data for MP-35N

Figure 27

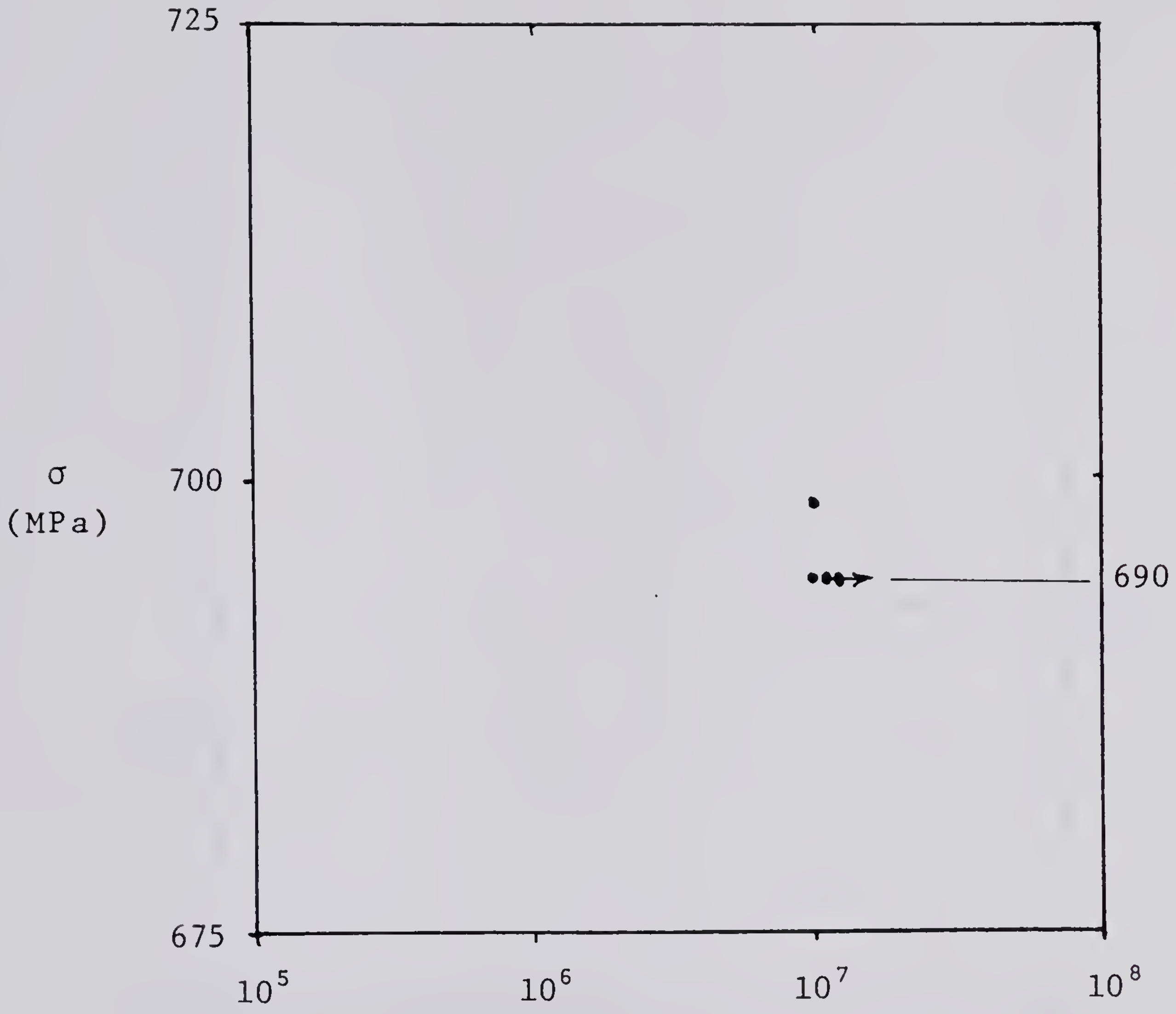

Cycles to Failure

Fatigue Data for Ti-6Al-4V

Figure 28

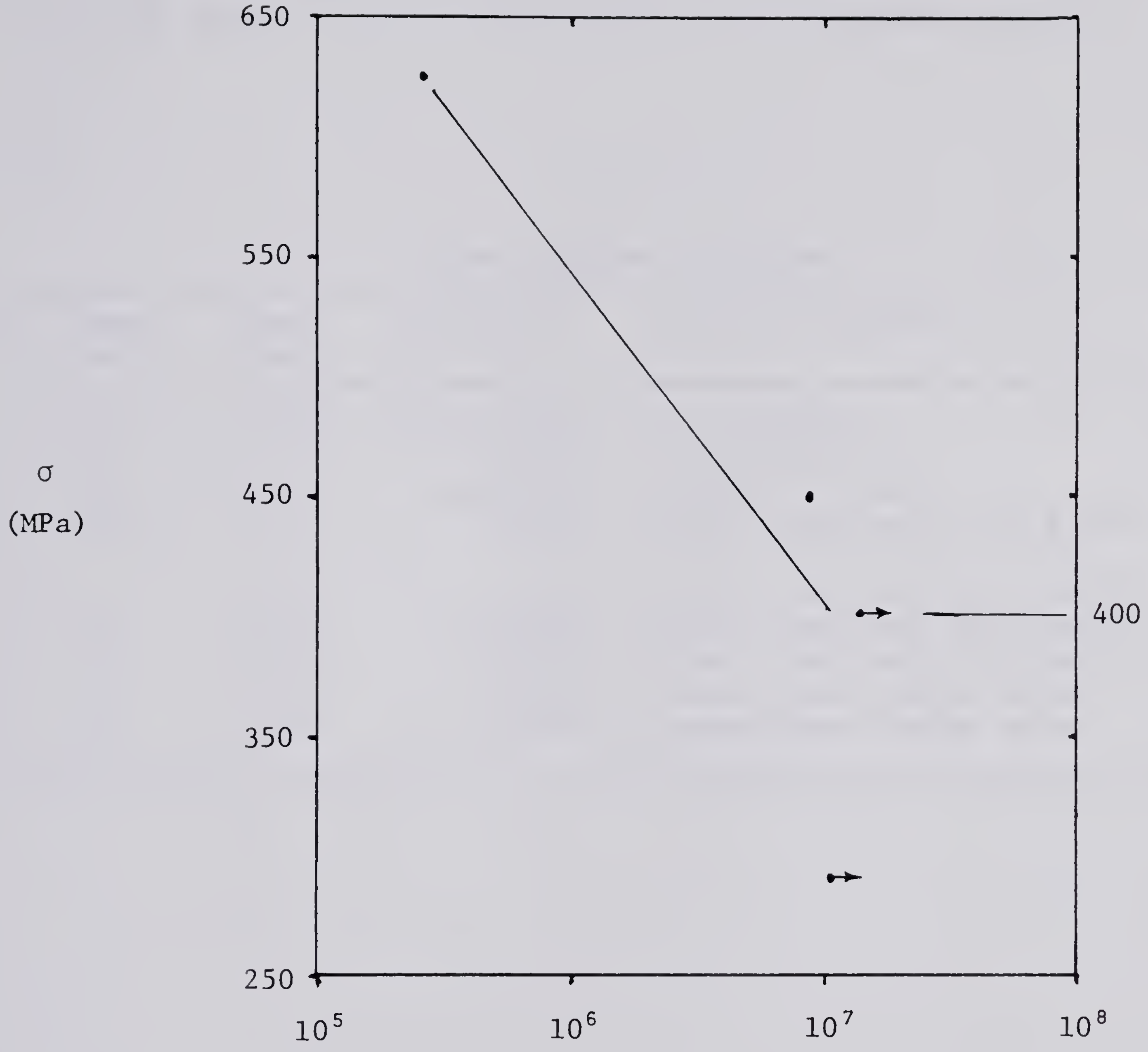

Fatigue Data for Cast Cobalt-Chrome

Figure 29

Tube-Mounted Stem Fatigue Results

Table 8 presents the data from the fatigue loading of the tube-mounted stems. As can be seen, the majority of the aluminum tubes did not stand up to the fatigue loading.

Table 8

Stem Fatigue Results

Stem No.	Load (kN)	Cycles to Failure	Mode of Failure
5-s	3.43	10,500,000	no failure
6-s	5.49	74,500	tube split
7-s	3.43	4,000,000	fatigue crack
19-s	5.47	19,000	bent stem and tube split
8	5.49	11,000	bent stem and tube split
10	3.43	135,900	bent stem and tube split
11	5.49	26,700	bent stem and tube split
13	5.49	145,200	tube break below stem
22	5.49	53,000	tube break below stem

Charpy V Notch Test Results

Table 9 presents the results of the Charpy V Notch tests. The corresponding material fracture toughness values are also listed. They were calculated using the formula presented in the section entitled 'Determination of Material Toughness ($K1_c$)' located in the Appendix.

As was noted earlier, two of the hot isostatically pressed specimens were fatigue cracked, but due to a shortage of material for test pieces and the possibility of breaking the specimens, no attempt was made to fatigue the other materials.

Table 9

Charpy V Notch Results

Material	No. of Specimens	Minimum Charpy (Nm)	$K1_c$ (MPa m$^{.5}$)
HCC	2	18	177
Pre-cracked	2	3.7	99
FCC	4	60	319
TAV	1	37	172
CSS	1	60	291

Results of Improper Stem Positioning

Figure 30 displays the effects of varying the position of the distal end of stem #23 from the medial side of the tube to the lateral side of the tube, or from the varus to the valgus position. It can be seen that the maximum stress is increased by placing the stem in a valgus position, and decreased by placing the stem in a varus position.

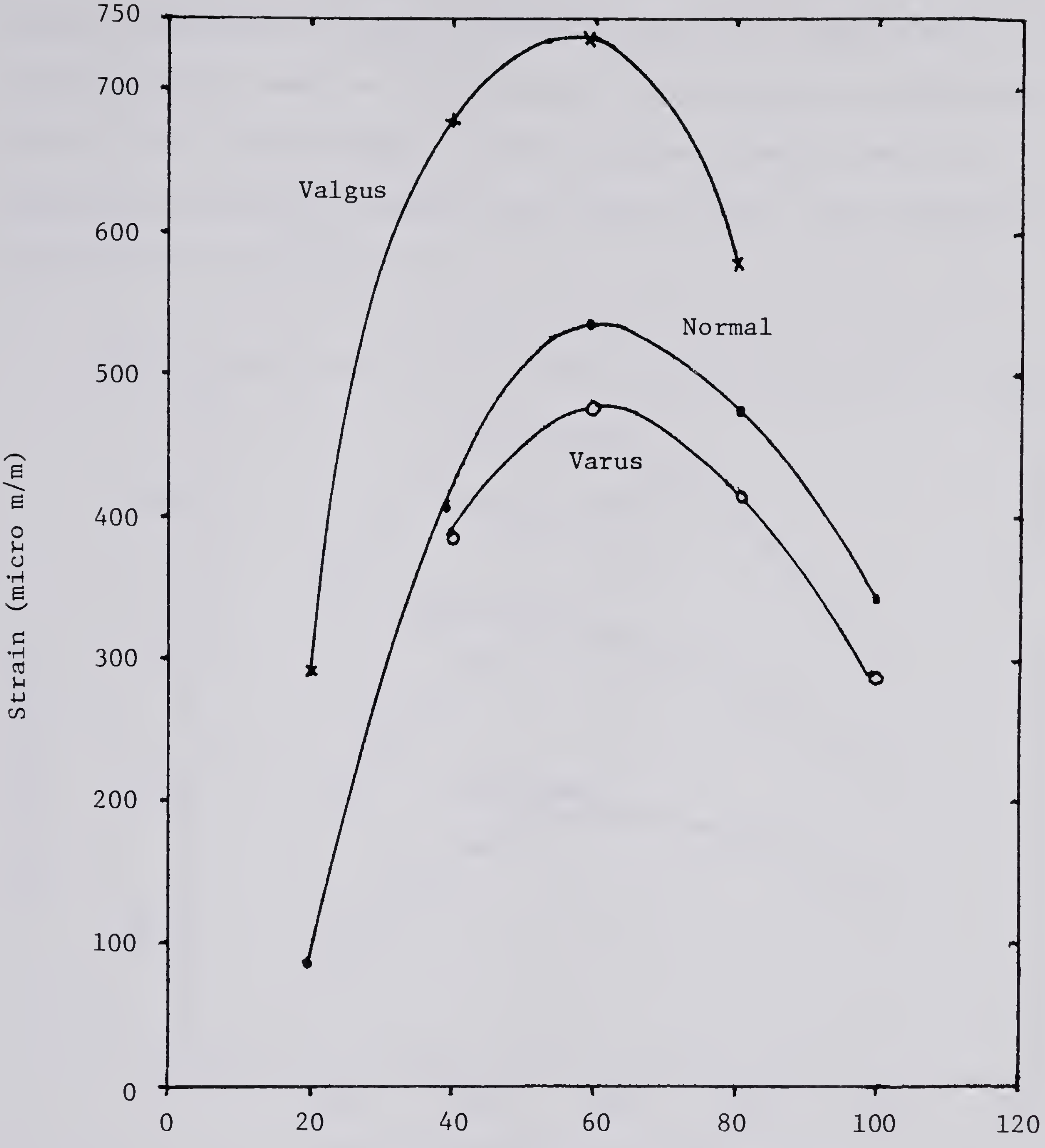

Lateral Face Strains Measured on

Stem #23 in Three Positions

Figure 30

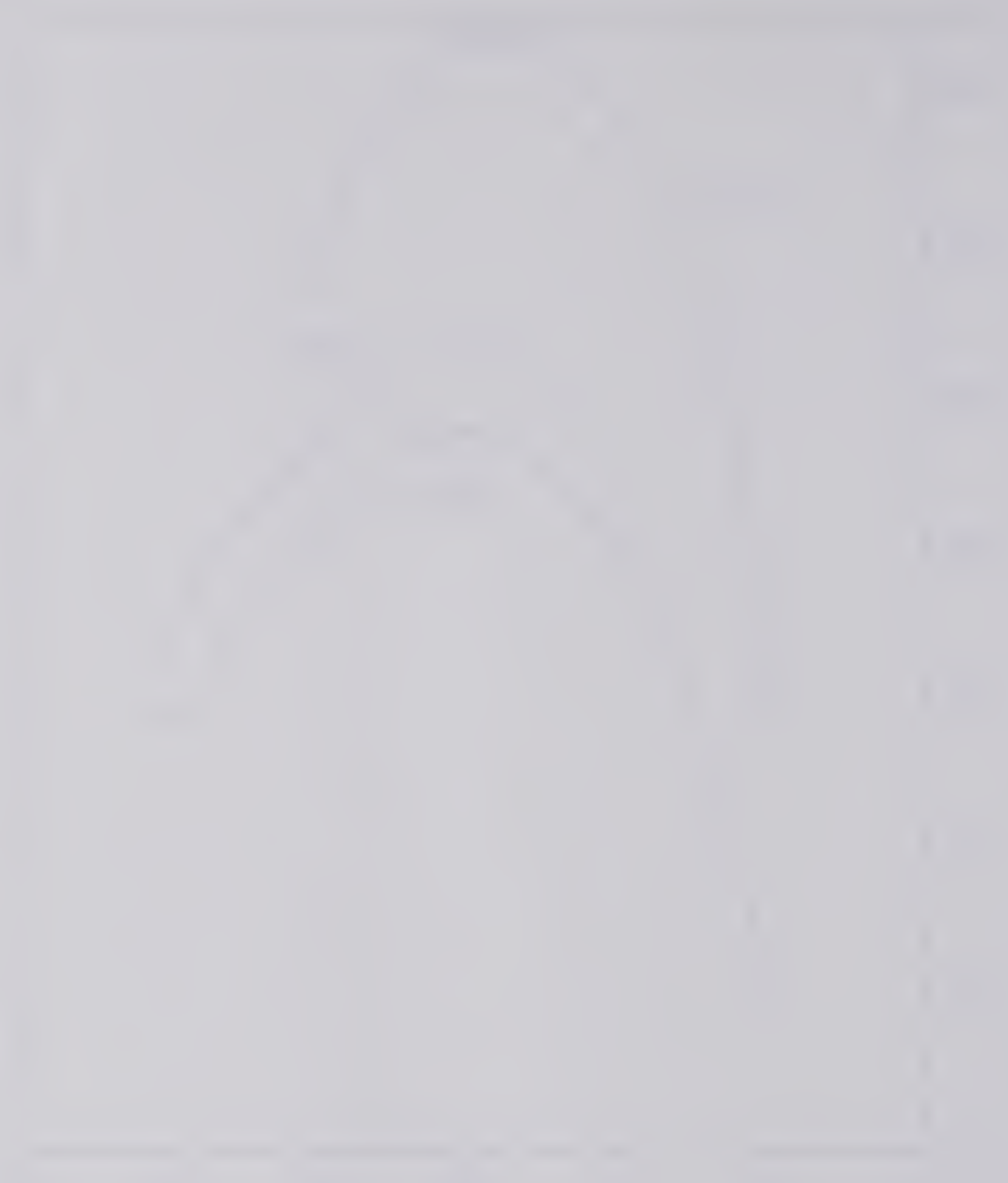

[illegible]

The change in stem strain due to altering the knee position varied depending on which stem was used. The increase in the maximum strain due to a bowlegged knee position ranged from 29% to 58%. The decrease in the maximum strain due to a knock-knee position ranged from 25% to 54%. This change is illustrated in Figure 31.

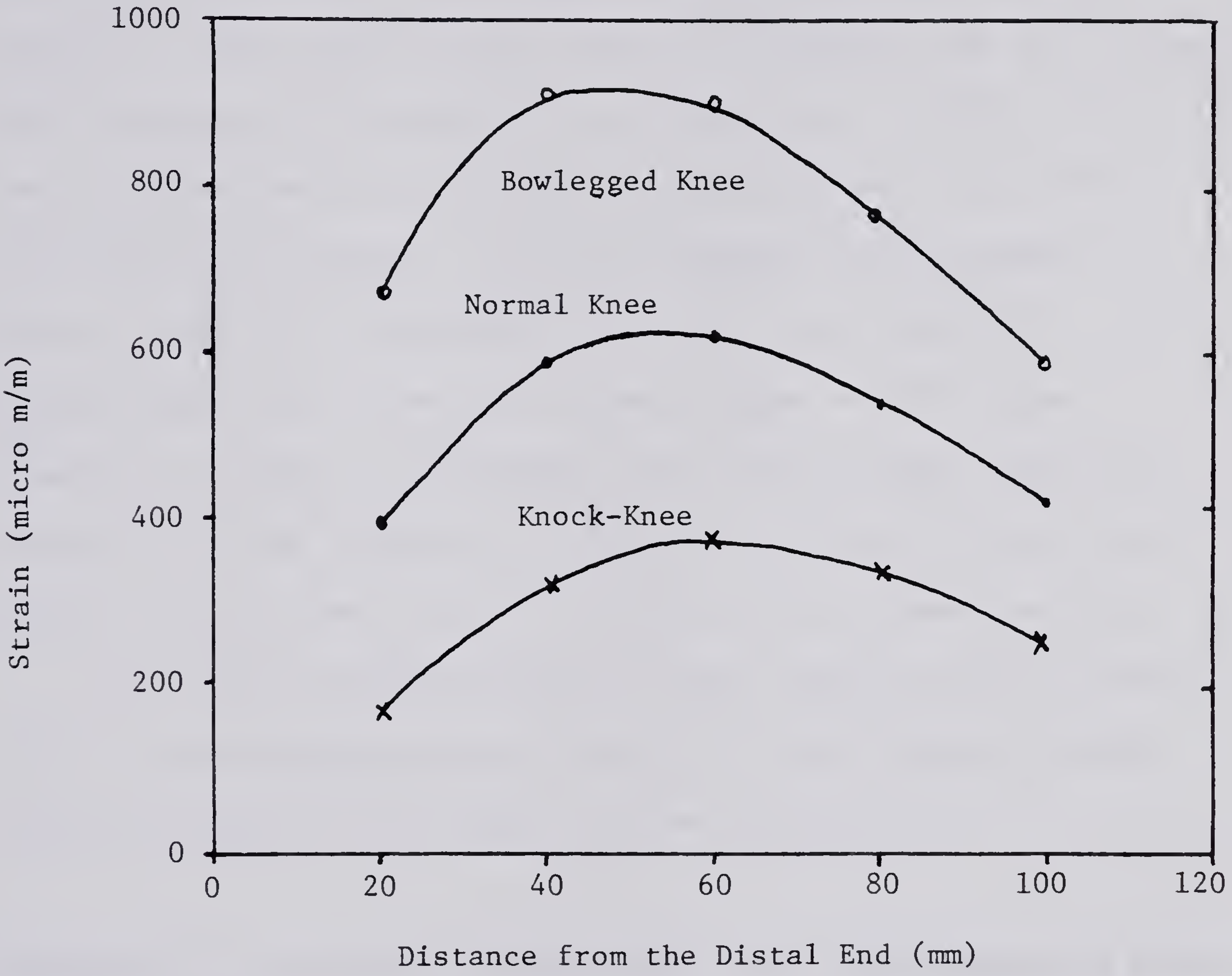

Lateral Face Strains Measured on

Stem #18 in Various Knee Positions

Figure 31

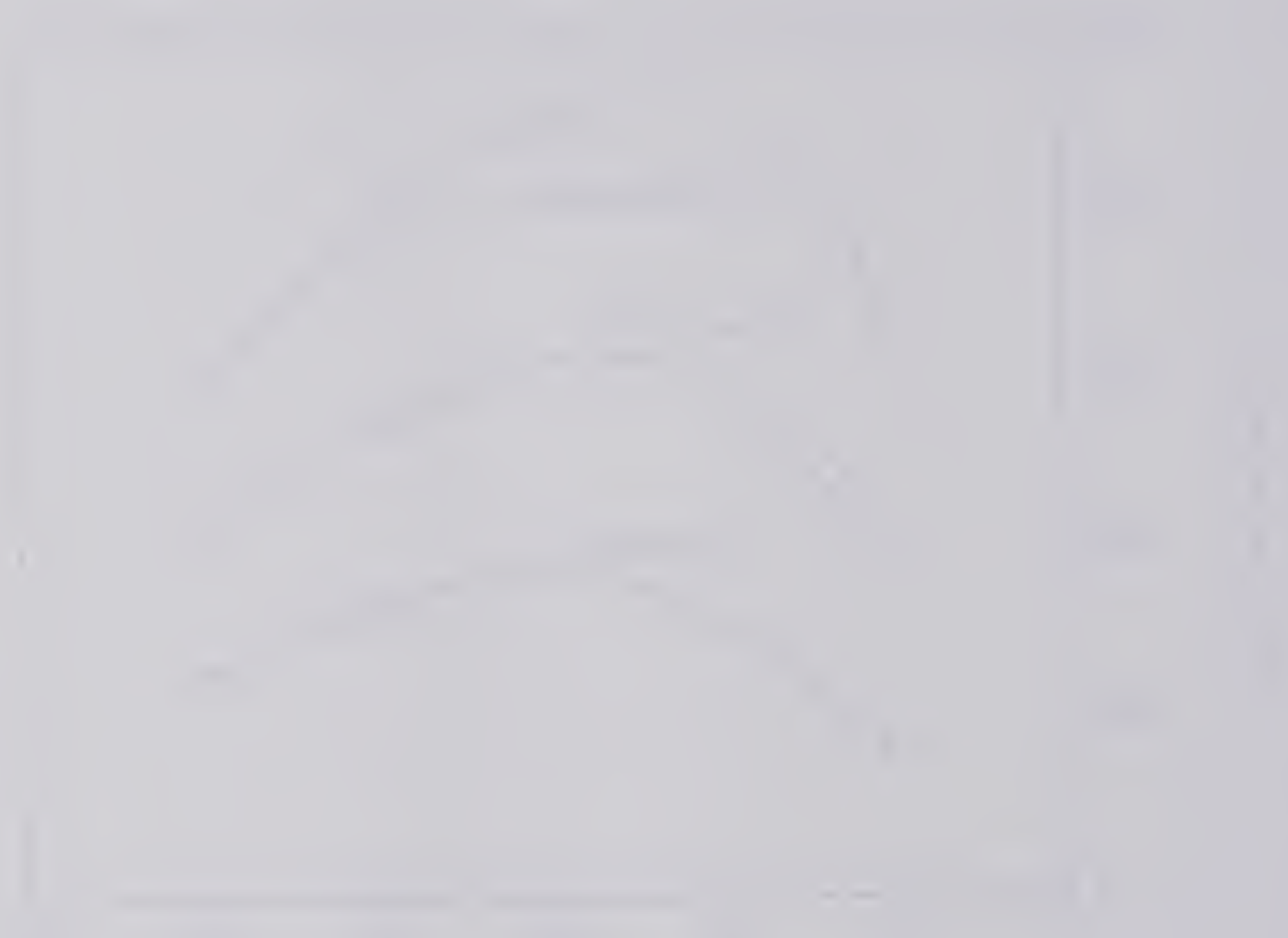

IV. Interpretation of the Results

Precision of the Stem Testing Method

Figures 18 and 19 show that, for the steel and forged cobalt-chrome prostheses tested, repeatable measurements were obtained. Much more scatter was evident in Figure 17 which shows the behavior of the Ti-6Al-4V stem. This implies that the stress in this stem is more sensitive to small errors in stem positioning. This is probably due to the much lower modulus of elasticity of Ti-6Al-4V, 110 GPa versus 207 GPa for steel and 248 GPa for cobalt-chrome. In a stem positioned in valgus, the lower modulus would cause a greater shift of the neutral axis of the stem-tube combination, away from the lateral face of the stem, compared to that of a stiffer stem. This would cause an increase in the stress, on the lateral face of the lower modulus stem, over that of a stem with a higher modulus.

The tests yielded maximum strain measurements within ±5% of the average maximum strain for the higher modulus materials, and within ±20% for the Ti-6Al-4V.

Comparison of Results Between Tube- and Femur-Mounted Stems

As shown in Figures 20 though 23, the maximum strains measured in the stems when the aluminum tubes were used, were in general similar to those measured when the stems were mounted in femurs. There is a discrepancy in the distal part of the stems. However, this is a less critical area, from the point of view of this study, since the stresses are

much lower near the end of the stem, and hence fracture would not be expected to occur in this area.

Maximum Stem Stresses at 1kN Load

The semi-round and the trapezoidal cross sections had much sharper lateral corners than the rest of the stems. To ensure that the strains used for evaluation purposes were indeed the maximum stem strains, it was necessary to calculate the strains at the lateral corners of these stems.

The strains listed in Table 4 are the maximum strains measured on the centerlines of the lateral faces of the stems. The strains in Table 5 are the strains measured on the centerlines of the front faces of four stems. These gages were shown in Figure 11. Assuming linear elastic behavior, the strain in one corner of the stem will be the corresponding lateral face strain plus the front face strain. The front face strain can be either compressive (negative) or tensile (positive). Therefore, the maximum stem strain was taken as the greater of the lateral face strain or the sum of the lateral face strain and the front face strain.

> The stems that were affected by the above calculation were all of the semi-round types, #2, #4, #8, #9, #10, and #11. The worst case was used in all instances, that is, the maximum lateral face strain was increased by 54 micro m/m for stems #2, #8, #9, #10, and #11, and by 76 micro m/m for stem

#4. As was noted in the section entitled 'Results', the trapezoidal stems did not exhibit a tensile front face strain, so the maximum stem strain, in the case of these stems, is the maximum strain measured on the lateral face. The maximum stem strain for each stem is listed in Table 10. It should be noted that, it was not necessary to add on the front face strain in the case of stems with rounded cross sections.

To calculate the maximum stem stress at a load of 1 kN the maximum stem strain at a load of 1 kN was multiplied by the modulus of elasticity of the material.

Table 10

Maximum Stem Stress at 1 kN Load

Stem No.	Maximum Strain (micro m/m)	Maximum Stress (MPa)
	Small Stems	
5-s	538	133
6-s	557	138
7-s	953	197
19-s	598	138
	Medium and	Large Stems
1	496	123
2	471	97
4	745	82
8	500	104
9	530	110
10	710	147
11	614	147
12	338	84
13	342	85
14	248	62
15	276	68
16	338	84
17	606	140
18	615	142
20	383	95
21	343	71
22	328	68
23	539	112
24	506	105
25	274	63

Effective Knee Joint Force

The maximum stress calculated at 1 kN load, presented in Table 10, was used to calculate the maximum stress possible under in vivo loading conditions. To do this it was necessary to know the magnitude of the force at the knee joint, the magnitude of the force applied by the abductor muscles, and the effect of the abductor muscle force on stem strain or stress.

The knee joint force, calculated in the section entitled 'Mounting and Loading Apparatus', is equal to 3.3 W, where W is the weight of the body.

The force applied by the abductor muscles is F_t, where F_t is given by equation (2):

$$F_t = 446 * W / x$$

The distance 'x', in mm, was measured for each stem by positioning the stem on a template, as shown in Figure 32. With the reference point 'A' fixed and the bottom end of the stem on the femur centerline, 'x' could be measured directly.

Ideally each stem tested would have been subjected to both a knee force and an abductor muscle force. Since it would have been very difficult to attach the trochanter force to the tubes in a way that simulated the femur loading conditions, a theoretical method of taking into account the abductor muscle force was needed.

The values of the stem strain produced by the abductor

muscle force were displayed in Table 7. Comparing these strains with the strains displayed in Table 6, it can be seen that the maximum effect of a 1 kN abductor muscle force is a strain of approximately 50% of the strain that would be produced by a knee force of 1 kN. This implies that adding 50% of the calculated abductor muscle force to the knee force would produce the same maximum stem strains as a separate abductor muscle force and knee joint force. The 'effective knee joint force' is defined as the knee joint force necessary to produce a stem strain equal to that produced when the knee joint force and the abductor muscle force are both applied.

$$\text{Effective Knee Joint Force} = 3.3\ W + 0.5\ F_t$$

$$=(3.3 + 223/x) * W$$

As mentioned previously, the body weight used for medium and large stems was taken as 784 N, and for small stems 468 N. The effective knee joint force for each stem is listed in Table 11.

Valgus Placed Stems

As indicated in Table 4 there were six stems that were not on the centerline of the tubes when they were tested. Four of these stems were relatively large and could not be positioned on the centerline easily, #14, #15, #21, #22. The other two stems were positioned incorrectly and were damaged before they could be remounted. The #19-s stem positioning was only slightly

valgus and this malposition probably did not raise the strains measured significantly.

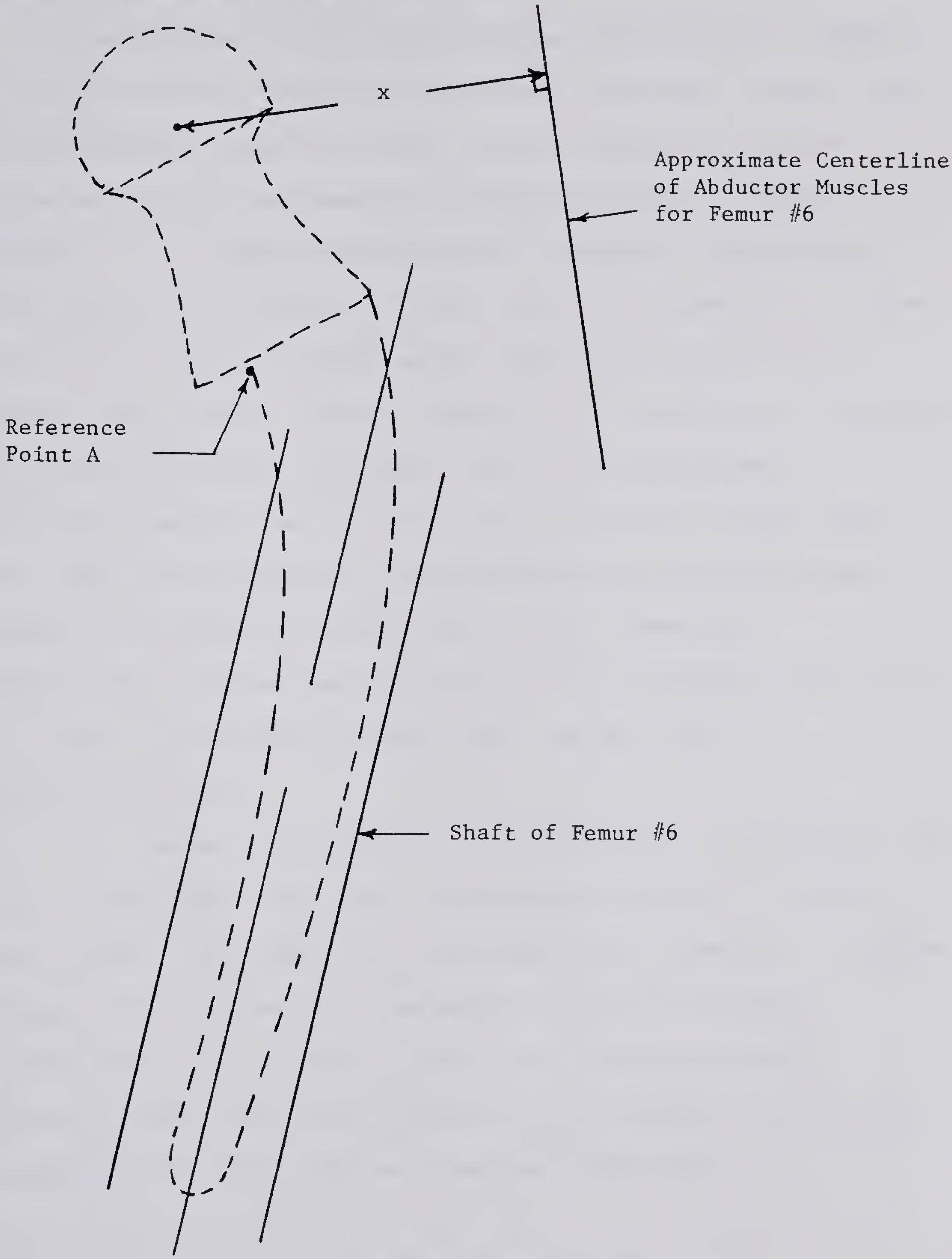

x Distance Template

Figure 32

Ranking the Stems

As mentioned in the Introduction, resistance to fatigue failure has been shown to be the most important factor, from the engineering point of view, in the choice of a stem. A simple method for determining the resistance to fatigue failure is to compare the endurance limit of the material with the maximum stress that is likely to occur in the stem. This can be done by dividing the endurance limit by the maximum stem stress. If the ratio is 1.0 or greater the stem is unlikely to break, assuming that the conditions postulated earlier are correct. If the ratio is less than 1.0, then there would be a possibility of a stem fatigue failure. It should be noted that, since there is considerable scatter in all fatigue test results, stems with a fatigue coefficient greater than 1.0 may still occasionally fail.

This number also allows a simple method for ranking the stems. The higher the ratio of endurance limit to maximum stem stress, the less likely the stem will undergo a fatigue failure. This ratio has been given the name 'fatigue coefficient'. It appears in Table 11, along with the endurance limit of the material and the maximum stem stress calculated assuming in vivo loading conditions.

Table 11

Fatigue Coefficients

Stem No.	Effective Knee Joint Force (kN)	Max. Stress (MPa)	Endurance Limit (MPa)	Fatigue Coef.
		Small	Stems	
5-s	3.3	439	800	1.8
6-s	3.3	455	830	1.8
7-s	3.6	709	435	0.6
19-s	3.2	442	775	1.8
	Medium and	Large	Stems	
1	5.7	701	400	0.6
2	5.3	514	207	0.4
4	5.7	467	690	1.5
8	5.1	530	207	0.4
9	5.2	572	207	0.4
10	5.3	779	207	0.3
11	5.1	648	207	0.3
12	5.6	470	800	1.7
13	6.1	519	400	0.8
14	5.9	366	400	1.1
15	5.7	388	830	2.1
16	5.7	479	830	1.7
17	5.5	770	775	1.0
18	5.4	767	775	1.0
20	5.8	551	800	1.5
21	5.4	383	435	1.1
22	5.9	401	435	1.1
23	5.9	661	650	1.0
24	5.5	577	650	1.2
25	5.5	347	775	2.2

Stem-Tube Fatigue

As seen in Table 8, most of the attempts to fatigue the stems mounted in tubes were unsuccessful because of failure of the aluminum tube. It was possible, however, to cycle the #5-s stem to 10.5 million cycles without failure of the stem, and to fatigue crack the #7-s stem after 4.6 million cycles. These stems are shown in Plate 17.

These two results lend support to the ranking system and the fatigue coefficient. The fatigue coefficient for the #5-s stem was 1.8, so it should not have failed at the load applied. On the other hand, the fatigue coefficient for the #7-s stem, 0.6, indicated that a fatigue failure was probable before 10 million load cycles.

The results also show that this method of fatigue loading may be practical for testing small stems but does not appear practical for medium and large size stems.

Fatigue Loaded Stems (1/2 X)

Plate 17

[illegible]

Fracture Toughness Testing

The relatively few specimens available for the Charpy V Notch testing preclude anything but a general statement about the fracture toughness of the materials. That is, use of either of the formulae, given in the Appendix, shows that it is unlikely that the stems would fail due to brittle failure, or lack of toughness. This is due both to the high fracture toughness of the material, and the small maximum possible flaw size which may be present in the material after inspection, as explained in the Appendix. For this reason, it is expected that stems will fracture only after an initial crack has been caused by fatigue.

Malpositioning of the Stem

Figure 30 shows that significant increases in stem stresses are possible if the stem is inserted in a valgus position, as shown in Figure 4. This would indicate that it is advantageous, from an engineering viewpoint, to insert the stem in a varus or a neutral position.

Figure 31 shows that a stem inserted in a bowlegged patient may be subjected to significantly higher stresses than one inserted in a patient with normal or knock-kneed legs.

V. Conclusion

A. Summary

An experimental model was developed to simulate mechanical in vivo loading conditions for total hip replacement stems. The fatigue strength and fracture toughness of the materials used in these stems were investigated. 24 stems were tested and ranked according to their ability to resist fatigue failure. These results appear in Table 12.

A fatigue coefficient of 1.0 or greater indicates that the stem is unlikely to fail in fatigue under the loading conditions assumed. A fatigue coefficient of less than 1.0 indicates the stem may fail in vivo. The higher the fatigue coefficient the less likely a fatigue failure will occur. It should be noted, however, that for many people, the assumed loads may never occur, so that a fatigue coefficient of 1.0 or less does not necessarily imply failure.

The effects of malpositioning of the stem were also investigated. It was found that, compared to a normally positioned stem, significantly higher stresses will be produced in stems that are inserted in a valgus position in the femur or into a bowlegged person.

As shown in Table 12, many of the stems tested are not likely to fail by fatigue in vivo. The stems that were ranked below 1.0 are of a relatively outdated design, or material or both.

The precision of the strain measurement, ±5% for most stems, and the probable error in the established endurance limits, less than ±5%, would lead to a grouping of the stems as shown in the table. The ±5% maximum probable error in the endurance limit would take into account the error in the Vibrophore testing machine and any possible dimensional measurement error. The small stems, #5-s, #6-s, #19-s, were all ranked equally, with the #7-s stem being ranked considerably lower. The medium and large stems were divided into three categories, those which are very unlikely to break in vivo, those which are essentially just above the borderline, and those which may break in vivo.

Table 12

Stem Ranking

Stem No.	Distributor and Description	Fatigue Coef.
	Small Stems	
5-s	Zimmer, TR-28, Straight Stem, Medium Neck	1.8
6-s	Howmedica, HD-2, Small Stem	1.8
19-s	Depuy, Protasul 10, Short Neck, Short Stem	1.8
7-s	Zimmer, T-28, Medium Neck, Small Stem	0.6
	Medium and Large Stems	
25	Depuy, Protasul 10, Large Stem	2.2
15	Howmedica, HD-2, Medium Neck, Large Stem	2.1
16	Howmedica, HD-2, Medium Neck, Medium Stem	1.7
12	Zimmer, TR-28, Long Neck, Large Stem	1.7
20	Zimmer, TR-28, Medium Neck, Large Stem	1.5
4	Zimmer, STH, Tivanium	1.5
24	Richards, Small Straight, 1 3/4" Neck	1.2
14	Howmedica, CAD, Large Stem	1.1
21	Richards, Medium Stem, 1 3/4" Neck	1.1
22	Richards, Medium Stem, 2 1/4" Neck	1.1
17	Depuy, Std. Neck, Std. Stem	1.0
18	Depuy, Long Neck, Std. Stem	1.0
23	Richards, Small Straight, 2 1/4" Neck	1.0
13	Howmedica, CAD, Medium Stem	0.8
1	Zimmer, Medium Neck, Long Stem	0.6
2	Richards, 3/8" Reg. Stem, 2 1/4" Neck	0.4
8	Richards, 3/8" Str. Stem, 1 3/4" Neck	0.4
9	Richards, 3/8" Reg. Stem, 1 3/4" Neck	0.4
10	Richards, 5/16" Reg. Stem, 1 3/4" Neck	0.3
11	Richards, 5/16" Str. Stem, 1 3/4" Neck	0.3

In summary, a number of total hip stem types presently on the market have been evaluated on a fatigue failure basis. A new technique has been devised for the testing of the stems, and standard engineering practice has been followed to establish important properties of the stem materials. The results may be used by any orthopaedic surgeon or hospital and should aid their choice of prosthesis. It should be noted that the fatigue failure aspect is only one point that a surgeon or hospital must consider when choosing a prosthesis, and it is the only point dealt with here.

B. Limitations

The technique of stem evaluation presented here is not without its limitations.

Factors Unaccounted For

The forces acting on the femur were simplified in order that they could be experimentally reproduced. This is a source of criticism of this method but it was a necessary step in attaining a solution of the loading problem. However, the stems were all treated in the same manner, and so the results are at least very useful on a comparative basis, and to a high degree are representative of what occurs in vivo.

The effect of environment on both the endurance limit

and fracture toughness was not investigated in this study. This is mainly due to the time required to do comprehensive corrosion fatigue tests. A corrosion fatigue test, on one sample, could conceivably take up to four months. In addition, there have been no reported cases of corrosion fatigue in the literature, although fatigue has been found many times.

Size and Material Limitations

The bulk of the specimens for the fatigue and Charpy tests were obtained from stems, which put a practical upper limit on their sizes. This limit was, for the endurance limit specimens, about one millimeter smaller in diameter than the ASTM recommended minimum.

Significant scatter in strain measurements on similarly mounted stems was shown for the Ti-6Al-4V material. This may mean that the method of centering the stem in the tube is not precise enough even using the methymethacrylate plug centering method.

As is shown in the Appendix, Charpy V notch specimens are not large enough to allow accurate determination of minimum fracture toughness values. Only estimates may be obtained. They were, however, the largest specimens that could be cut from stems and correlated to fracture toughness values.

Anomalies

The strain readings on the TR-28 stems, #12 and #20, are a minor source of concern. Both of the stems were supposed to have the same stem length and cross section, however, although the #12 stem had the longer neck, it had a lower maximum strain. The longer stem neck would be expected to cause higher strains in the stem, so this result indicates either a slight difference in stem cross sections, or a slight placement difference between the stems, or both. The fatigue coefficients are close, however, as are the fatigue coefficients of other similarly sized pairs of stems.

Number of Subjects and Specimens

Only a limited number of stems and a limited quantity of stem material were available for the testing program. Most of the stems tested were donated by the manufacturers. The high cost of each stem, about $400, made it impractical to buy a large number of stems for testing. Ideally, more stem types could have been tested, and each type tested more times, to give greater confidence in the results. Material was always scarce and in several instances only a few specimens were tested. This is especially the case in the Charpy V Notch testing, where in some instances only one or two specimens were tested.

Recommendation for Further Investigations

Further work should be undertaken to refine the method for centering the stems in the tubes. This would enable more precise testing of all the stems and in particular the Ti-6Al-4V stem.

The lack of sufficient material prevented the establishment of totally reliable endurance limits for either cast cobalt-chrome or Ti-6Al-4V, although the endurance limit for Ti-6Al-4V estimated here agrees with that found in the literature. These endurance limit estimates should be reinforced with more material testing. More testing is also necessary to establish minimum fracture toughness values for all the materials.

V. Appendix

Fracture Toughness

Brittle fracture is characterized by plane strain boundary conditions. Considering the usual dimensions of total hip stems, the assumption of plane strain is a conservative one, as will be shown later. A simplified diagram of the loading on a section of a stem can be seen in Figure 33. This type of loading, considering that the stresses produced by the moment are much greater than those produced by the axial load, can lead to what is known as the opening mode or 'mode 1' fracture. This is shown in Figure 34. The crack tip stress intensity factor for this type of loading is denoted by K1. For mode 1 fracture, given slow loading rates and plane strain conditions, the material toughness is denoted by $K1_c$.

Maximum Permissible Flaw Size

With the current non-destructive testing techniques used by the manufacturers, the maximum length of crack present in a prosthesis after inspection would probably be in the order of 0.25 mm (0.01 inch). It should be noted, however, that cracks, which initially are small, may grow due to fatigue or stress corrosion.

The maximum permissible flaw size can be calculated, knowing the material toughness and the maximum stress, by using the basic formula:

$$K1_c = \sigma_y (\pi * a)^{.5}$$

Where 'a' is one half of the crack length, and σ_y is the maximum nominal stress, namely the stress that would occur if there were no crack. The maximum nominal stress can be assumed to be the maximum occurring on the lateral face of the stem. This is a conservative method of calculating the flaw size, since it assumes that the stress is a constant across the cross section, as shown in Figure 34.

If the crack is assumed to traverse the stem, as in Figure 35, the stem becomes an edge-cracked bend specimen. Wilson [14], using a boundary collocation method, has derived an expression which he proposes may be used to determine a more accurate stress intensity factor for this type of specimen:

$$K1 = 3.99\ M/(D-a)^{1.5}$$

Where 'M' is the moment per unit width, 'D' is the specimen depth, and 'a' the crack depth. The critical flaw size can be determined by substituting $K1_c$ for K1 and using the maximum possible moment for 'M'. The assumption of a transverse crack, across the stem width, is an exaggerated representation of the case that might be encountered in total hip prostheses.

---

[14] Wilson, W.K.; Stress Intensity Factors For Deep Cracks in Bending and Compact Tension Specimens, Engineering Fracture Mechanics, Vol.2, 1970-71, pg.169-171, Ed. H. Liebowitz, Pergamon Press, Toronto.

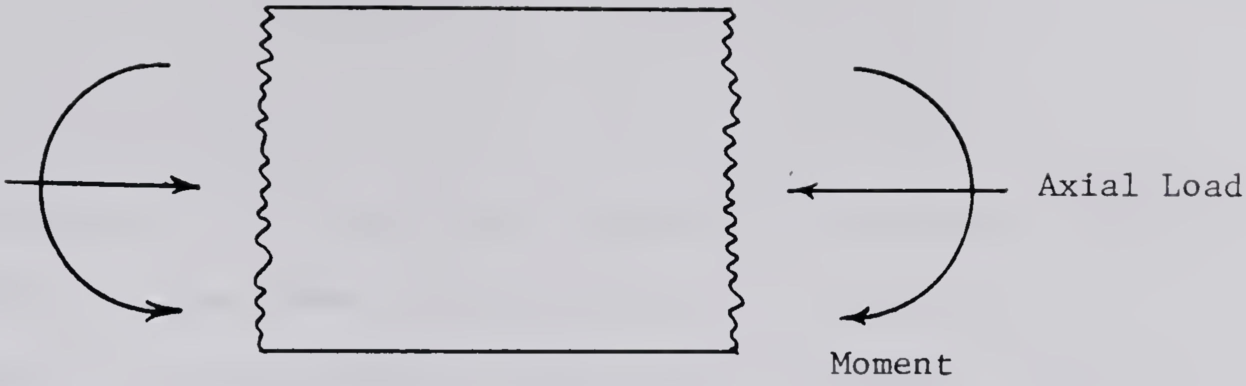

Simplified Stem Loading

Figure 33

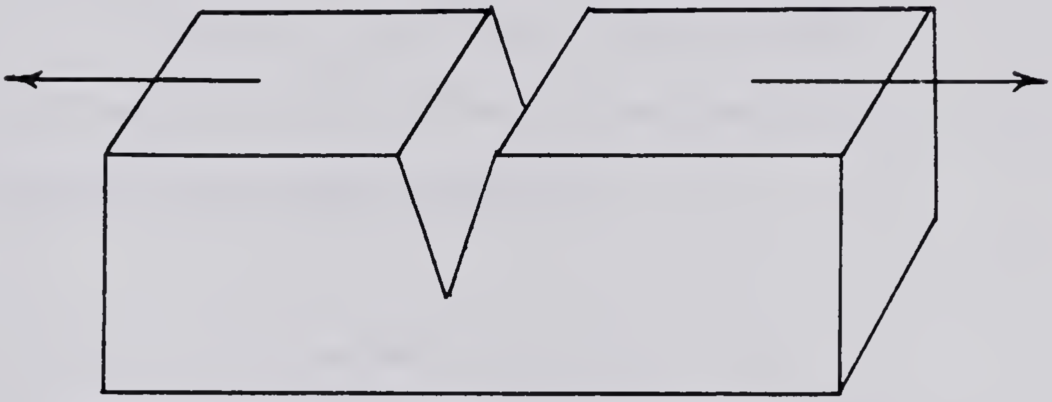

Mode 1 Fracture

Figure 34

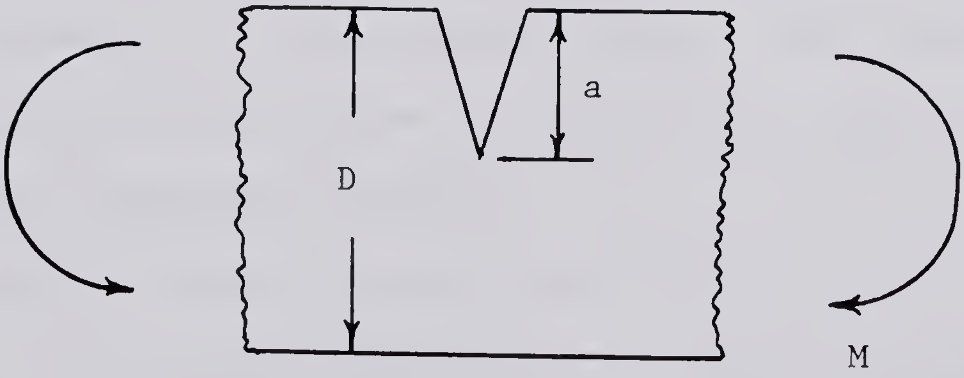

Edge-Cracked Bend Specimen

Figure 35

Crack Tip Yielding

Yielding will occur at the crack tip as the bending stresses in the stem approach the yield stress. To account for this probable crack tip yielding, Irwin [15] has suggested increasing the actual crack length by an amount R_y. He gives R_y as:

$$R_y = (K1_c / \sigma_y)^2/(6 * \pi)$$

Where σ_y is the yield stress.

This adjustment in crack length is necessary in both of the aforementioned expressions.

Determination of Material Toughness ($K1_c$)

It would have been desirable to measure $K1_c$ directly, for each particular material. The materials, however, were not available in the large sizes necessary to carry out the standard tests recommended by ASTM. It was necessary to use Charpy V notch test specimens and a theoretical correlation between Charpy impact values and fracture toughness values.

Charpy impact values can be used to obtain impact, fast loading rate, values for fracture toughness. It is, however, a generally accepted and conservative practice to use the impact value to obtain the material toughness when the actual loading rate is uncertain and may be

---

[15] Irwin, G.R.; Linear Fracture Mechanics, Fracture Transition, and Fracture Control, Engineering Fracture Mechanics, Vol.2, 1968.

slow or intermediate.

The theoretical relationship between $K1_c$ and the Charpy impact value can be expressed as:

$$K1_c{}^2 = E * (W/A)/(2 * (1- \nu^2))$$

Where: E = modulus of elasticity

ν = Poissons ratio

W = Charpy impact value

A = area of the fracture surface

The factor of 2 in the denominator takes into account the forming of two fracture surfaces. Ronald, as quoted by Rolfe and Barsom [16], has shown good correlation between values calculated using this method and actual $K1_c$ measurements for titanium and steel. He used precracked Charpy V notch specimens subjected to slow bend loading.

The Plane Strain Assumption

To ensure elastic plane strain behavior, and therefore a minimum $K1_c$ value, the following minimum specimen size requirements have been established by Brown and Srawley [17]:

$$a \geq 2.5 * (K1_c / \sigma_y)^2$$

$$B \geq 2.5 * (K1_c / \sigma_y)^2$$

---

[16] Rolfe, S.T. and Barsom, J.M.; Fracture and Fatigue Control in Structures, 1977, Prentice-Hall Inc., New Jersey, pg.50,193.

[17] Brown Jr., W.F.; Srawley, J.E.; Plain Strain Crack Toughness Testing of High Strength Metallic Materials, ASTM 410, American Society for Testing and Materials, Philadelphia Pa. 19103. pg.26.

$$D \geq 5.0 * (K1_c / \sigma_y)^2$$

Where 'B' is the specimen width, 'D' is the specimen depth, and 'a' is the crack depth.

Use of the above formula shows the dimensions of the Charpy V notch specimen to be insufficient in all cases. That is, the minimum fracture toughness calculated for any of the materials was 99 MPa $m^{.5}$ for the hot isostatically pressed cobalt-chrome. This material also exhibited the highest yield strength of those tested, 920 MPa. The minimum values of 'a', 'B', and 'D' calculated for this material would thus be the lowest for any of the materials. These calculated values, however, are still larger than the dimensions of the Charpy V notch specimens.

Strain Gage Specifications

The strain gages were either EA-06-062AP-120, EA-13-062AP-120, or CEA-06-062UW-120 type gages manufactured by Micro Measurements of Romulus, Michigan. The gage factor for the EA-06 gages was 2.045, for the EA-13 gages 1.99, and for the CEA-06 gages 2.10.

Stem Strains at 1 kN Load

The following table lists the strains produced in each stem tested in the aluminum tube mounting apparatus. As was noted earlier, the values presented below are the average of strain measurements from at least three stem loadings, and in some cases also include the results from two or more implantations into different tubes.

Table 13

Stem Strains at 1 kN Load

Stem No.	Gage Position (mm),Strain (micro m/m)				
	20	40	60	80	100
1	-	-	448	496	-
2	264	403	432	417	350
4	253	497	585	669	326
5-s	250	499	538	510	448
6-s	133	349	542	557	269
7-s	96	650	891	953	755
8	117	320	399	446	385
9	179	340	445	476	-
10	172	503	641	656	320
11	120	348	516	560	448
12	243	320	338	329	319
13	-	201	342	296	143
14	112	201	248	157	-
15	124	228	276	240	-
16	118	271	338	315	149
17	323	551	606	509	404
18	395	589	615	530	417
19-s	384	522	598	457	357
20	133	288	358	383	345
21	175	311	343	318	248
22	223	288	328	304	266
23	85	405	539	474	341
24	214	443	506	425	-
25	123	234	274	255	216

Chemical Composition of Stem Materials

Table 14

Composition of Implant Metals and Alloys (%)

Element	CSS &FSS	CCC	FCC	TAV	MP35N	HCC
H	-	-	-	0.0125	-	-
C	0.03	0.35	0.05	0.08	0.025	.23
O	-	-	-	0.13	-	-
N	-	-	-	0.05	-	-
Al	-	-	-	5.5-6.5	-	-
Si	0.75	1	1	-	0.15	.70
P	0.025	-	-	-	0.15	-
S	0.010	-	-	-	0.010	-
Ti	-	-	-	balance	-	-
V	-	-	-	3.5-4.5	-	-
Chr	17-20	27-30	26-28	-	19-21	28.8
Mn	2.0	1	1	-	0.15	.40
Fe	balance	0.75	0.75	0.25	1.0	.15
Co	-	balance	balance	-	balance	balance
Ni	12-14	2.5	1.0	-	33-37	.14
Mo	2-4	5-7	5-7	-	9-10	5.81

Bibliography

Andriacchi, T.P.; Galante, J.O.; Belytschko, T.B.; Hampton, S.; A Stress Analysis of the Femoral Stem in Total Hip Prostheses, The Journal of Bone and Joint Surgery, Vol.58-A, July 1976, pg.618-624, The Journal of Bone and Joint Surgery Inc., Boston, Massachusettes.

Brown Jr., W.F.; Srawley, J.E.; Plain Strain Crack Toughness Testing of High Strength Metallic Materials, ASTM 410, American Society for Testing and Materials, Philadelphia Pa. 19103. pg.26.

Brown Jr., W.F.; Srawley J.E.; Commentary on Present Practice, Review of Developements in Plane Strain Fracture Toughness Testing, ASTM STP 403, American Sociey for Testing and Materials, Philadelphia Pa. 19103, Pg 229.

Charnley, J.; Biomechanical Considerations in Total Hip Prosthetic Design, The Hip 1973, The C.V. Mosby Company.

Collins, D.K.; Femoral Stem Failure in Total Hip Replacement, The Journal of Bone and Joint Surgery Vol.59-A Dec. 1977, pg. 1033-1041. The Journal of Bone and Joint Surgery Inc., Boston, Massachusettes.

DePuy; A Case for Strength.......Protasul-10, Report issued by DePuy, Division of Bio-Dynamics, Inc., P.O. Box 988, Warsaw, Ind., printed in the USA.

DePuy; Report 7601 Protasul-10, Technical Bulletin issued by DePuy, Warsaw, Indiana.

Evans, F.G.; Significant Differences in the Tensile Strength of Adult Human Compact Bone, Bone and Tooth Symposium, 1963, Macmillan, New York.

Ford, G.; Mec. E. 685 Class Notes.

Galante, J.O.; Rostoker, W.; Doyle, J.M.; Failed Femoral Stems in Total Hip Prostheses, The Journal of Bone and Joint Surgery March 1975, pg. 230-236, The Journal of Bone and Joint Surgery Inc., Boston, Massachusettes.

Hille, G.H.; Titanium for Surgical Implants, Journal of Materials, Vol.1, No.2, June, 1966, pg.373. American Society for Testing and Materials, Philadelphia.

Howmewdica Co.; Metallurgy of Orthopaedic Implant Materials, Report issued by Howmedica, Inc. Orthopaedics Division, 359 Veterans Blvd., Rutherford, N.J.

Howmedica Co.; Vitallium Alloy Group, Report issued by Canadian Howmedica Limited, 90 Woodlawn Road W., Guelph, Ontario.

Irwin, G.R.; Linear Fracture Mechanics, Fracture Transition, and Fracture Control, Engineering Fracture Mechanics, Vol. No.2, 1968.

Markolf, K. and Amstutz, H.; A Comparative Experimental Study of Stresses in Femoral Total Hip Replacement Components: The Effects of Prosthesis Orientation and Acrylic Fixation, J. Biomechanics, Vol.9, 1976, pg. 73-79 , Pergamon Press, New York.

Martens, M.; Aernoudt, E.; de Meester, P.; Ducheyne, P,; Mulier, J.C.; de Langh, R.; Kestelyn, P.,; Factors in

the Mechanical Failure of the Femoral Component in Total Hip Prosthesis, Acta Orthop. Scand. 45, 693-710, 1974, Munksgaard International Booksellers and Publishers Ltd., Copenhagen K, Denmark.

Milch, Henry; Osteotomy at the Upper End of the Femur, The Williams & Wilkins Company, Baltimore, 1965. pg.9.

Morral, F.R.; Cobalt Alloys as Implants in Humans, Journal of Materials, Vol.1, No.2, June, 1966, pg.384, American Society for Testing and Materials, Philadelphia.

Muller, M.E.; Osteotomy of the Greater Trochanter, The Hip 1974, The C.V. Mosby Company, pg.231-251.

Newman, P.H.; Development of Total Hip Replacement, Total Hip Replacement, Jayson, M., J.B.Lippincott Company Toronto,1971, pg. 13-25.

Page, D.l., Bardos, D.I., Ph.D.; Mechanical Testing of Total Hip Femoral Prosthesis Stems, Warsaw, Indiana, January 28, 1975.

Paris, C.P. and Sih, G.C.; Stress Analysis of Cracks, Fracture Toughness Testing and Its Applications, ASTM STP #381, American Society for Testing and Materials, Philadelphia, 1965.

Peterson, M.H.; Brown, B.F.; Newbegin, R.L.; Groover, R.E.; Stress Corrosion Cracking of High Strength Steels and Titanium Alloys in Chloride Solutions at Ambient Temperature, Corrosion, 23, 1967, National Association of Corrosion Engineers, Inc., Houston, Texas.

Richards Manufacturing Co.; Inspection Quality Control,

Technical Information issued by Richards Manufacturing Co., 1450 Brooks Rd., Memphis, Tenn.

Rolfe, S.T. and Barsom, J.M.; Fracture and Fatigue Control in Structures,1977, Prentice-Hall Inc., New Jersey, pg.50,193.

Rydell, N.W.; Intravital Measurements of Forces Acting on the Hip Joint , Acta. Orthop. Scand. Suppl.88;37:1, 1966 Munksgaard International Booksellers and Publishers, Ltd., Copenhagen K, Denmark.

Shigley, J.E.; Mechanical Engineering Design, McGraw- Hill Book Company, Toronto, 1963, pg. 177-183.

Speidel, M.O.; Blackburn, M.J.; Beck, T.R.; Feeney, J.A.; Corrosion Fatigue and Stress Corrosion Crack Growth in High Strength Aluminum Alloys, Magnesium Alloys, and Titanium Alloys Exposed to Aqueous Solutions, Corrosion Fatigue: Chemistry, Mechanics and Microstructure, NACE-2, National Association of Corrosion Engineers, Houston, 1972, pg.330.

Smith, Wayne T.; Metals Used in Orthopedic Implants, distributed by Richards Manufacturing.

Stulberg, D. and Harris, W.H.; Acetabular Dysplasia and Development of Osteoarthritis of Hip, The Hip, The C.V. Mosby Company, 1974, pg.82 to 91.

Walker, Peter S.; The Optimun Use of Materials In Total Hip Design, The Hip 1973, The C.V. Mosby Company, pg.46-66.

Weisman, Sidney; Surgical Implant Materials, Standardization News, Vol.4, No.11, American Society for Testing and

Materials, 1916 Race Street, Philadelphia, Pa.19103, 1976.

Weightman, B.; The Stress In Total Hip Prosthesis Femoral Stems: A Comparative Experimental Study, Advances in Artificial Hip and Knee Joint Technology, Ed. M. Schaldach and D. Holmann, Spinger-Verlag, 1976, pg.138-147.

Weisman, Sidney; The Skeletal Structure of Metal Implants, Biomechanical and Human Factors Symposium 1967, The American Society of Mechanical Engineers, 345 East 47th Street, New York, New York 10017.

Weisman, Sidney; Metals for Implantation in the Human Body, Annals of the New York Academy of Sciences Volume 146, Article 1, Pg.80-95, January 8, 1968.

Williams and Svensson; A Force Analysis of the Hip Joint, Bio-Medical Engineering, Vol. 3, 1968, United Trade Press Limited, London.

Wilson, W.K.; Stress Intensity Factors For Deep Cracks in Bending and Compact Tension Specimens, Engineering Fracture Mechanics, Vol.2, 1970-71, pg.169-171, Ed. H. Liebowitz, Pergamon Press, Toronto.

United States of America Department of Defense; Military Standardization Handbook, Metallic Materials and Elements for Aerospace Vehicle Structures, MIL-HDBK-5C, Naval Publications and Form Center, Philadelphia.

Zarek, J.M., Smith, A.S., A.E.F. Wilkinson; Sintering-Cobalt-Chrome-Molybdenum Alloys for

Osteosynthesis, Nature August 22, 1964, pg. 909.

Zimmer Co.; *Cast Stainless Steel*, Technical Report B-58 issued by Zimmer Co.

Zimmer Co.; *Micro-grain Zimaloy*, Technical Report issued by Zimmer Co.

Zimmer Co.; *Tivanium a new orthopaedic alloy from Zimmer-USA*, Technical Report issued by Zimmer Co.

Zimmer Co.; *Tivanium*, Technical Report issued by Zimmer Co.

Zimmer Co.; *The STH Total Hip Prosthesis*, Surgical Technique Report issued by Zimmer Co.

Zwicker, H.U. and Schmid, H.J.; *Mechanical Properties of Metallic Materials for Longterm Use in Highly Stressed Locomotor Systems*, Engineering in Medicine Vol.2, Institution of Mechanical Engineers, pg. 347-361.